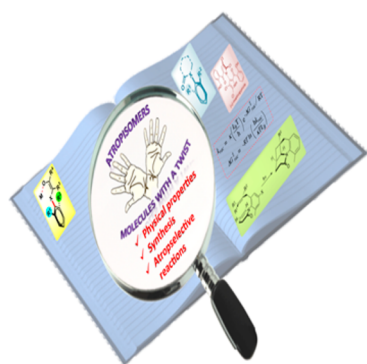


Nonbiaryl and Heterobiaryl Atropisomers: Molecular Templates with Promise for Atropselective Chemical Transformations

Elango Kumarasamy, Ramya Raghunathan, Mukund P. Sibi,* and J. Sivaguru*

Department of Chemistry and Biochemistry, North Dakota State University, Fargo, North Dakota 58108, United States



CONTENTS

1. Introduction	11239
2. Synthesis	11241
2.1. Anilides	11241
2.2. Amides	11243
2.3. Imides	11247
2.4. Indole Derivatives	11248
2.5. Pyrrole and Pyrazole Derivatives	11249
2.6. Lactams	11250
2.7. Quinazolinone Derivatives	11251
2.8. Ureas	11252
2.9. Atropisomers Based on Restricted C–O Bond Rotation	11252
2.10. Atropisomers Based on Restricted C–S Bond Rotation	11254
2.11. Other Systems	11255
3. Physical Characteristics	11255
3.1. Calculation of Racemization Kinetics	11256
3.2. Various Mechanisms of Racemization	11262
3.3. Racemization vs <i>E</i> – <i>Z</i> Isomerization vs Slow Rotation	11262
3.4. Importance of Physical Processes in Atropisomerism in Drug Discovery	11263
4. Applications	11264
4.1. Atropselective Reactions	11264
4.1.1. Cyclization Reactions	11264
4.1.2. [4 + 2]-Cycloaddition	11265
4.1.3. [3 + 2]-Cycloaddition	11265
4.1.4. Radical Cyclizations	11266
4.1.5. Heck Cyclization	11268
4.1.6. Anionic Cyclization	11269
4.1.7. Iodolactonization	11269
4.2. Addition of Nucleophiles	11270
4.3. Reactions with Electrophiles	11272
4.3.1. Enolate Chemistry	11272
4.3.2. <i>Ortho</i> and Lateral Lithiation	11274
4.4. Rearrangements	11276

4.5. Catalysis	11277
4.5.1. Desymmetrization	11277
4.5.2. Grignard Coupling	11278
4.5.3. Asymmetric Heck Reaction	11278
4.5.4. Suzuki–Miyaura Cross Coupling	11278
4.5.5. Benzoin and Stetter Reaction	11279
4.5.6. Michael Addition	11280
4.5.7. [3 + 2]-Cycloaddition	11281
4.6. Atropselective Photoreactions	11281
4.6.1. 6 π -Photocyclization	11281
4.6.2. 4 π -Photocyclization	11283
4.6.3. [2 + 2]-Photocycloaddition	11283
4.6.4. Hydrogen Abstraction	11285
4.6.5. Photochemistry of Chiral Crystals	11285
4.6.6. Photochemistry of Atropisomeric Compounds under Elevated Pressures	11285
4.7. Molecular Machines and Gears	11286
4.8. Stereochemical Relay through Conformation Control	11289
5. Conclusion and Outlook	11290
Author Information	11290
Corresponding Authors	11290
Notes	11290
Biographies	11290
Acknowledgments	11291
Abbreviations	11291
References	11291

1. INTRODUCTION

Chirality plays a crucial role in life-sustaining processes, and for this reason asymmetric synthesis has been a central research theme in many research groups in the field of organic chemistry. While earlier research mainly focused on central chirality (a central atom that has different substituents), other motifs that feature axial chirality, helical chirality, and planar chirality (Chart 1) have recently been investigated for their potential use in synthesis, in asymmetric catalysis, and as chiral perturbers. Axially chiral compounds, unlike molecules that feature central chirality (point chirality), lack stereogenic center(s) yet exist as enantiomers. Atropisomers belong to the class of axially chiral compounds; however, in this case the enantiomers exist due to the restricted rotation around a single bond.

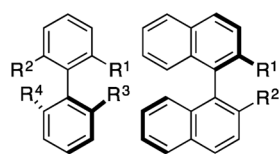
While the atropisomers are usually defined by the chirality rule, viz., *R* (or *R_a*) and *S* (or *S_a*) nomenclature using Cahn–Ingold–Prelog rules, it is also often represented in terms of helicity rules, viz., *P* (positive helix) and *M* (negative helix) nomenclature. For

Received: March 5, 2015

Published: September 28, 2015

Chart 1. Exemplars Featuring Various Forms of Chiralities

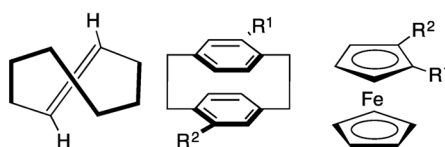
Biaryl atropisomers



Biphenyl

Binaphthyl

Planar chiral molecules



(E)-Cyclooctene

Paracyclophanes

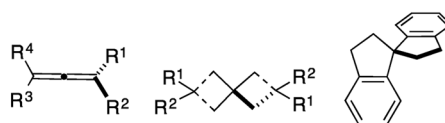
Ferrocenes

Helical chiral molecules



Helicenes

Axial chiral molecules

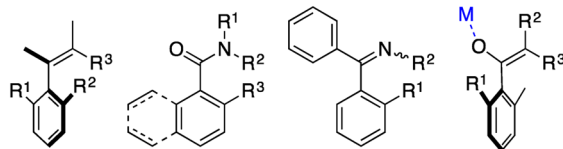


Allenes

Spiranes

Spiro-indanes

Atropisomers around C-C chiral axis



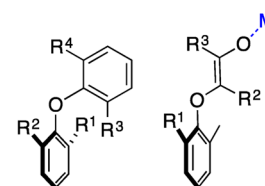
Styrenes

Amides

Imines

Transient
(M= metal)

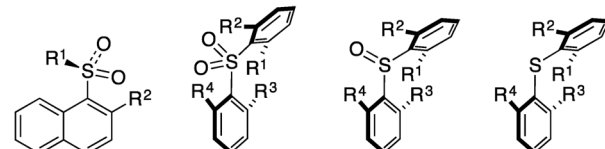
Atropisomers around C-O chiral axis



Diaryl ethers

Transient
(M= metal)

Atropisomers around C-S chiral axis



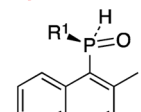
Sulfones

Sulfones

Sulfoxides

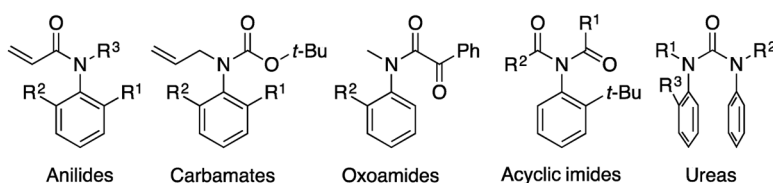
Sulfides

Atropisomers around C-P chiral axis



Phosphine oxides

Atropisomers around C-N chiral axis



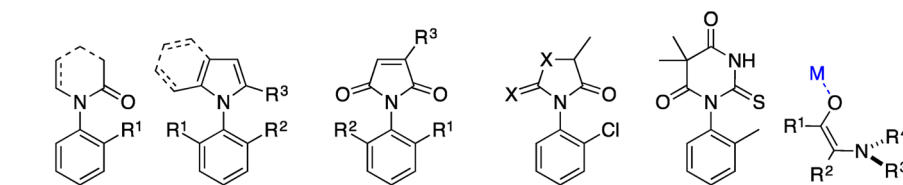
Anilides

Carbamates

Oxoamides

Acyclic imides

Ureas



Lactams

Pyrrole/Indoles

Imides

Azolidine-4-ones
X= O, S

Barbiturates

Transient
(M= metal)

a detailed understating of these nomenclature and concepts, we refer to an excellent review article published elsewhere.¹

The phenomenon of restricted bond rotation was first identified by Christie and Kenner in 1922 while investigating biaryl 6,6'-dinitro-2,2'-diphenic acid.² The term "atropisomer" was coined by Kuhn (derived from Greek, where *a* means "not" and *tropos* means "turn").³ Oki proposed that the atropisomers should be separable if they exhibit a half-life of at least 1000 s (16.7 min).⁴ Progress in this area saw a steep increase after the advent of biaryl based atropisomeric catalysts⁵ and discovery of many natural products with atropisomeric skeleton(s).^{6,7} The

use of atropisomeric compounds as ligands in metal mediated catalysis has revolutionized the fields of organometallic chemistry and asymmetric synthesis. Owing to the high demand and importance of these chiral biaryl scaffolds, numerous synthetic procedures, reviews, and concepts have been published in the literature.^{6–10} Although similar investigations were carried out on nonbiaryl atropisomers, most of them were restricted to analysis of their physical characteristics such as the energy barrier to rotation, racemization, and conformational analysis. It was not until the seminal work of Curran and Clayden that many research groups began to appreciate and investigate the potential of

nonbiaryl atropisomers as an avenue to perform stereospecific/stereoselective reactions and catalysis.¹¹ Curran and co-workers coined the term “atropselective” for reactions featuring atropisomers with stereocontrol.

This review highlights those investigations that describe nonbiaryl and heterobiaryl atropisomers as potential chiral catalysts or substrates that can induce selectivity in chemical transformations. For nonbiaryl atropisomers (i.e., nonbiphenyl and nonbinaphthyl atropisomeric systems), we will focus on stereogenic axis that arise due to restricted rotation about the C(sp²)-X bond (where X is a heteroatom N, O, and S) and C-C bond (e.g., atropisomeric amides), and for heterobiaryl systems we will restrict our scope to select examples that feature atropisomerism around the C-N_{Aryl} bond (e.g., atropisomeric indoles, bis-indoles and pyridones). There are few review articles available in the literature^{12–17} that cover various aspects of atropisomers, and this review will include the latest developments and improvements involving nonbiaryl atropisomers that complement existing reports in this research area.

The review contains three main sections: (i) synthesis, (ii) physical characteristics, and (iii) applications of nonbiaryl atropisomers in synthetic transformations. In the **Synthesis section (Section 2)**, the preparation of various atropisomeric functionalities is organized based on different methodologies that feature (a) racemic, (b) chiral pool, (c) organometallic, and (d) asymmetric (stoichiometric/catalytic) synthesis. The **Physical Characteristics** section highlights parameters such as the rate constant (k_{rac}), half-life ($\tau_{1/2}$), and energy barrier ($\Delta G_{\text{rac}}^\ddagger$) for racemization. This **section (Section 3)** also features various modes of racemization, differences between racemization and slow rotation, as well as the influence of atropisomerism in drug discovery. Finally, the **Applications section (Section 4)** emphasizes the use of atropisomers for different reactions including cycloadditions, radical reactions, nucleophilic and electrophilic additions, catalysis, photoreactions, and the use of atropisomers in molecular devices.

2. SYNTHESIS

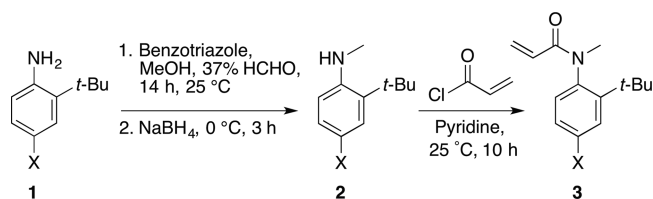
Though the first observation on atropisomerism was documented in 1922, most of the atropisomeric compounds synthesized later were not investigated in the context of atropisomerism. This may be in part due to the lack of appreciation of the importance of axial chirality in atropisomeric compounds. After isolation of several atropisomeric natural products, subsequent work led to a better understanding of the importance of atropisomers/axial chirality leading to greater scrutiny of atropisomeric compounds.^{6,7} These include axially chiral amides, anilides, benzamides, ureas, *N*-aryl pyrroles, *N*-aryl indoles, sulfones, sulfides, *N*-aryl carbamates, diaryl ethers, and carbazoles. Each of these classes of compounds is discussed below in some detail with an emphasis on stereocontrolled synthesis.

2.1. Anilides

Anilides were one of the first systems employed for “atropselective” reactions. Curran et al. documented the synthesis of axially chiral anilides,¹⁸ and their early work focused on synthesizing them as racemates. The racemic anilides were screened for atropselective reactions. A prototypical racemic atropisomeric anilide synthesis is shown in **Scheme 1**.

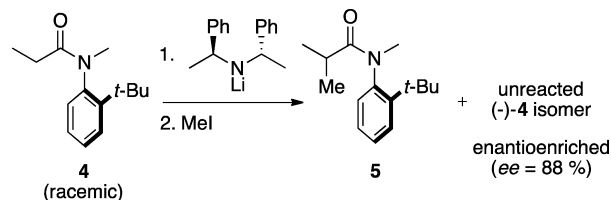
The atropselective chemistry of anilides led many researchers to synthesize them in enantiopure form. For example, Simpkins and co-workers attempted the synthesis of enantiopure anilide **4**

Scheme 1



through kinetic resolution of the corresponding racemate (**Scheme 2**).¹⁹ Treating racemic **4** with a substoichiometric

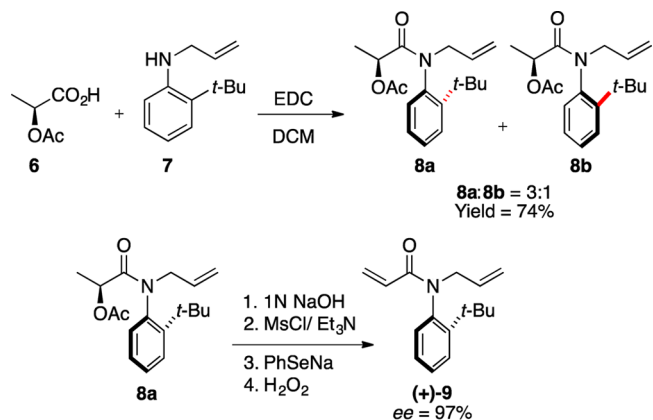
Scheme 2



amount of chiral lithium amide base followed by electrophilic quenching with MeI resulted in the recovery of unreacted starting material **4** with enantiomeric excess of 88%.

While the above attempt gave acceptable enantiopurity, it opened up avenues to access anilides with high enantiomeric purity. Taguchi succeeded in obtaining enantiomerically pure *N*-acryloyl-*N*-allyl anilide **9** through a chiral pool approach (**Scheme 3**).^{20,21} Reaction of *N*-allyl-*o*-*tert*-butylaniline **7** with (*S*)-*O*-acetyl lactic acid **6** resulted in carboxamides **8a** and **8b**, a separable mixture of diastereomers in a ratio of 3:1.

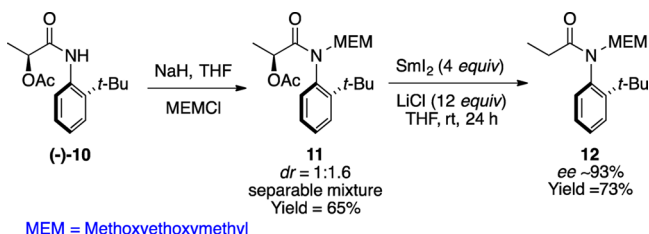
Scheme 3



EDC = 1-Ethyl-3-(3-dimethylaminopropyl)carbodiimide

The crystal structures of **8a** and **8b** revealed that the amide and the aryl functionalities were oriented at $\sim 83^\circ$. The diastereomeric carboxamides **8a/8b** were converted to the corresponding anilide **9** with high enantiopurity (ee = 97%). Following a similar protocol, Simpkins and co-workers reported reduction of α -acetoxy anilides **11** using a combination of SmI₂ and LiCl to furnish enantiomerically enriched anilides **12** (**Scheme 4**).^{22,23} Apart from the acetoxy group, this method also smoothly reduced OBn and Br groups. The presence of LiCl was indispensable as it accelerated the reaction resulting in higher product yields. These optically pure amides were then subjected to alkylation with very

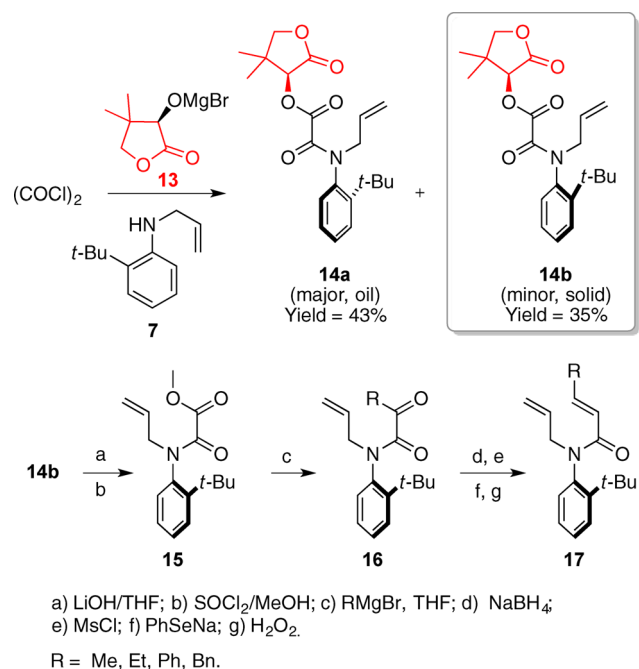
Scheme 4



high atropselectivity (>25:1). However, this method suffered from long reaction times (>24 h) as well as the need to use superstoichiometric amounts of SmI_2 (4 equiv) and LiCl (12 equiv).

Taguchi et al. reported yet another chiral pool approach for the synthesis of enantiomerically pure atropisomeric anilides **17** through resolution of amide esters **14a** and **14b** derived from pantolactone **13** (Scheme 5).²⁴ These amide esters were then

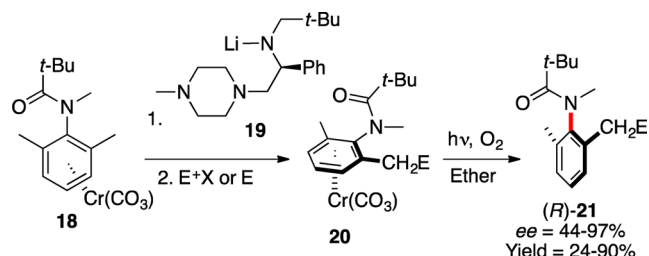
Scheme 5



converted to their corresponding α -ketoamides **16** and α,β -unsaturated anilides **17** without loss of stereochemical integrity. They also demonstrated the successful recovery and reuse of the optical resolving agent pantolactone **13** and validated the potential advantage of this methodology for large-scale preparation.

The first asymmetric synthesis of atropisomeric anilides was reported by Uemura and co-workers through enantioselective lithiation of prochiral tricarbonyl(*N*-methyl-*N*-pivaloyl-2,6-dimethylaniline)-chromium complex **18** with a chiral lithium amide base **19** followed by quenching with an electrophile (Scheme 6).^{25,26} The stereoselective deprotonation occurred due to the conformational orientation of prochiral chromium complex **20** in which the amido carbonyl oxygen was oriented *trans* to the chromium complexed phenyl ring. Exposure of an ethereal solution of chiral chromium complex **20** to sunlight resulted in decomplexation to furnish optically pure anilides **21** without the loss of optical purity.

Scheme 6

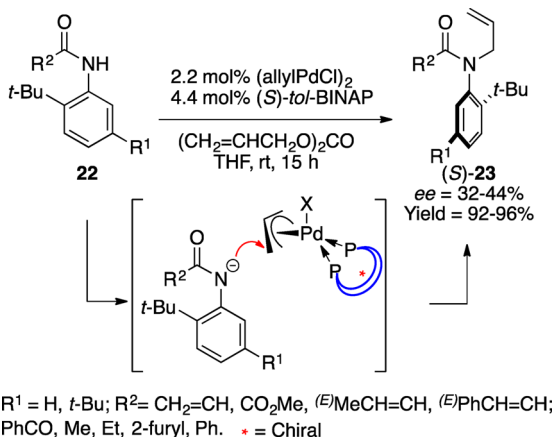


$\text{E}^+\text{X} = \text{MeI}$, PhCH_2Br , $\text{CH}_2=\text{CH}-\text{CH}_2\text{Br}$, $\text{MeC}\equiv\text{C}-\text{CH}_2\text{Br}$, $\text{PhC}\equiv\text{C}-\text{CH}_2\text{Br}$, PhCOCl .

E = Benzophenone, cyclohexanone.

Taguchi and Curran independently reported the first catalytic asymmetric synthesis of atropisomeric anilides. The protocol involved the employment of chiral π -allyl palladium intermediates (Scheme 7).^{27,28}

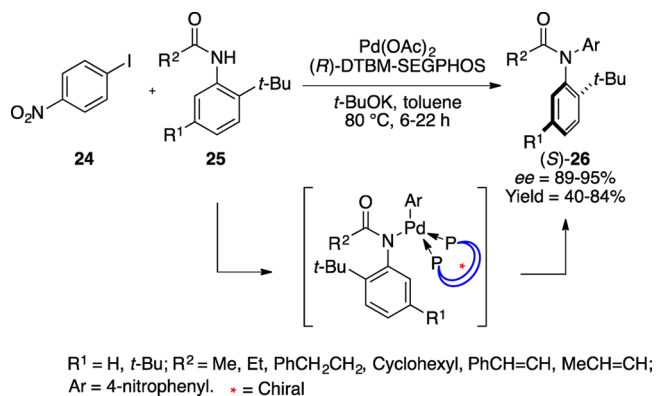
Scheme 7



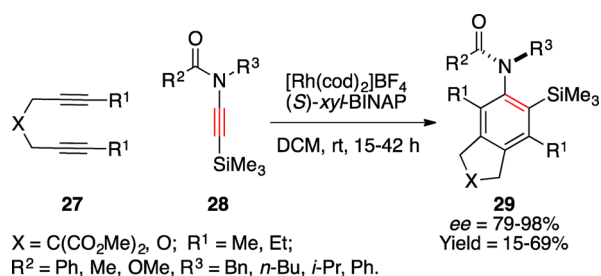
Though these two methods gave excellent chemical yields, the stereoselectivities were rather low. The lower selectivity was attributed to poor facial discrimination during the nucleophilic attack on the π -allyl carbon by the soft anilide anion from the opposite side of the coordinated Pd atom resulting in diminished asymmetric induction. Nevertheless, this work provided initial insights into the catalytic asymmetric synthesis of nonbiaryl atropisomeric systems. Building on this precedence, Taguchi et al. reported a successful catalytic asymmetric synthesis of atropisomeric anilides **26** through intra- and intermolecular *N*-arylation of achiral anilides **25** by a chiral Pd catalyst with very high stereoselectivity (Scheme 8).²⁹⁻³¹ Higher selectivity in these experiments was attributed to the formation of C–N bond near the chiral ligand of the Pd catalyst. Though excellent selectivity and chemical yield was obtained in these experiments, the coupling partner was limited to *p*-nitroiodobenzene **24**. The temperature (80 °C, 22 h) required for efficient conversion in the above method was detrimental for accessing atropisomeric anilides that have lower barriers for C– N_{Aryl} restricted bond rotation, as racemization of the product became unavoidable at elevated temperatures.

Tanaka and co-workers reported rhodium catalyzed enantioselective intermolecular [2 + 2 + 2]-cycloaddition of trimethylsilylnamides **28** with 1,6-diyne **27** to access enantioenriched atropisomeric anilides **29** (Scheme 9).³² The

Scheme 8



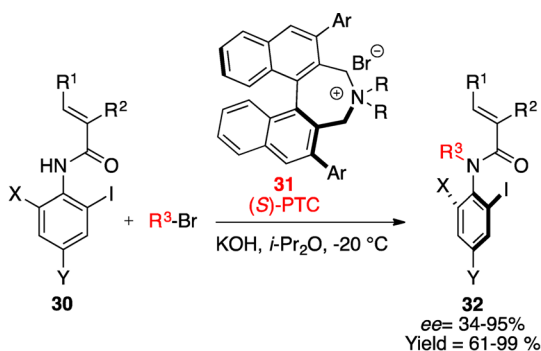
Scheme 9



reaction proceeded smoothly at ambient conditions with very high enantioselectivity and moderate chemical yields. The major side reaction was the homo [2 + 2 + 2]-cycloaddition of 1,6-diynes. Similarly, Hsung and co-workers reported Rh(I) catalyzed asymmetric [2 + 2 + 2]-cycloaddition of ynamides that facilitated the establishment of both C–C and C–N chirality in one synthetic step.³³

Maruoka and co-workers reported a highly efficient catalytic asymmetric synthesis of *o*-iodoanilides **32** through an *N*-alkylation reaction of **30** promoted by quaternary chiral ammonium phase transfer catalyst **31** (Scheme 10).^{34,35} Based on the crystal structure of the catalysts they proposed a transition state model for the observed enantioselectivity, where the catalyst could recognize the steric difference at the *ortho*-position of the anilide (X vs I; refer to Scheme 10). Their hypothesis was bolstered by the dependence of enantioselectivity on the size of the halide substituent at the *ortho*-position of the anilide **30**

Scheme 10

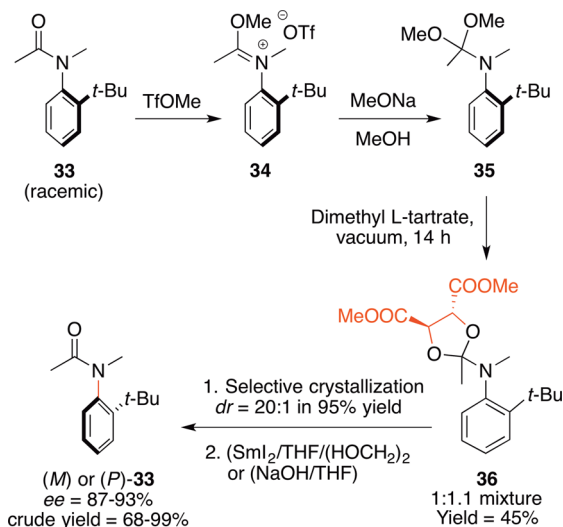


$\text{Ar} = 3,5\text{-}[(t\text{-Bu})_2\text{C}_6\text{H}_3]_2\text{-C}_6\text{H}_3; R = n\text{-Hex}; X = \text{Me}, \text{Et}, \text{OMe}, \text{F}, \text{Cl}, \text{Br}; Y = \text{Me}, \text{H}, \text{Br}, \text{I}; R^1 = \text{H}, \text{Me}; R^2 = \text{Me}, \text{Ph}; R^3 = \text{Bn}, 4\text{-Me-C}_6\text{H}_4\text{-CH}_2, 4\text{-CF}_3\text{-C}_6\text{H}_4\text{-CH}_2, \text{CH}_2=\text{CH-CH}_2, n\text{-Bu}.$

(varying the X substituent from F, Cl, and Br varied the enantioselectivity from 80, 58, and 31%, respectively).

Curran et al. reported a novel method based on crystallization-induced asymmetric transformation of **36** to obtain optically pure anilides **33** (Scheme 11).³⁶ Upon crystallization, one of the

Scheme 11

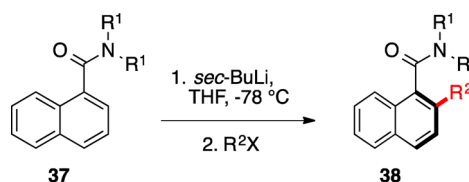


diastereomers of **36** was isolated in a diastereomeric ratio (dr) of 20:1 even though *trans*-ketalization of *o*-anilide **35** afforded **36** in a dr of 1:1:1. The enriched diastereomer of **36** underwent samarium iodide reduction or base hydrolysis to furnish enantiomerically enriched axially chiral anilides **33**. The dr of **36** dictated the ee in **33** that suggested that the reduction/hydrolysis occurred much faster than the C–N_{Aryl} bond rotation. While this method employed stoichiometric amount of tartaric acid for resolution, two important hypotheses were introduced in order to obtain optically pure axially chiral anilides. First, the asymmetric hydrolysis of *o*-anilide in the presence of a chiral environment is difficult; viz., the rate of hydrolysis must be faster than the rate of C–N_{Aryl} bond rotation of ketal-anilide, but slower than the C–N_{Aryl} bond rotation of the keto anilide product. Second, in the asymmetric acylation protocol, the ketal formation step (tetrahedral intermediate) must be selective rather than the hydrolysis step as the former determines the ee of the final anilide product. This is because the rate of hydrolysis is much faster than the rate of C–N_{Aryl} bond rotation of the *o*-anilide.

2.2. Amides

Aromatic amides with a general formula ArCONR₂ with sufficiently bulky *ortho* substituents exist as atropisomers (Scheme 12). The plane of the amide carbonyl is almost perpendicular to the aromatic ring. Axially chiral amides have

Scheme 12

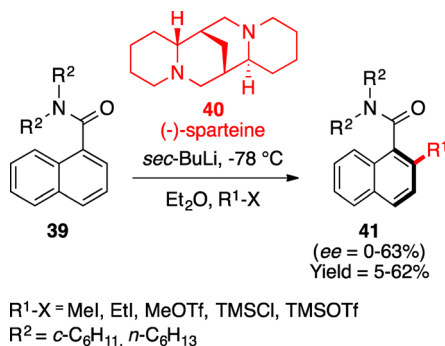


$R^1 = \text{Et}, i\text{-Pr}; R^2X = \text{MeI}, \text{TMSCl}$

been under intense scrutiny starting from 1966 and have been well studied for their physical characteristics (interesting landmarks will be discussed in section 2). Pioneering work by Clayden and co-workers has highlighted the versatility of atropisomeric amides in asymmetric synthesis. They reported the first stereoselective synthesis of axially chiral amides **38** through *ortho* metalation of **37** followed by electrophilic quenching (Scheme 12).^{37,38}

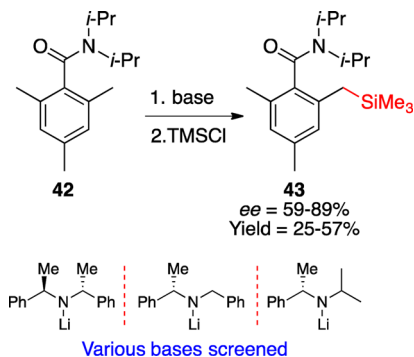
Following a similar protocol, Beak et al. achieved the first enantioselective synthesis of axially chiral amides with the use of (–)-sparteine **40** (Scheme 13).^{39,40} They rationalized the

Scheme 13

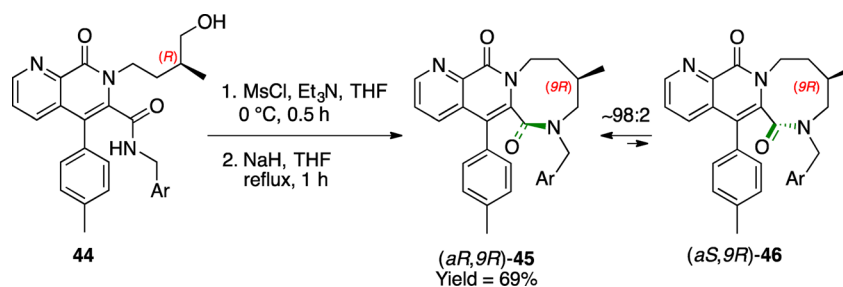


observed enantioselectivity on the asymmetric deprotonation of the naphthamides **39** using *sec*-BuLi/sparteine complex followed by electrophilic quenching. Similarly, Clayden and co-workers reported a method to access optically pure atropisomeric amides involving desymmetrization of enantiotopic *o*-methyl substituents using chiral lithium amide bases followed by electrophilic quenching (Scheme 14).⁴¹ *sec*-BuLi complexed

Scheme 14



Scheme 15

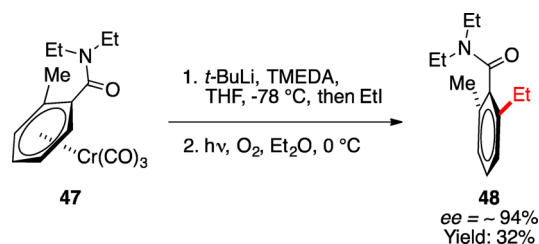


with chiral diamine such as (–)-sparteine or chiral lithium amide bases were both efficient in deprotonating **42** with the later combination giving the product in appreciable enantioselectivity and chemical yields.

Natsugari et al. reported a diastereoselective cyclization of **44** leading to potent NK₁ receptor antagonist **45** and carried out extensive studies on its pharmacological properties (Scheme 15).^{42–44} The newly formed eight-membered ring in the cyclized product reached an equilibrium of 98:2 ((*aR,9R*)-**45**:(*aS,9R*)-**46**) in solution in approximately 60 h at 37 °C. In a similar manner, the enantiomer of **45** (*aS,9S*) was synthesized and tested for its antagonistic activity. Structure–activity studies revealed that the axial chirality had significant influence on the NK₁ antagonistic activity. For example, the (*aR,9R*)-**45** isomer had an IC₅₀ of 0.45 nM compared to its enantiomer (*aS,9S*)-**45** whose IC₅₀ value was 340 nM.

Uemura and co-workers succeeded in obtaining highly enantioenriched axially chiral benzamides **48** using a planar chiral arene chromium complex **47** (Scheme 16).⁴⁵ The

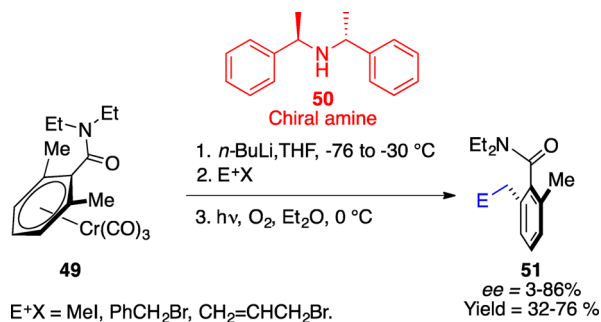
Scheme 16



orientation of the amide NEt₂ substituent was *anti*, while the amide carbonyl oxygen was *syn* to the aryl coordinated chromiumtricarbonyl functionality. Such an orientation allowed excellent stereoselectivity in the *ortho*-lithiation step followed by stereoselective quenching by electrophiles. Additionally, several other substituents were investigated at the *ortho* position for their influence on the stability of the atropisomers. The same group reported an enantiotopic lithiation of prochiral benzamide derivatives **49** in the presence of a chiral lithium amide base **50** to access optically pure atropisomeric benzamides **51** (Scheme 17).²⁶ Among various chiral amines screened, only monoamines gave respectable enantioselectivity. Further optimization to obtain higher selectivity by varying the solvent and additives such as LiCl were not fruitful.

Clayden and co-workers reported the asymmetric synthesis of atropisomeric amides through dynamic thermodynamic resolution with proline-derived diamine derivative **53** (Scheme 18).⁴⁶ Coupling of optically pure resolving agent **53** with **52** resulted in **54** with high yield and diastereoselectivity. After thorough

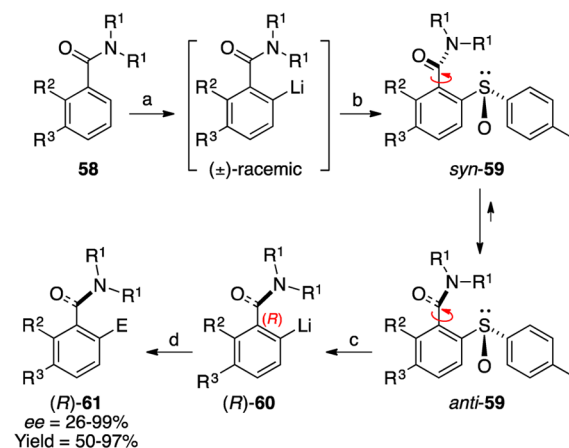
Scheme 17



investigations they concluded that the aminal was formed initially as a mixture of diastereomers **54/55**. Under the reaction conditions **55** epimerized to more stable atropisomer **54** leading to higher diastereoselectivity (dynamic kinetic resolution). The diastereomerically enriched **54** was sequentially hydrolyzed and reduced to obtain the optically pure amide **57** (as the aldehyde derivative **56** featured a lower energy barrier for racemization). This methodology was extended to benzamides; however, the lower energy barrier for rotation in the product resulted in partial racemization leading to poor enantioenrichment in the final product. The same group also employed various chiral resolving agents such as (–)-ephedrine, proline-derived imidazolines, and ephedrine-derived oxazolindines to achieve higher enantioenrichment in naphthamide and benzamide derivatives.^{47,48}

In an elegant report, Clayden and co-workers employed enantiomerically pure sulfoxide *anti*-**59** as a temporary handle to achieve excellent thermodynamic control over the stereochemistry of amides **61** (Scheme 19).⁴⁹ Racemic amide **58** on metalation followed by quenching with menthylsulfonate gave *syn*-**59** that underwent dynamic resolution under thermodynamic control to yield *anti*-**59** exclusively. This thermodynamically stable sulfoxide *anti*-**59** reacted with *t*-BuLi generating the *ortho*-lithiated intermediate **60**. As the axial chirality was preserved at -78 °C, this intermediate **60** was trapped by electrophilic quenching resulting in enantioenriched amides **61**. The conversion of enantiomerically pure atropisomeric amides to amide free derivatives such as benzofuranones through memory of chirality exemplified the versatility of this strategy.

Scheme 19



$\text{R}^1 = i\text{-Pr}$; Et ; $-\text{CMe}_2\text{CH}_2\text{OCMe}_2-$

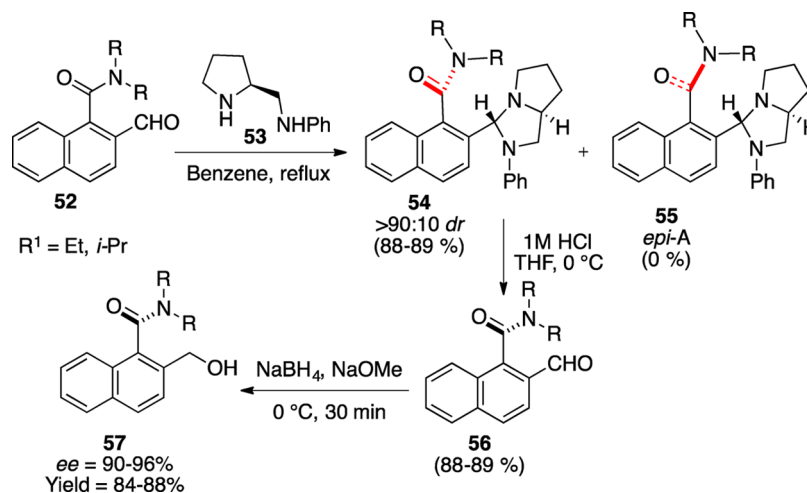
$\text{E}^+ = \text{Me}$, Et , Ph_2CO , $(\text{CH}_2)_2\text{CO}$, $\text{C}_2\text{H}_4\text{Br}_2$, $\text{C}_2\text{H}_4\text{I}_2$, EtI ; a) *sec*-BuLi, THF, -78 °C; b) (1*R*,2*S*,5*R*,*Ss*)-(–)-menthyl-*p*-toluenesulfonate, -78 °C to 0 °C then NH_4Cl ; c) *t*-BuLi (3 equiv), THF, -78 °C, 5 min; d) E^+

Walsh and co-workers reported a catalytic kinetic resolution method to obtain optically pure atropisomeric amides **62** using commercially available Sharpless asymmetric dihydroxylation agent (AD) (Scheme 20).⁵⁰ They anticipated that the presence of a chiral axis will impact the relative rates of dihydroxylation of the enantiomers. The analysis revealed that the relative rate (k_{rel}) of dihydroxylation was as high as 32 with the use of AD-mix α . The absolute stereochemistry of the resolved enantiomer **62** as well as the diol **63** was not reported.

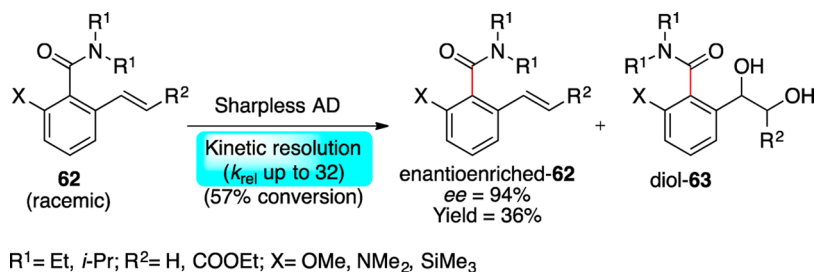
While benzamides were superior for kinetic resolution, substituents at the *ortho* position and at the amide nitrogen of benzamides had a significant influence on the k_{rel} of the reaction. This is due to the epimerization of the atropisomers over time that reduced the diastereoselectivity in the diol product **63**.

Addition of pyridine to accelerate the dihydroxylation did not affect the initial outcome of the diastereomeric excess (de) in the diol product, thus allowing them to conclude that the kinetic diastereoselectivity was substrate controlled rather than catalyst controlled. Dai and co-workers also reported a similar type of kinetic resolution to obtain enantioenriched atropisomeric naphthamide derivatives containing oxygenated functionalities.⁵¹

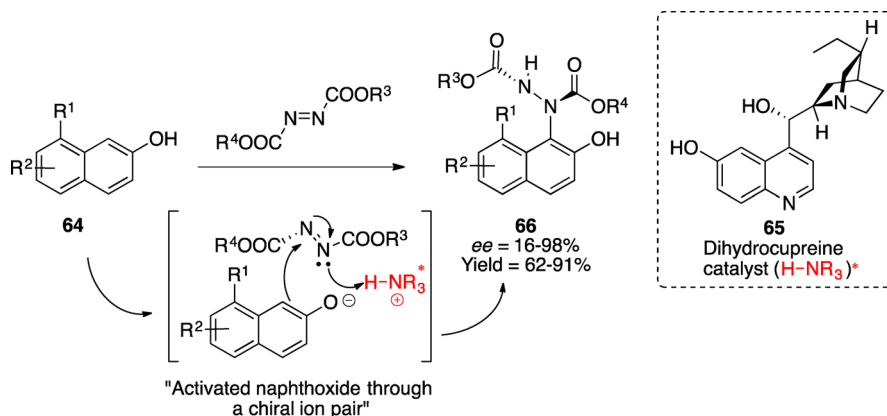
Scheme 18



Scheme 20



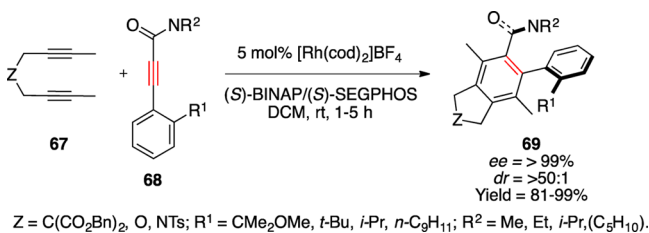
Scheme 21



Jørgensen and co-workers documented cinchona-alkaloid based organocatalytic enantioselective synthesis of naphthamides and carboxamides through asymmetric Friedel–Crafts reaction (Scheme 21).⁵² The reaction proceeded through an activated naphthoxide that in the presence of catalyst **65** formed a chiral ion pair with azodicarboxylate complex, which further reacted to form naphthamides **66** with excellent stereo- and regiocontrol (if unsymmetrical azodicarboxylate was employed). Interestingly, the catalyst itself underwent Friedel–Crafts reaction under forcing conditions (under the asymmetric reaction conditions, only **64** reacted preferentially compared to the catalyst) resulting in new class of cinchona-alkaloid that accelerated the reaction much more efficiently giving rise to products with high optical purity and enabling access to both enantiomers of the product.

Tanaka and co-workers reported the first catalytic enantioselective synthesis of atropisomeric benzamides through cationic rhodium catalyzed [2 + 2 + 2]-cycloaddition of 1,6-diyne **67** with *N,N*-dialkylalkynylamide **68** (Scheme 22).⁵³ This methodology tolerated several substitutions and was also useful in the synthesis of substrates featuring two axial chiral units, viz., aryl-aryl and aryl-carbonyl axial chiralities with excellent control over enantio- and diastereoselectivities. Employing this methodology,

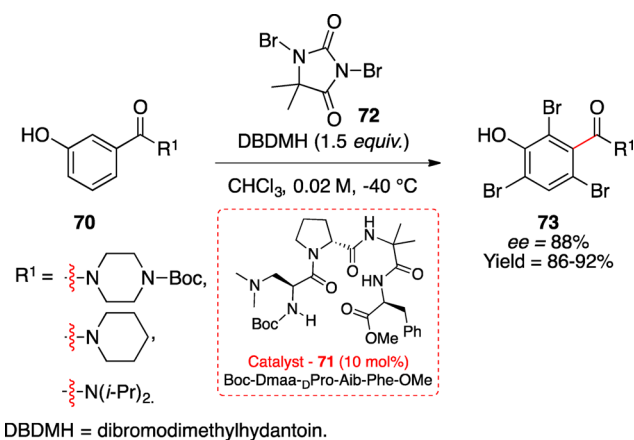
Scheme 22



the same group demonstrated the synthesis of axially chiral 2-pyridones with reasonable enantiomeric excess (up to 87% ee).⁵⁴

Miller and co-workers reported an interesting catalytic enantioselective method to synthesize axially chiral benzamides through peptide catalyzed aromatic substitution reactions involving bromination (Scheme 23).⁵⁵ The tetrapeptide bearing

Scheme 23

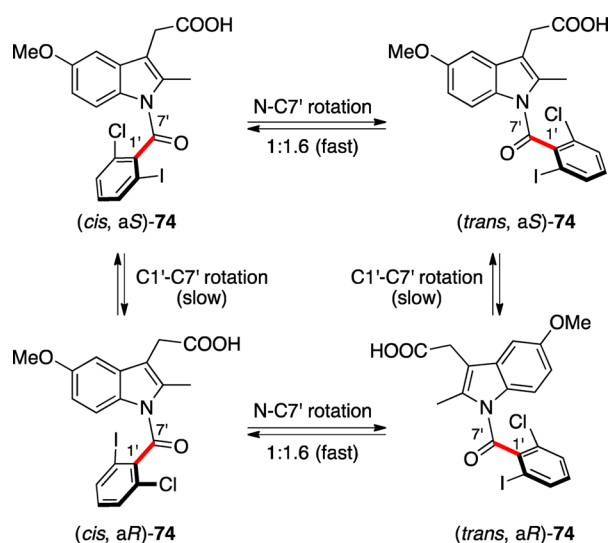


a tertiary amine catalyst **71** acted as a Brønsted base in promoting the reaction. The phenolic group in the substrate **70** coordinated to the catalyst (likely through H-bonding) and directed the bromination. The origin of enantioselectivity during this multibromination reaction was evaluated by monitoring the progress of reaction at an early stage. The results revealed that the initial bromination occurred near the prochiral axis (*ortho* to phenol and the amide carbonyl) dictating the stereochemistry in the product. The advent of several catalytic enantioselective

methods provided an easy access to the axially chiral amides that can further be employed for atropselective reactions (*vide infra*).

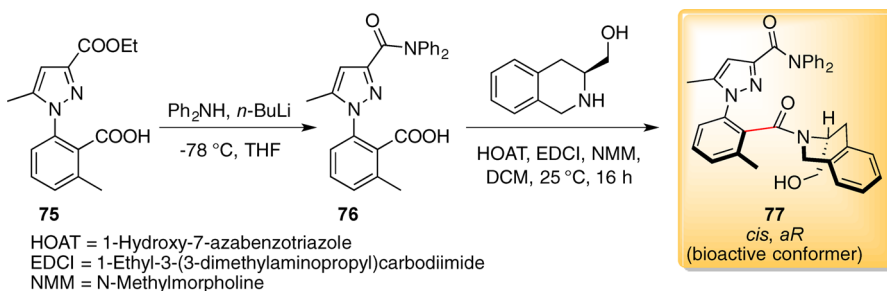
Indometacin **74**, a nonsteroidal anti-inflammatory drug, has been the subject of extensive studies to understand its reactive conformation and interactions with the cyclooxygenase (COX) active site. For a long time indometacin was assumed to be a planar molecule (atropisomerism was overlooked), which led to several misconceptions. Natsugari and co-workers prepared and analyzed derivatives of indometacin and showed that the axial chirality greatly affects the recognition of COX isoforms (Scheme 24).⁵⁶ The ester derivatives of **74** were separated on a chiral stationary phase using preparative HPLC and subsequently hydrolyzed to get the target analyte.

Scheme 24



While the interconversion of N–CO conformers that exist in a ratio 1:1.6 was fast, the interconversion of C–CO atropisomer was slow due to a higher energy barrier to rotation around the C(sp²)–C(O) chiral axis (25.7 kcal·mol⁻¹). Analysis of the racemate and individual enantiomers revealed that only (*cis,aR*)-**74** showed potent activity against COX-1 (IC₅₀ of 15.6 ± 1.8 μM). Just like central/point chiral molecules, each isomer/conformer of the atropisomeric compounds can have different biological activity. For example, Porter and co-workers reported the synthesis of atropisomeric 1,2,3,4-tetrahydroisoquinoline amide **77** as Bcl-2 ligands for proteins that are well-known for their *anti*- and *pro*-apoptotic activity (Scheme 25).⁵⁷ Further separation of rotamers and conformers allowed them to identify the biologically active conformer (eutomer) *cis-aR*-**76**. The result was further bolstered by Bcl-2 affinity analysis in which only *cis*-

Scheme 25

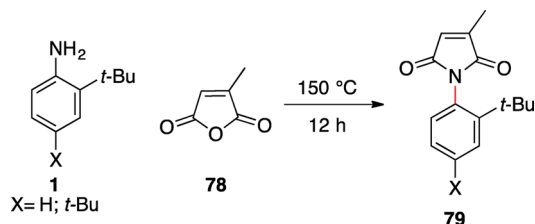


aR-**77** bound to the protein. Structure–activity relationship (SAR) studies revealed that changing NPh₂ substituent to NBU₂ in the pyrazole group resulted in improved potency against Bcl-2.

2.3. Imides

One of the features of *N*-aryl maleimides is the orthogonal orientation of the amide and aryl functionalities.⁵⁸ This has been exploited for a wide variety of reactions.⁵⁸ Based on this precedence, axially chiral maleimides were reported by Curran *et al.* through desymmetrization of the maleimide motif that resulted in an N–C_{Aryl} chiral axis (Scheme 26).¹⁸ While the

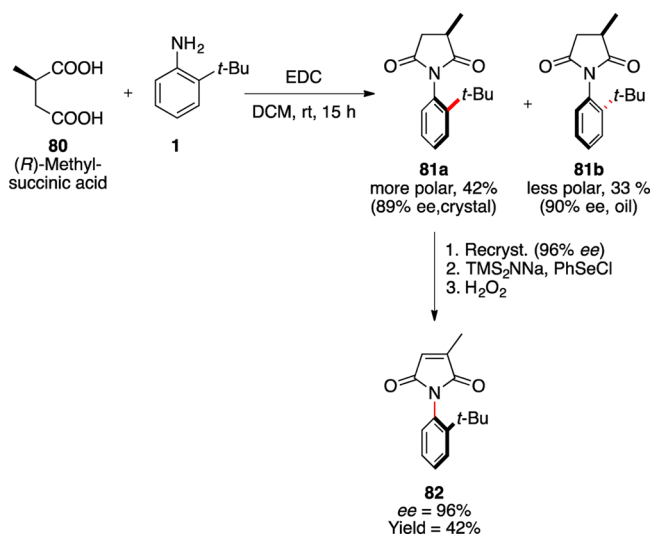
Scheme 26



individual atropisomers of **79** were not resolved, the presence of an *o*-*tert*-butyl group inhibited racemization at room temperature providing the necessary control of facial selectivity during chemical transformations.

Taguchi and co-workers reported a chiral pool approach to access optically pure atropisomeric maleimides (Scheme 27).²¹

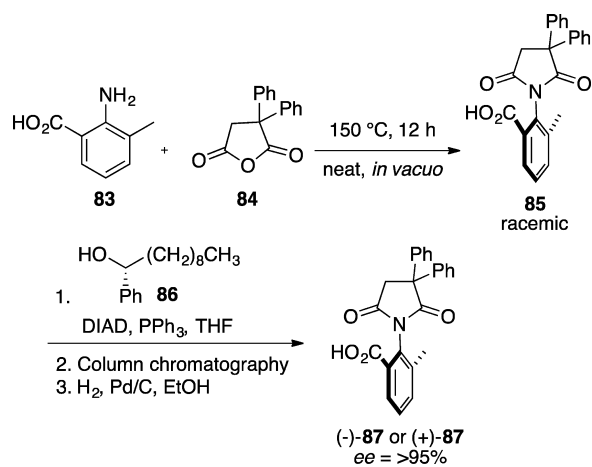
Scheme 27



The coupling reaction between *o*-*tert*-butylaniline **1** and (*R*)-methyl succinic acid **80** promoted by EDC resulted in high conversion at a high concentration (3 M) leading to a mixture of diastereomeric imides **81a** and **81b**. The diastereomers were easily separated by chromatography followed by recrystallization to yield optically pure **81a**, which was further converted to the corresponding maleimide **82** without the loss of optical purity.

Shimizu and co-workers carried out resolution using the chiral resolving agent (*S*)-1-phenyl decanol **86** under Mitsunobu conditions to access enantiomerically pure *N*-aryl imide **87** (Scheme 28).⁵⁹ The optically pure imide esters (formed from

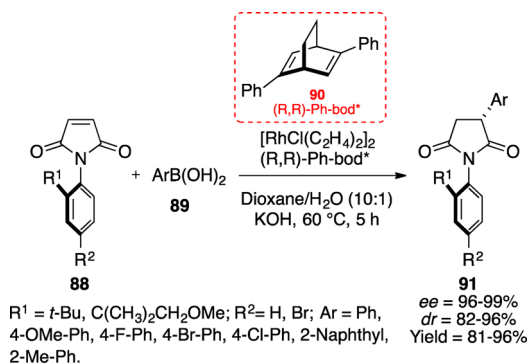
Scheme 28



coupling of **85** and **86**) obtained by chromatographic separation were subjected to hydrogenolysis followed by recrystallization in acetone to obtain optically pure *N*-aryl imide **87** that possessed a high energy barrier for C_{Aryl}–N bond rotation (>30 kcal·mol⁻¹). Following a similar protocol, the same group reported the synthesis of enantiomerically pure axially chiral *N*-aryl imide monodentate phosphine ligand that was employed for Pd catalyzed asymmetric allylic alkylation reaction.⁶⁰

Hayashi and co-workers reported catalytic asymmetric synthesis of *N*-aryl imides through rhodium catalyzed asymmetric 1,4-addition reaction (Scheme 29).⁶¹ Excellent enantio- and diastereoselectivities were obtained through this methodology. The observed selectivity was explained based on the approach of the Rh complex from the side opposite to the bulky *t*-Bu substituent, thus avoiding unfavorable steric interactions. The succinimide **91** was oxidized using a DEAD/K₂CO₃ mixture to

Scheme 29



corresponding maleimides without loss of stereochemical integrity (axial chirality).

Bencivenni and co-workers reported an enantioselective desymmetrization approach involving aminocatalytic vinylogous Michael addition to access optically pure imide derivatives **95** (Scheme 30).⁶² The reaction proceeded smoothly with excellent control over the prochiral axis resulting in very high stereoselectivity in the product. The catalyst **94** was able to exert its stereochemical influence at the prochiral axis of the maleimide double bond resulting in desymmetrization (favoring the *P*-isomer). Replacing the *ortho* substituent of the maleimide **93** from a bulky *t*-Bu group to a less bulky group such as iodo, SiEt₃, or Ph resulted in epimerization due to lower energy barrier for N–C_{Aryl} bond rotation. The same authors have also reported highly atropselective Diels–Alder desymmetrization of *N*-arylmaleimides catalyzed by the organocatalyst **94**.⁶³

2.4. Indole Derivatives

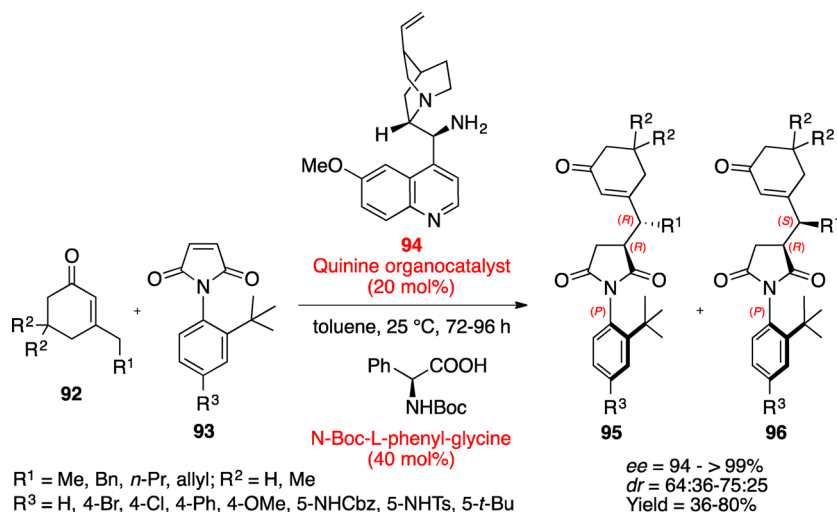
In 2001, Bringmann and co-workers reported the first total synthesis of murrastifoline-F **98**, a heterobiaryllic bis-carbazole alkaloid with an N–C_{Aryl} chiral axis, through oxidative non-phenolic coupling of **97** (murrayafoline-A)⁶⁴ promoted by Pb(OAc)₄ (Scheme 31).⁶⁵ The authors were the first to explore atropisomerism in **98** even though the natural product had prior literature precedence. The liquid chromatography circular dichroism (LC-CD) spectra of **98** in a stopped flow mode confirmed the presence of enantiomers due to restricted N–C_{Aryl} bond rotation. The optically pure atropisomers were accessed through derivatization of **98** with a chiral auxiliary (Mosher's acid) followed by chromatographic separation of the diastereomers. The individual diastereomers were characterized, and their absolute configurations were determined. Analysis of the naturally occurring murrastifoline-F revealed that the *M*-isomer was favored over the *P*-isomer in a ratio ranging from 55:45 to 58:42.

Uemura and co-workers reported diastereoselective synthesis of axially chiral indoles through stereoselective nucleophilic aromatic substitution of planar chiral chromiumtricarbonyl complex **99** (Scheme 32).^{66,67} Coordination of electron withdrawing chromium complex activated the aryl ring toward nucleophilic attack of the indole anion **100**.

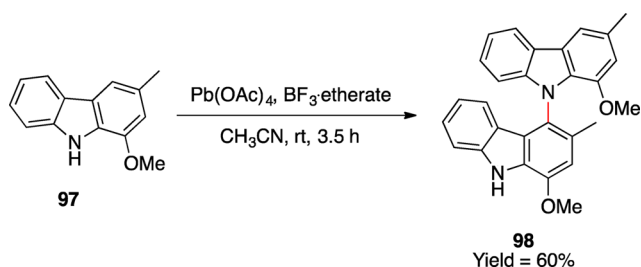
Interestingly, the product stereochemistry was dictated by the substitution at the 2-position (R²) of indole **100**. The chromium functionality was oriented *anti* (**101**) to the indole benzene ring in the case of unsubstituted and 3-methyl substituted indoles, while it was oriented *syn* (**102**) in the case of 2-substituted indoles. Theoretical calculation revealed that the rate-determining step was the elimination of fluoride ion that had the highest energy barrier of all the steps. In addition, the most stable conformation featured the methyl group of the indole orienting away from the leaving group (F⁻).

Kitagawa and co-workers reported the first asymmetric synthesis of axially chiral indole **104** through 5-*endo*-hydroaminocyclization of **103** mediated by a Pd catalyst (Scheme 33).⁶⁸ Reaction with the aromatic alkyne **103** resulted in good yields of the product. In contrast, the reaction was sluggish with aliphatic and deactivated aromatic substituents (*o*-nitro derivatives). Addition of AgOTf (5 mol %) accelerated the reaction by the formation of reactive cationic Pd species. One interesting note was that if the R¹ group contained an *ortho*-substituted phenyl group (e.g., 2-Me-Ph), the product was obtained with higher selectivity. The observed selectivity was attributed to the generation of dynamic axial chirality around C_{alkynyl}–C_{phenyl} that

Scheme 30



Scheme 31



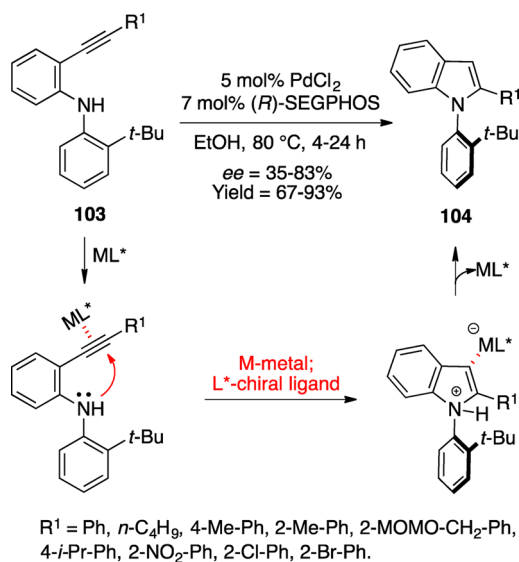
efficiently translated the chiral information from (*R*)-SEGPHOS to the newly forming C–N chiral axis.

2.5. Pyrrole and Pyrazole Derivatives

N-Arylpyrroles (e.g., **108**), are one of the earliest nonbiaryl atropisomeric compounds that were documented by Bock and Adams in 1931 (Scheme 34).⁶⁹ This was followed by several other reports, which were focused on understanding the rotational barriers and racemization processes of the atropisomers through HPLC separation on a chiral stationary phase and analysis of their kinetic parameters.

Sarli and co-workers reported an improved procedure for the total synthesis of marine alkaloid (\pm)-marinopyrrole-A **112** (Scheme 35).⁷⁰ The copper mediated arylation of **109** and **110** under microwave conditions was employed to access the 1,3'-bipyrrole core **111**. The synthesis was accomplished in six steps with 22% overall yield compared to the previous report by Li and

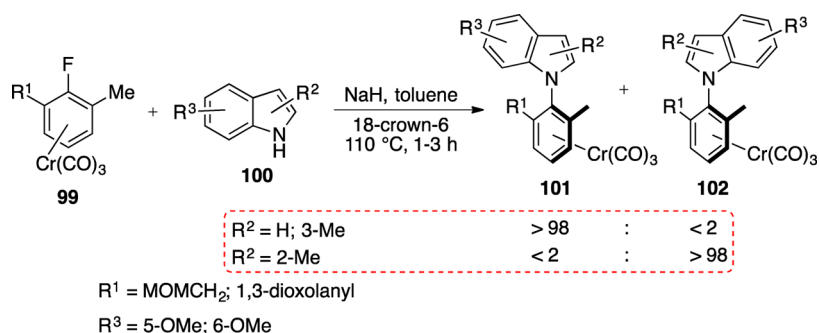
Scheme 33



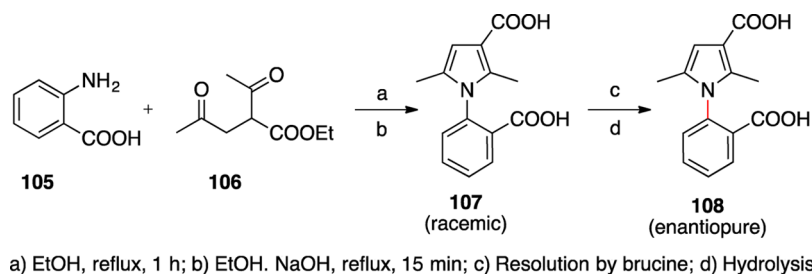
co-workers that involved nine steps with 30% overall yield.⁷¹ Similarly, Fenical and co-workers reported access to marinopyrroles A–F through the cultivation of actinomycete strain CNQ-418.⁷² These stable axially chiral natural products possessed only (*M*)-configuration.

Sugane and co-workers reported a concise method and resolution procedure to access enantiomerically pure triazoles

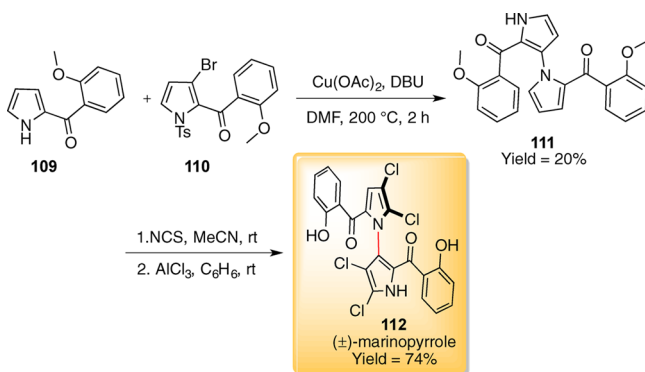
Scheme 32



Scheme 34

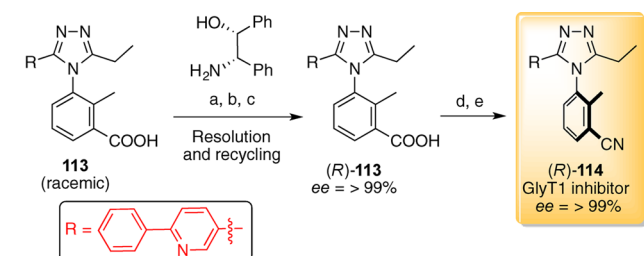


Scheme 35



derivative **114**, which was an active GlyT1 inhibitor (Scheme 36).⁷³ The active (*R*)-enantiomer **114** was synthesized from (*R*)-

Scheme 36



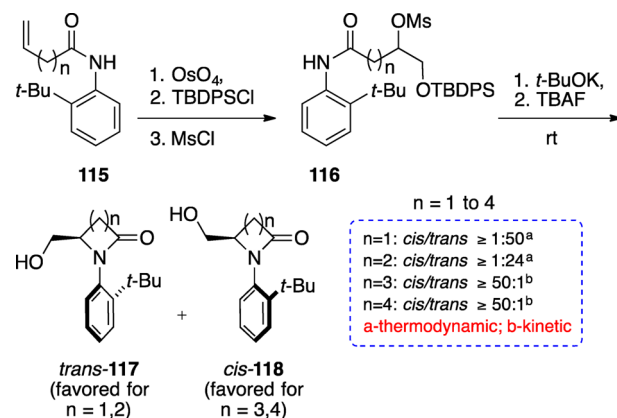
(a) (i) (1*R*,2*S*)-(-)-2-amino-1,2-diphenylethanol, EtOH/H₂O (1:3); (ii) recryst. from EtOH/H₂O (1:3), 41%; (b) 1 M HCl aq, 95%; (c) (i) DMA, 155 °C; (ii) 1 M HCl aq, 98%. (d) EDC·HCl, HOBT, NH₄Cl, Et₃N, DMF, rt, 86%; (e) POCl₃, DMF, 0 °C, 81%.

113. The undesired (*S*)-**113** enantiomer obtained after resolution was converted back to a racemate by heating at 155 °C in *N,N*-dimethylacetamide (DMA). This process enabled recovery and reuse of undesired (*S*)-**113** isomer taking advantage of thermal isomerization of axially chiral molecules.

2.6. Lactams

In the course of their continued interest in atropisomeric compounds, Taguchi and co-workers devised a strategy to synthesize optically active axially chiral lactams through aminocyclization of the mesylate derivative **116** (Scheme 37).^{74,75} The ring size of the lactam had considerable influence on the stereochemical outcome of the diastereomeric products **117**/**118**. In four- and five-membered lactams, the *o*-*tert*-butyl functionality was oriented *trans* (as in **117**) with respect to C-4 or C-5 substituent. On the other hand, in six- and seven-membered ring lactams, the *o*-*tert*-butyl functionality was *cis* (as in **118**) with respect to C-4 or C-5 substituent. After careful analysis of the reaction, the authors concluded that the

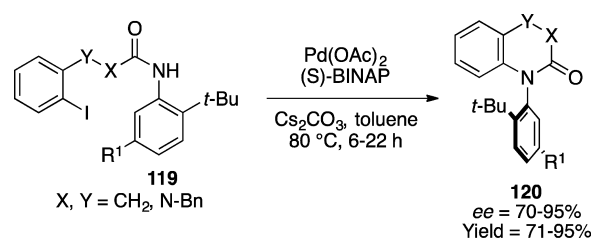
Scheme 37



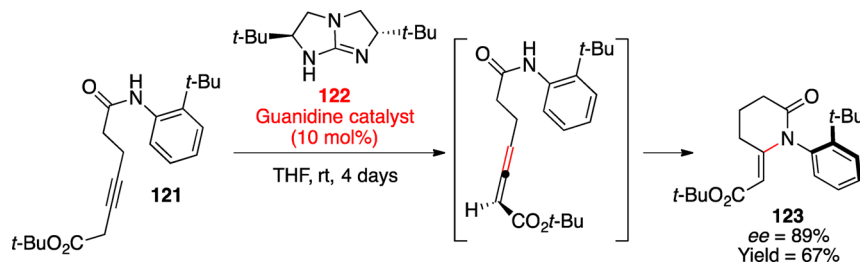
thermodynamic product dominated in the case of four- and five-membered lactams where the initially formed *cis* product **118** (kinetic product) isomerized to thermodynamically stable *trans*-**117** through C_{Aryl}-N bond rotation. This bond rotation was facilitated by the reduced bond angle in the four- and five-membered lactams. On the other hand, in the case of six- and seven-membered ring lactams, the *cis* product **118** formed under kinetic conditions did not convert to *trans*-**117** due to the large rotational barrier (as C-N-C bond angles are larger for six- and seven-membered lactams). They also found that the N-C_{Aryl} bond rotation is more facile in the four-membered ring system (even with the *ortho tert*-butyl substitution in the N-Phenyl ring) and as the ring size increases the barrier for rotation becomes higher. Taguchi and co-workers also reported the synthesis of optically pure atropisomeric lactams **120** through the catalytic asymmetric N-arylation reaction of **119** promoted by Pd in the presence of BINAP (Scheme 38).²⁹ The resulting lactam was subjected to atropselective reactions to furnish compounds that were biologically active NET inhibitors.^{31,76}

Tan and co-workers reported an enantioselective synthesis of axially chiral lactam **123** through tandem isomerization-aza-Michael reaction of amide **121** in the presence of a chiral guanidine catalyst **122** (Scheme 39).⁷⁷ While the reaction

Scheme 38



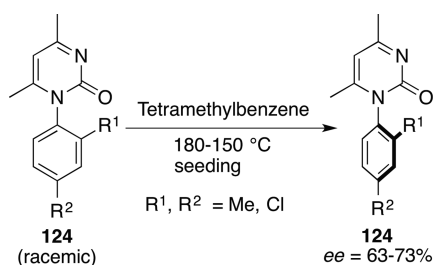
Scheme 39



proceeded smoothly, the method was rather limited in scope due to the difficulty in securing various substituted alkynes. The reaction failed in the aza-Michael cyclization step for substrates with higher chain lengths and gave only enantioenriched allenes.

In 2003, Sakamoto and co-workers reported a spontaneous induced crystallization method to access optically pure *N*-arylpyrimidinones **124** (Scheme 40).⁷⁸ For a successful resolution, it

Scheme 40



was essential that the racemate crystallize in a chiral space group (as conglomerates). In the absence of seeding, when a melt crystal or a solution at high temperature (150–180 °C) was slowly cooled, chiral symmetry breaking⁷⁹ occurred favoring one enantiomer over the other resulting in chirally enriched *N*-arylpyrimidinones (ee ranging from 13 to 66%). The authors report unpredictability of the crystallized enantiomer as well as the inconsistency in getting the same optical purity. They overcame this limitation by externally adding optically pure crystals to melt that gave the same optical isomer of the seeded crystal with consistent results. These enantioenriched crystals were further subjected to simple crystallization to yield atropisomeric compounds with high optical purity (>99%).

2.7. Quinazolinone Derivatives

Several of the axially chiral quinazolinone derivatives such as methaqualone,⁸⁰ CP-465022,⁸¹ and benzomalvin A and D⁸² possess interesting biological and medicinal properties. These compounds also possess high rotational energy barriers around 31 kcal·mol⁻¹ making them attractive chiral ligands for asymmetric catalysis.

Virgil and co-workers reported a racemic synthesis and resolution of optically pure atropisomeric quinazolinone **127** (Scheme 41).⁸³ The resolution of racemic **127** was carried out using (–)-(*S*)-**128** (a conventional resolving agent for phosphine ligands), leading to (*S,R*)-**129** in 99% ee. They simplified their approach by employing camphorsulfonic acid for large-scale resolution without compromising the optical purity.

Chenard and co-workers synthesized derivatives of piriqualone **130** and carried out detailed structure–activity relationship (SAR) on the A, B, and C rings of the skeleton (Figure 1). Compound (+)-**131** (CP-465,022) had high affinity binding to

Scheme 41

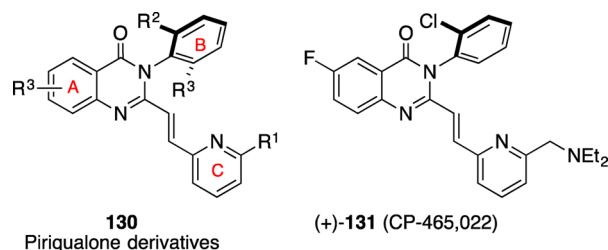
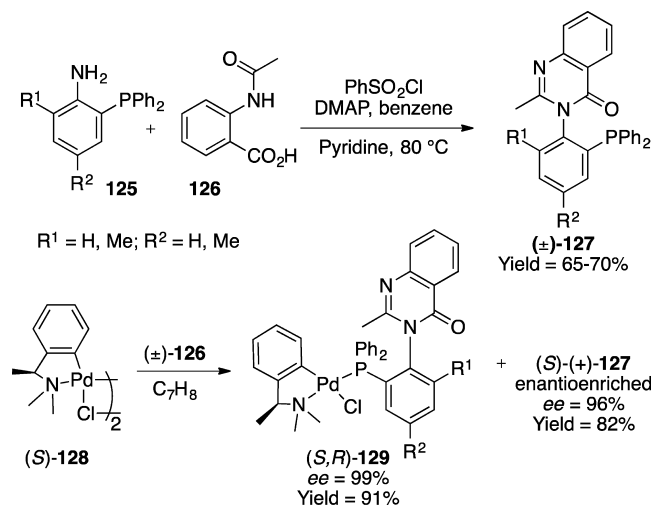


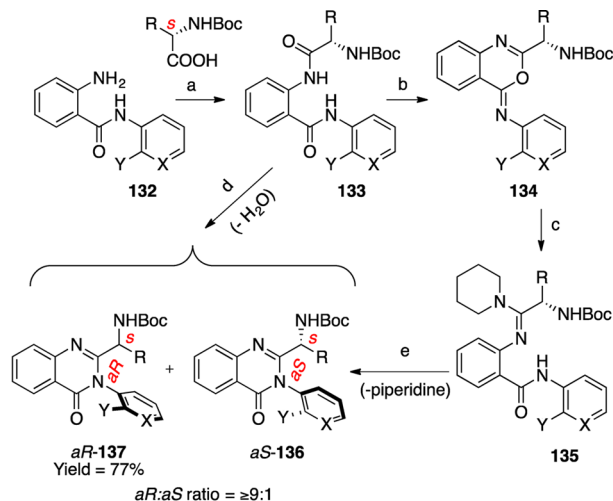
Figure 1.

α -amino-3-hydroxy-5-methyl-4-isoxazolepropionic acid (AMPA) and showed potent anticonvulsant activity.⁸¹ The optical purity had a dramatic effect on the activity of these compounds.

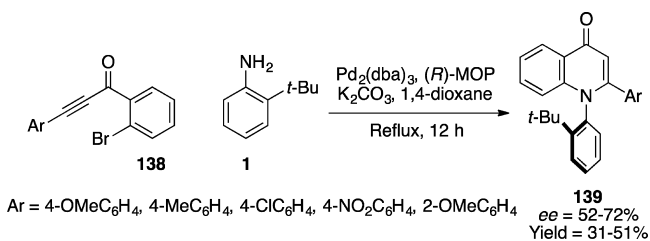
Natsugari and co-workers documented two approaches for diastereoselective synthesis of atropisomeric quinazolinone derivatives **136/137** through dehydrative cyclization of carbamic acid *tert*-butyl ester **133** that features a central chiral amino acid substituent (Scheme 42).⁸⁴ The diastereoselectivity was dependent on the type of substrate and reaction conditions with the best result yielding diastereoselectivity as high as 9:1 (**137**:**136**). Racemization kinetics data revealed that the *aR*-**137** was more stable (31.6 kcal·mol⁻¹) than *aS*-**136** (30.9 kcal·mol⁻¹).

Kitagawa and co-workers reported a catalytic enantioselective synthesis of axially chiral 2-aryl-quinolinones **139** through a tandem amination of **138** by 2-*tert*-butylaniline **1** mediated by (*R*)-MOP-Pd₂(dba)₃ (Scheme 43).⁸⁵ The *t*-Bu group at the *ortho* position was critical for achieving high enantioselectivity in the product. The reaction worked well in most cases, but suffered from several drawbacks. The reaction failed in the case of nonaromatic ethynyl ketones and gave lower yields when

Scheme 42



Scheme 43

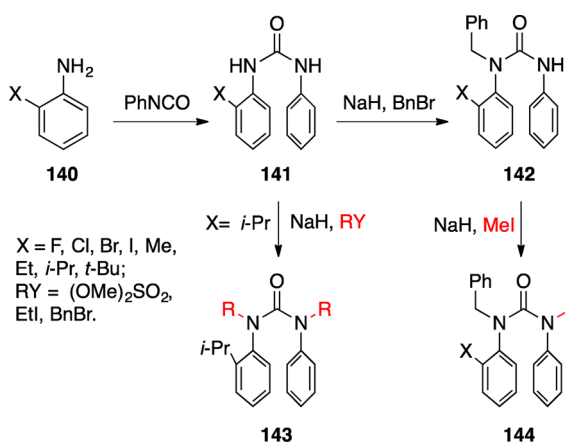


electron-withdrawing groups such as Cl and NO₂ were present on the aryl (Ar) substituent. The reaction required large steric bulk to avoid thermal racemization of the products.

2.8. Ureas

Urea derivatives have been investigated extensively due to their interesting conformational features. Except for NMR analysis, studies to explore rotational barriers were not investigated in detail.⁸⁶ *N,N'*-Diarylureas preferentially exist in a conformation that puts the two aryl rings *cis* to each other. Studies on these motifs were initiated by Clayden and co-workers, who reported several interesting structural features (Scheme 44).⁸⁷ Mono-

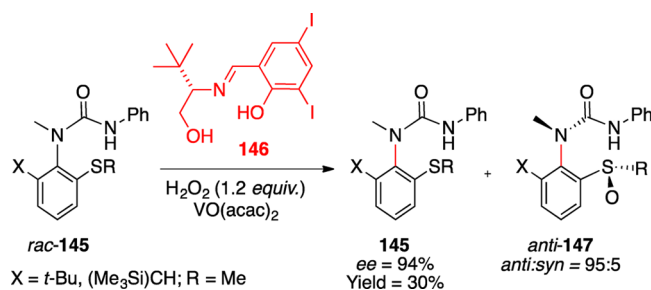
Scheme 44



alkylated ureas **142** have a higher rotational energy barrier over their doubly alkylated counterparts **143** and **144** by approximately 2.4 kcal·mol⁻¹, an effect attributed to decreased ground state strain. Additionally, the size of the X group had little influence on racemization in monoalkylated diaryl ureas. Conformational and stereodynamic studies on *ortho*-disubstituted *N,N'*-diarylurea⁸⁸ revealed that, among multiple *cis* conformations of diarylureas (two phenyl rings *cis* to each other), the one that places the *ortho* substituents *anti* on the N(aryl) ring was preferred. However, if the substituents are bulky, then the *cis* conformation of the phenyl ring collapses where the two aryl rings may settle into an *anti* conformation. These studies provided crucial information on design and development of atropisomeric urea derivatives for synthesis and catalysis.

Clayden and co-workers developed a method to access enantioenriched atropisomeric ureas **145** (Scheme 45) by

Scheme 45



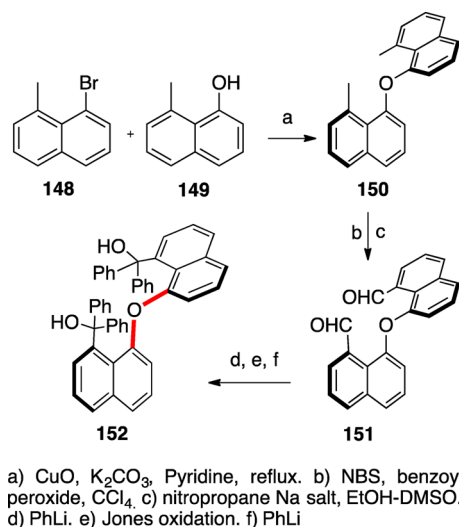
oxidative kinetic resolution using vanadium and (*S*)-*tert*-leucine derived imine ligand **146**.⁸⁹ The resolution also led to sulfoxide **147** with an *anti:syn* ratio of 95:5. The reaction ceased to proceed beyond 50% despite the presence of 1.2 equiv of H₂O₂ oxidant. The recovered **145** was enantioenriched (*ee* = 94%) with a selectivity factor (*s*) as high as 300. Racemization studies on optically pure sulfide **145** (X = *t*-Bu) revealed a racemization energy barrier of 31.6 kcal·mol⁻¹. These sulfides were oxidized to their corresponding sulfinyl derivatives whose thermodynamic conformational selectivities were significantly poorer than those previously reported for *N,N'*-dialkyl-*N,N'*-diarylureas.

2.9. Atropisomers Based on Restricted C–O Bond Rotation

Compounds containing imbedded C–O axial chirality are present in several natural products and interlocked macrocyclic ring systems such as vancomycin.^{90,91} In contrast, molecules featuring isolated C–O chiral axes are less common. Highly substituted biaryl ethers along with several other stringent conditions exhibit atropisomerism. The idea of atropisomerism in biaryl ethers itself was conceived around 1958 by Dahlgard and Brewster.⁹² Spectroscopic and chromatographic observations in the case of small molecules was documented around 1968 by Kessler and others.^{93–95} In 1998, Fuji and co-workers reported the first resolution of atropisomeric biaryl ethers **152** (Scheme 46).⁹⁶ They introduced bulky groups (C(Ph)₂OH) that were necessary in order to obtain diaryl ethers with stable chiral axis. The individual atropisomers were separated by preparative chromatography and also by derivatization techniques such as esterification with optically pure ester followed by resolution.

In 2006, based on extensive analysis of simple diaryl ethers, Clayden and co-workers established empirical rules for biaryl ethers to be atropisomeric.⁹⁷ They synthesized a collection of diaryl ether scaffolds using different synthetic techniques

Scheme 46



including nucleophilic aromatic substitution, metal catalyzed coupling, and directed *ortho* metalation (Figure 2).^{98–101} The

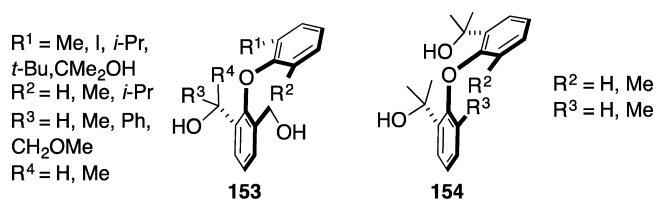
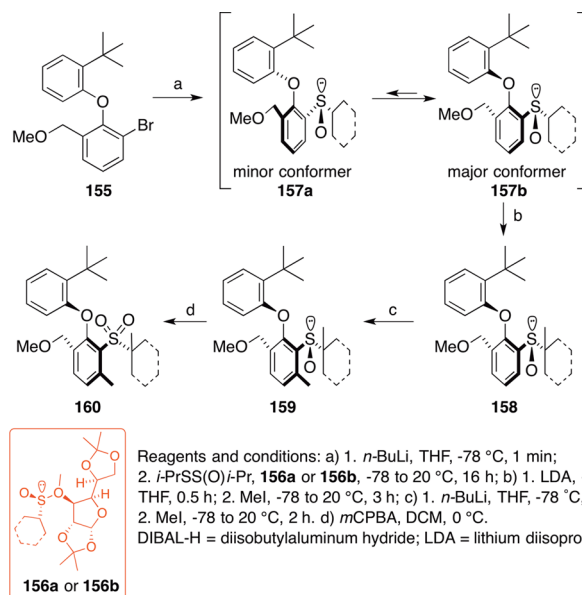


Figure 2. Atropisomers based on restricted C–O bond rotation.

racemization of minimally substituted or less bulky diaryl ethers was followed by variable temperature NMR studies. These studies provided insights into the activation parameters such as the half-life of racemization and activation energy for racemization. Diaryl ethers with *t*-Bu substituents were resistant to racemization on the NMR time scale. These compounds were separated by HPLC on a chiral stationary phase. The racemization kinetics was followed by HPLC analysis at elevated temperatures (40 and 70 °C). Based on kinetic analysis and theoretical calculations (molecular mechanics), the atropisomerism was rationalized to heavily rely on substitution pattern rather than number of substituents. Diaryl ethers will not exhibit atropisomerism if one of the aryl rings is symmetrically substituted (R¹ = R²) due to concerted bond rotation of their stereoisomers.⁹⁷ Also, at least one of the substituents should be as large as *t*-Bu in order for diaryl ethers to exhibit stable atropisomerism. On a similar note, Kan and co-workers reported a new class of atropisomeric biphenanthryl ether with a fluoro substituent scaffold that displayed both axial and helical chirality.¹⁰² The helical structure in the solid state was organized through a series of C–H⋯F hydrogen bonding interactions.

In 2008, Clayden and co-workers reported the first enantioselective synthesis of atropisomeric diaryl ethers (Scheme 47).¹⁰³ The strategy involved the incorporation of a temporary chiral group (sulfoxide) that can influence the adjacent C–O chiral axis after which it was transformed into a bulky group preserving the axial chirality.¹⁰⁴ The authors term this process as dynamic-thermodynamic resolution. While conformational control in the initial sulfinylation was rather poor (157a, 157b), series of further alkylations biased the process toward the

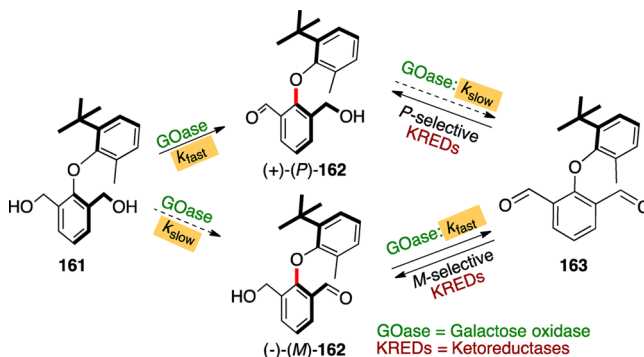
Scheme 47



major conformer (157b) with *dr* up to 98:2. The sulfinyl group was converted to the corresponding sulfone, eliminating the temporary chiral center and turning it to a bulky group that locked the C–O chiral axis.

Clayden, Turner, and co-workers documented a biocatalytic desymmetrization approach to access enantiomerically pure atropisomeric diaryl ethers (Scheme 48).¹⁰⁵ The reaction

Scheme 48



proceeded through enantioselective oxidation of diol 161 by galactose oxidase (GOase), resulting in monoaldehyde (*P*)-162 with 88% ee. Surprisingly, longer reaction times led to an increase in enantiomeric purity in 162 (up to 94% ee). This enantioenrichment was explained by the erosion of enantiomer (*M*)-162 which was converted to achiral dialdehyde 163 (a combination of enantioselective desymmetrization and kinetic resolution process). The kinetic resolution was confirmed by employing racemic 162 in the presence of GOase that resulted in dialdehyde 163 after 24 h with 84% conversion. In addition, analysis of the unreacted 162 revealed an optical purity in excess of 99%. These observations led the authors to hypothesize that the resolution process occurred slower than the desymmetrization step (selectivity factor, *E* = 4). They further extended their studies in which they carried out the asymmetric reduction of dialdehyde 163 to (*P*)-162 using ketoreductases (KREDs) with very high enantiomeric excess (up to 99% ee). The authors

further disclosed access to enantiomerically enriched bi-phosphine ligands that possessed diaryl ether skeletons by lithiation and enantioselective deprotonation techniques of the corresponding diaryl ether scaffolds.^{106,107}

2.10. Atropisomers Based on Restricted C–S Bond Rotation

Studies on C–S axial chirality started at the time when C–O axial chirality was systematically being probed.¹⁰⁸ Highly substituted sulfides, sulfoxides, and sulfones exhibit atropisomerism (Figure 3). However, due to the bulk of the sulfur atom and a longer C–S

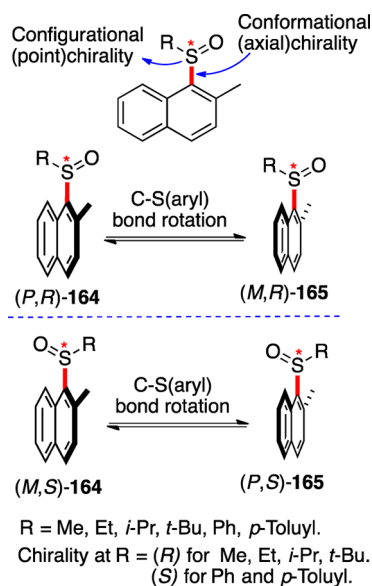


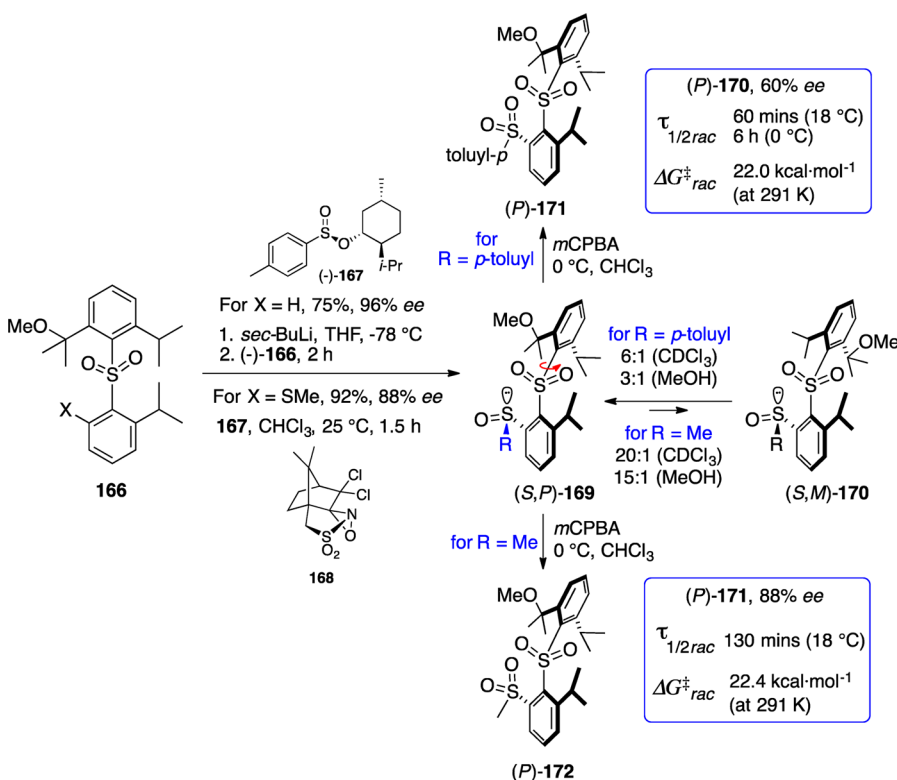
Figure 3. Atropisomers based on restricted C–S bond rotation.

bond length, these molecules tend to have slightly lower energy barriers for rotation than similarly substituted diaryl ethers. Aromatic sulfoxides when placed around bulky substituents display both configurational chirality (at the sulfur atom) and a conformational chirality (restricted bond rotation). The stereodynamics of these compounds, especially 2-naphthylsulfoxides (**164** and **165**), have been explored as early as 1993 by Casarini and others.^{109–111} Chirally enriched compound (at the central chirality *R*) was obtained either by Sharpless asymmetric epoxidation for alkyl substituents or by chiral auxiliary method using Anderson's reaction.¹⁰⁹ While the compounds were not stable atropisomers at ambient conditions, some of the conformers were separated through chiral HPLC at low temperatures (*R* = *t*-Bu was separated at $-35\text{ }^{\circ}\text{C}$) and the barrier to interconversion was established to be 18–19 kcal·mol⁻¹.

Based on ¹H NMR studies, Jennings and co-workers investigated 9-anthryl sulfoxides that do not feature bulky substituents and observed restricted bond rotation around the C–S bond at $-50\text{ }^{\circ}\text{C}$.¹¹² Structural and conformational preferences of C–S atropisomers have been studied in detail by Baker, Mazzanti, and others.^{113–115}

Clayden and co-workers reported the first asymmetric synthesis of diaryl sulfones by dynamic resolution under thermodynamic control (Scheme 49).¹¹⁶ This is a popular strategy to access atropisomeric compounds where an optically pure chiral auxiliary that was installed next to a developing axial chiral center influenced the conformational equilibrium leading to diastereo control in the product.^{117–119} Unlike diaryl ethers, the C–S chirality requires all four *ortho* positions *S*–C_{Aryl} substituent (e.g., **169**) to be substituted with considerable bulk (*t*-Bu and *i*-Pr). Tetrasubstituted sulfides, in which one of the substituents is a sulfinyl chiral auxiliary, led to separable

Scheme 49

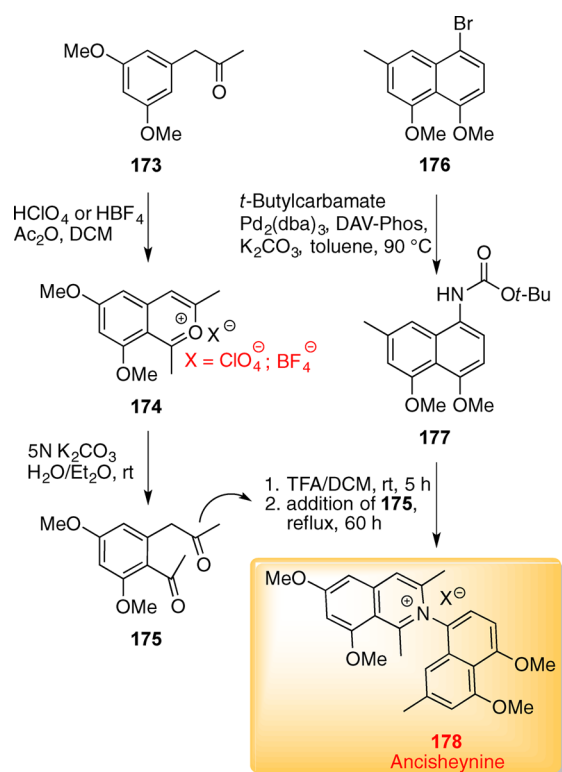


atropisomers that rapidly equilibrated under ambient conditions. On the other hand, tetrasubstituted sulfones **166** were easily synthesized and converted to sulfinyl sulfones **169** (sulfinyl is a point central auxiliary and exerts conformational control) that showed excellent diastereomeric control ($dr > 20:1$ in the case of $R = Me$) depending on the R group ($R = Me, p\text{-toluyl}$). The reason for such high selectivity was attributed to the dipole interaction between sulfoxide sulfur and sulfone oxygen. The sulfinyl chiral auxiliary in **169** was oxidized to bissulfones **171/172** (eliminating central chirality) with moderate enantioselectivity.

2.11. Other Systems

In 2006, Bringmann and co-workers reported the first total synthesis of ancisheynine **178**, an $N\text{-C}_{\text{Aryl}}$ atropisomeric alkaloid (Scheme 50).¹²⁰ The convergent synthesis involved the

Scheme 50



condensation of diketone **175** and naphthalene derivative **177** obtained through Pd catalyzed amination reaction. The counteranion played a critical role in stabilizing ancisheynine (trifluoroacetate counteranion was found to be the best choice). The presence of atropisomerism was established through LC-CD studies that showed opposite Cotton signs for individual atropisomers. This was further confirmed by theoretical calculations involving PM3 methods and CD calculations using the OM2 Hamiltonian.

In 2009, Kawabata and co-workers reported atropisomeric biaryl amine analogues **182** as H-bonding biaryl surrogates (Scheme 51).¹²¹ The amines **182** were obtained through cross-coupling reactions. The important prerequisite for maintaining the axial chirality was the strong intramolecular H-bonding between the N-H-N atoms in an *s-cis* conformation. To increase the strength of the H-bond, strong electron-withdrawing nitro groups were installed on the top pseudo naphthalene ring and steric bulk (Me groups) was introduced on the lower

naphthalene ring to stabilize the chiral axis. The authors hypothesized that the hydrogen of the N-H resides in a chiral microenvironment presenting opportunities to employ these newly synthesized scaffolds as chiral proton donors.

Ávalos and co-workers published a series of papers on the synthesis and structural characteristics of carbohydrate ($\alpha\text{-D}$ -glucofurano derivatives) derived atropisomeric imidazolidine-2-ones **183** and imidazolidine-2-thione **184** derivatives (Figure 4).^{122–124} The individual atropisomers were isolated (**184**, $\text{X} = \text{O}$; $\text{R}^1 = \text{NO}_2$) as acetylated derivatives and the absolute configurations were determined by single crystal X-ray analysis. The examination revealed that the compound exists as a *P*-atropisomer exclusively. Dynamic NMR studies along with theoretical calculation revealed that these compounds possessed a barrier of rotation in the vicinity of $20\text{--}22\text{ kcal}\cdot\text{mol}^{-1}$.

3. PHYSICAL CHARACTERISTICS

Unlike point chiral molecules (atoms connected to different substituents/configurational isomers), the element of chirality in atropisomers is instilled in a rotational axis (typically anchored by a pivotal bond). For a large number of atropisomers the interconversion of one isomer to the other by simple bond rotation (other mechanisms of isomerization also exist that include bond breaking) is a plausible process. The energy required for such rotation is influenced by the steric hindrance, electronics, solvents, and temperature. In addition to the slow rotation of the stereogenic axis in atropisomers, restricted bond rotations impart dynamic features in these systems leading to chiral rotamers (e.g., *E/Z* rotamers in an atropisomeric anilide). In recent years, these dynamic aspects have become quite important for contemporary investigations. Detailed understanding of the conformational and configurational stability as well as dynamics offer insights for designing molecular architectures for various applications such as nanomachines, nanomotors, molecular clefts, catalysis, and resolving agents, to name a few. The stability of atropisomeric molecules is often evaluated by kinetics measurements (enantiomerization/racemization) that include various physical terms such as rate, half-life, and activation energy for the isomerization processes. Due to the importance of conformational/configurational isomers and their role in pharmacokinetics and drug administration, several books and articles have been published that extensively cover aspects such as dynamics, kinetics, etc.^{125–128} Wolf has detailed the treatment of physical processes in his book, and readers are strongly encouraged to refer to it for an in-depth analysis.¹²⁹ This review will provide a basic introduction to these terms and highlight some of the mechanistic details of the isomerization processes in atropisomeric compounds.

Some of the terms that are often used in the isomerization kinetics of these stereochemically labile compounds include “racemization”, “enantiomerization”, “diastereomerization”, and “epimerization”. Sometimes these terminologies have been used interchangeably, so it becomes imperative to understand their differences. Racemization is a macroscopic phenomenon where a nonracemic mixture (optically active) undergoes irreversible transformation to a racemic mixture (not optically active).¹²⁷ This statistical process can also be extended to nonracemic compounds such as interconversion of diastereomers (diastereomerization). Racemization is a process that describes the conversion of 50% of an enantiopure compound to its corresponding enantiomer (where the process is complete) and the corresponding half-life ($\tau_{1/2}$) of the racemization process is the time required for the reduction of optical purity to 50% of

Scheme 51

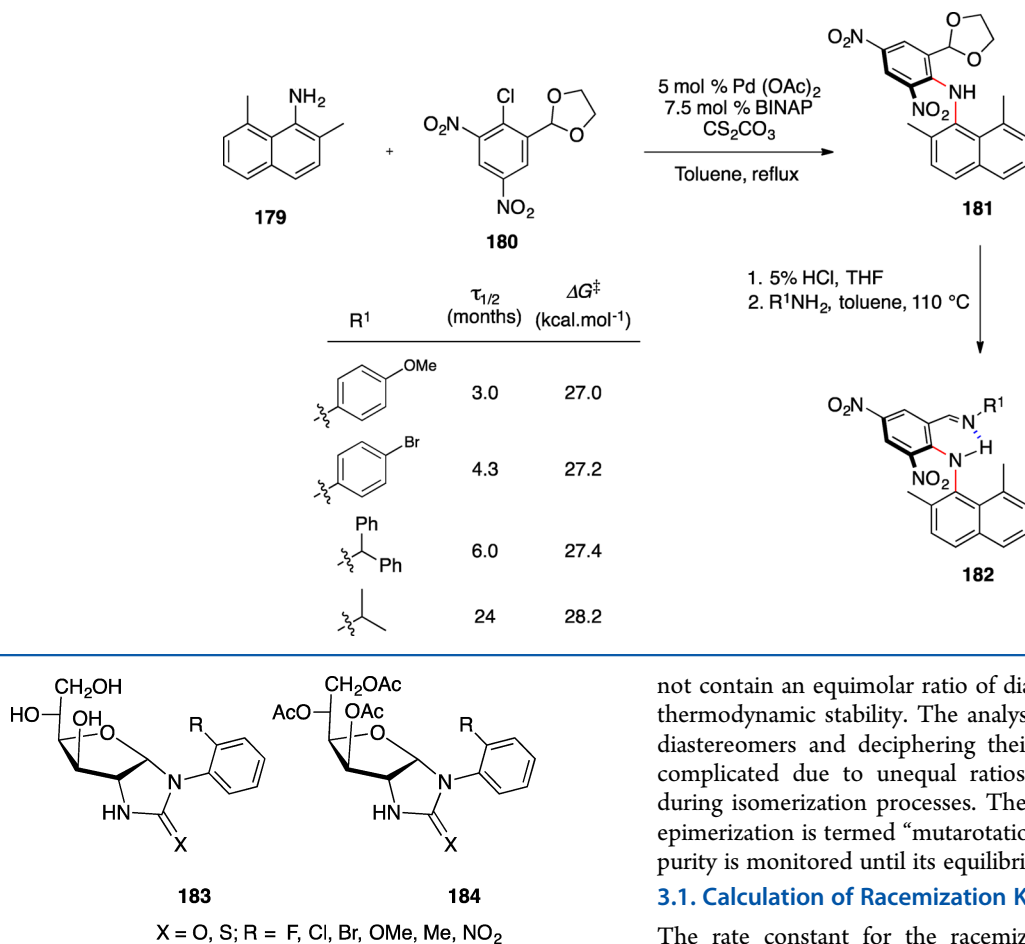
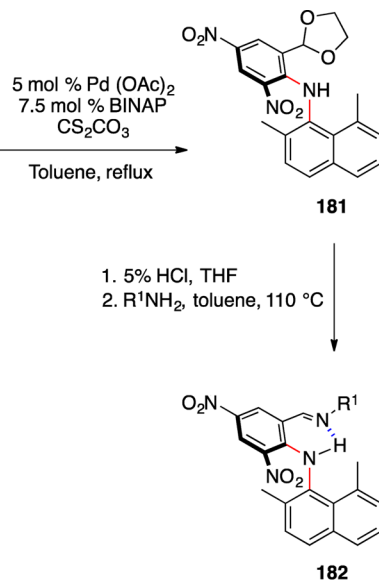


Figure 4. Carbohydrate derived atropisomeric imidazolidine-2-one and imidazolidine-2-thione.

its initial value. In the absence of external chiral influence, the rate of racemization for a pair of enantiomers is the same (as the activation energy for racemization is identical for a given pair of enantiomers) and can be monitored by several analytical techniques such as chiral chromatography, circular dichroism spectroscopy, and optical rotation measurements.

Enantiomerization is a microscopic process that is considered reversible and treats the process at a molecular level.¹³⁰ On the other hand, racemization is a macroscopic process that is considered irreversible. The rate constants for the two processes are related by the equation $k_{\text{rac}} = 2k_{\text{enant}}$, where k_{enant} is the rate constant for enantiomerization and k_{rac} is the rate constant for racemization. The corresponding half-life of enantiomerization represents the time required for the 50% interconversion of an enantiopure compound (going from 100% ee to 0% ee). On the other hand, the half-life of racemization represents the time required for conversion of an enantiopure compound to 50% enantiomeric excess.

Diastereomerization and epimerization are observed in molecules having more than one stereogenic center (can be a combination of configurational and conformational chirality) that features a dynamic functionality that can be influenced by an external perturbation (e.g., temperature). Diastereomerization and epimerization can often be followed by NMR techniques if the diastereomers/epimers involved have distinct resonances for a given functionality. Mostly, thermodynamic equilibrium does



not contain an equimolar ratio of diastereomers reflecting their thermodynamic stability. The analysis of kinetic parameters of diastereomers and deciphering their rate constants are often complicated due to unequal ratios of stereoisomers present during isomerization processes. The macroscopic treatment of epimerization is termed “mutarotation”, in which loss of optical purity is monitored until its equilibrium is reached.

3.1. Calculation of Racemization Kinetics

The rate constant for the racemization for a given pair of enantiomers can be calculated from monitoring the change in optical purity over time (through HPLC analysis, circular dichroism, or optical rotation) using the following Eyring equations:¹²⁹

$$k_{\text{rac}} = \kappa \left(\frac{k_{\text{B}} T}{h} \right) e^{-\Delta G_{\text{rac}}^{\ddagger} / RT} \quad (1)$$

$$\Delta G_{\text{rac}}^{\ddagger} = -RT \ln \left(\frac{h k_{\text{rac}}}{\kappa T k_{\text{B}}} \right) \quad (2)$$

where k_{rac} = racemization rate constant, $\Delta G_{\text{rac}}^{\ddagger}$ = energy barrier for racemization, T = temperature, R = gas constant, h = Planck constant, k_{B} = Boltzmann constant, and κ = kappa, transmission coefficient (which is usually unity for this calculation).

The half-life of racemization, $\tau_{1/2}$, can be calculated using the rate constant of racemization k_{rac} (assuming $S_0 = 0$ at $t = 0$).¹²⁹

$$\ln \left(\frac{x_{\text{eq}}}{x_{\text{eq}} - x} \right) = \ln \left(\frac{R_0}{2R - R_0} \right) = \ln \left(\frac{R + S}{R - S} \right) = 2k_{\text{enant}} t \quad (3)$$

$$\ln \left(\frac{R_0}{R_0 - x} \right) = k_{\text{rac}} t \quad (4)$$

where $k_{\text{rac}} = 2k_{\text{enant}}$, R_0 = initial concentration of (*R*)-enantiomer, and $x = R_0 - R, S$ (concentration of the racemate at time t). Note that $R_0 = R + S$.

At 50% ee, the equation becomes

Table 1. Half-Life ($\tau_{1/2}$), Racemization Rate Constant (k_{rac}), and Energy Barrier (ΔG_{rac}^\ddagger) to Racemization for Nonbiaryl Atropisomeric Compounds^a

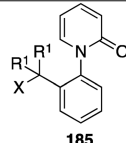
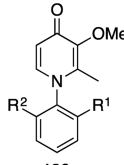
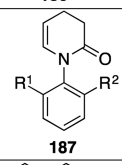
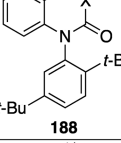
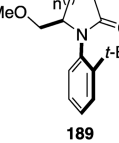
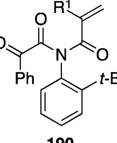
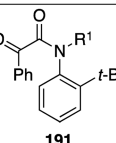
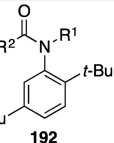
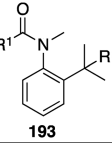
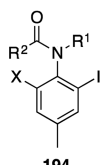
Ent.	Compound	Substituents	Solvent	<i>t</i> (°C)	Physical parameters			Ref
					k_{rac} (s ⁻¹)	$\tau_{1/2}$ (days)	ΔG_{rac}^\ddagger (kcal/mol)	
1		R ¹ , X = Me R ¹ = Me; X = OH R ¹ = Ph; X = OH	MeOH	65	3.4×10 ⁻⁷ 6.8×10 ⁻⁵ 7.1×10 ⁻⁴	24 2.8 ^b 0.3 ^b	29.9 26.3 24.7	133
2		R ¹ = Cl; R ² = H R ¹ = Me; R ² = H R ¹ = CN; R ² = H R ¹ = OMe; R ² = H R ¹ = Cl; R ² = Me	Diglyme Diglyme EtOH/H ₂ O Diglyme Diglyme	66 72 25 25 157	1.1×10 ⁻⁶ 1.0×10 ⁻⁶ 3.6×10 ⁻⁷ 6.1×10 ⁻⁷ 2.1×10 ⁻⁷	64 ^c 58 ^c 21 ^c 35 ^c > 12 ^c	26.2 26.6 22.3 22.6 >32.0	134
3		R ¹ = Me; R ² = allyl R ¹ = <i>t</i> -Bu; R ² = H	IPA CHCl ₃	75 60	8.2×10 ⁻⁷ -	9.8 21 ^h	30.2 26.9	135 136
4		X = CH ₂ X = NH	Toluene Toluene	110 110	- -	4.1 4.3 ^b	33.1 30.7	137
5		n = 1 n = 2	-	27	- -	14 ^b 602	- 28.3	75
6		R ¹ = Me R ¹ = Et	MeCN	50	1.3×10 ⁻⁶ 2.3×10 ⁻⁶	6.4 3.5	27.7 27.3	138
7		R ¹ = Me R ¹ = Cyclohexyl	IPA Oct./IPA	75 110	4.9×10 ⁻⁷ 9.8×10 ⁻⁶	8.2 0.4	30.5 31.3	139
8		R ¹ = Me; R ² = ^E MeCH=CH R ¹ = C ₃ H ₁₁ ; R ² = ^E MeCH=CH R ¹ = Me; R ² = C ₂ H ₅ R ¹ = C ₂ H ₅ ; R ² = 4-NO ₂ Ph	2-butanol Toluene	106 80	- - -	35 ^c 60 ^c 83 ^c 55 ^b	28.9 29.3 29.6 29.4	140 30
9		R ¹ = OTMS; R ² = ^E PhCH=CH R ¹ = OTIPS; R ² = ^E PhCH=CH	2-butanol 2-butanol	23 23	- -	42 ^b 141 ^b	25.4 26.1	140
10		R ¹ = Me; R ² = CH=CH, X = Me R ¹ = -CH=CH-CMe ₂ ; R ² = <i>p</i> -Br-Ph; X = Me R ¹ = allyl; R ² = Ph; X = Me R ¹ = allyl; R ² = C ₂ H ₄ -Ph; X = Me R ¹ = CHMePh; R ² = CH=CH ₂ ; X = H R ¹ = Me; R ² = CMe=CMeH; X = Me	IPA/hex. IPA/hex. Hex Hex	110 140 23 25	2.0×10 ⁻⁵ - - - 4.3×10 ⁻⁷	- - - - 4.7 ^b	30.8 29.7 30.7 32.7 22.6 26.0	141 142 143 144

Table 1. continued

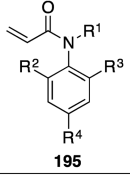
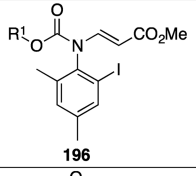
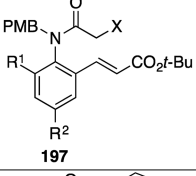
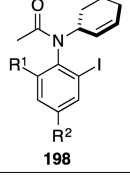
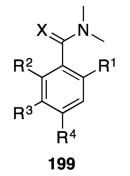
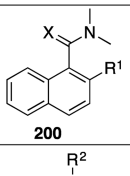
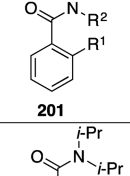
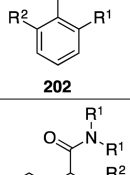
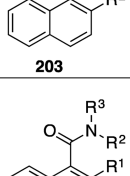
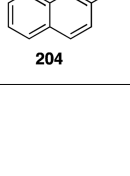
Ent.	Compound	Substituents	Solvent	<i>t</i> (°C)	Physical parameters			Ref
					<i>k</i> _{rac} (s ⁻¹)	$\tau_{1/2}$ (days)	$\Delta G^{\ddagger}_{rac}$ (kcal/mol)	
11		R ¹ = Me; R ² = I; R ³ = TMS, R ⁴ = H R ¹ = Me; R ² = I; R ³ = TMS, R ⁴ = H R ¹ = allyl; R ² = <i>t</i> -Bu; R ³ , R ⁴ = H	Hex -	100	-	-	30.8	145
				80	-	33 ^b	28.2 -	20
12		R ¹ = allyl R ¹ = <i>t</i> -Bu R ¹ = CH ₂ Ph	IPA/hex.	115	4.8×10 ⁻⁶ 6.2×10 ⁻⁶ 6.1×10 ⁻⁶	1.7 1.3 1.4	32.4 32.2 32.1	146
13		X = I; R ¹ = Me; R ² = Me X = I; R ¹ = Br; R ² = Me X = I; R ¹ = OMe; R ² = H	IPA/hex.	140	5.7×10 ⁻⁶	1.4	34.3	147
			IPA/hex.	143	9.8×10 ⁻⁶	0.8	34.2	
			IPA/hex.	55	2.1×10 ⁻⁵	0.4	26.3	
14		R ¹ = H, R ² = H R ¹ = Me, R ² = Me	EA/Hex	36	5.2×10 ⁻⁴	0.4 ^b	22.8	148
			EA/Hex	153	3.1×10 ⁻⁶	2.6	36.0	
15		R ¹ = <i>t</i> -Bu; R ² , R ³ , R ⁴ = H; X = O R ¹ = <i>t</i> -Bu; R ² , R ³ , R ⁴ = H; X = S R ¹ , R ² = OMe; R ³ = Br; R ⁴ = H; X = O R ¹ , R ² = OMe; R ³ = Br; R ⁴ = H; X = S R ¹ , R ² , R ³ , R ⁴ = Me; X = O R ¹ , R ² , R ³ , R ⁴ = Me; X = S	EtOH	13	-	-	20.8	149
			Diglyme	90	-	-	30.2	
			Dioxane	31	-	-	22.6	
			Diglyme	90	-	-	29.9	
			Dioxane	61	-	-	24.8	
			Diglyme	159	-	-	32.9	
16		R ¹ = Me; X = O R ¹ = Me; X = S	Dioxane	55	-	-	24.0	149
			Diglyme	159	-	-	33.2	
17		R ¹ , R ² = Et R ¹ = <i>i</i> -Pr, R ² = Et R ¹ = CHO; R ² = <i>i</i> -Pr	DMSO	35 ^e	-	0.002 ^d	14.2	150
			-	-	-	0.02 ^d	15.6	
			CDCl ₃	-10 ^e	36	5×10 ^{-4,d}	13.5	
18		R ¹ = CMe ₂ OH; R ² = Et R ¹ = Me; R ² = Et R ¹ = Ph ₂ PO; R ² = Et R ¹ = Ph ₂ P; R ² = Et R ¹ = OMe; R ² = -CH=CH ₂	Dioxane	93	1.0×10 ⁻⁵	30 ^{g,i}	29.9	151
			Dioxane	50	2.8×10 ⁻⁵	10 ^g	25.7	50
			Dioxane	50	7.7×10 ⁻⁵	3 ^g	25.0	
			Dioxane	55	1.9×10 ⁻⁴	2 ^g	24.9	
			Et ₂ O	4	1.1×10 ⁻⁶	7.5	23.8	
19		R ¹ = Et; R ² = H R ¹ = <i>i</i> -Pr; R ² = H R ¹ = CH ₂ Ph; R ² = H	DMSO	36 ^e	140	0.01	15.1 ^f	150
			DMSO	73 ^e	35	1	17.9 ^f	
			MeOH	40 ^e	64	0.03	15.8 ^f	
20		R ¹ = Et; R ² , R ³ = <i>i</i> -Pr R ¹ = Me; R ² , R ³ = <i>i</i> -Pr R ¹ = OMe; R ² , R ³ = <i>i</i> -Pr R ¹ = SiMe ₃ ; R ² , R ³ = <i>i</i> -Pr R ¹ = Me; R ² , R ³ = Me R ¹ = OEt; R ² , R ³ = (CH ₂) ₅ R ¹ = Me; R ² , R ³ = Cyclohexyl R ¹ = CH=CH ^L CO ₂ Et; R ^{2,3} = <i>i</i> -Pr	EtOH/Hex	47	4.4×10 ⁻⁵	86 ^{b,f}	25.1	150
			IPA/Hex	44	3.5×10 ⁻⁵	75 ^{b,f}	25.0	
			EtOH/Hex	48	2.0×10 ⁻⁴	19 ^{b,f}	24.3	
			-	-	-	< 0.2 ^{b,f}	< 21.5	
			IPA/Hex	25	-	30 ^{b,f}	24.5	
			IPA/Hex	45	-	0.7 ^{b,f}	22.3	
			EtOH/Hex	42	1.5×10 ⁻⁴	12 ^{b,f}	24.0	
			Et ₂ O	25	1.6×10 ⁻⁵	12 ^b	24.0	

Table 1. continued

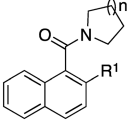
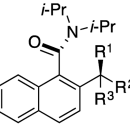
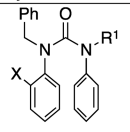
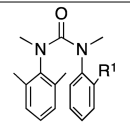
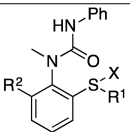
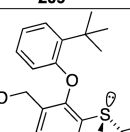
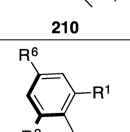
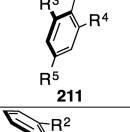
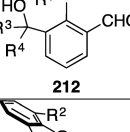
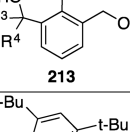
Ent.	Compound	Substituents	Solvent	<i>t</i> (°C)	Physical parameters			Ref
					<i>k_{rac}</i> (s ⁻¹)	$\tau_{1/2}$ (days)	ΔG_{rac}^\ddagger (kcal/mol)	
21		R ¹ = OMe; n = 2 R ¹ = OMe; n = 1 R ¹ = <i>n</i> -Bu; n = 1 R ¹ = <i>t</i> -Bu; n = 2	THF THF <i>n</i> -nonane <i>n</i> -nonane	15	1.6 × 10 ⁻⁴	11.8 ^{c,j}	21.2	152
				15	3.6 × 10 ⁻⁴	16.2 ^c	21.2	153
				40	-	93 ^c	24.4	
				100	-	53 ^c	28.8	
22 ^g		R ¹ = OH; R ² = Me; R ³ = H R ¹ = Me; R ² = SiMe ₃ ; R ³ = H R ¹ = OH; R ² = Et; R ³ = Me	Dioxane EtOH/Hex Dioxane	62	1.4 × 10 ⁻⁴	15.8 ^f	25.9	150
				45	4.5 × 10 ⁻⁵	5.8 ^f	25.0	
				55	<1.0 × 10 ⁻⁶	>4.6 ^{f,j}	>28.7	
23 ^l		R ¹ = H; X = I R ¹ = H; X = Me R ¹ = H; X = <i>t</i> -Bu R ¹ = Me; X = I R ¹ = Me; X = <i>t</i> -Bu	DMSO	- ^c	-	-	16.2	87
				-	-	-	15.4	
				-	-	-	16.7	
				-	-	-	13.6	
				-	-	-	19.1	
24		R ¹ = I R ¹ = <i>t</i> -Bu R ¹ = OCF ₃	Toluene Toluene Toluene	15 ^e	-	0.02 ^{d,g}	15	88
				110 ^e	-	>5.8 ^{d,g}	>20.1	
				-90 ^e	-	6 × 10 ⁻⁴ ^{d,g}	9.4	
25		R ¹ = Me; R ² = <i>i</i> -Pr, X = O R ¹ = Me; R ² = <i>t</i> -Bu, X = - R ¹ = Me; R ² = CH(SiMe ₃) ₂ ; X = -	Toluene Toluene Toluene	65	-	-	27.2 ^g	89
				110	-	500 ^{h,i}	31.5	
				110	-	56	26.8	
26		R ¹ , R ² = Me R ¹ , R ² = (CH ₂) ₅	DCM/Hex DCM/Hex	40	-	5.6	27.2	103
				40	-	10.8	26.7	
27		R ¹ , R ⁴ = PPh ₂ ; R ² , R ³ = Me; R ⁵ , R ⁶ = Me R ¹ = Me; R ² = <i>t</i> -Bu; R ³ = CH ₂ OH; R ⁴ = CHO; R ⁵ , R ⁶ = H	Hex/IPA Heptane	63	-	84 ^h	27.0	106
				90	1.6 × 10 ⁻⁶	5	>31.1	105
28		R ¹ = <i>t</i> -Bu; R ² = H; R ³ , R ⁴ = Me R ¹ = <i>i</i> -Pr; R ² = H; R ³ , R ⁴ = Me R ¹ = <i>t</i> -Bu; R ² ; R ³ = Me; R ⁴ = H	DMSO	25	-	>2 ^{b,e,h} 3 ^{d,e,h} 6 × 10 ^{3,i}	23.2 18.8 -	97
				-	-	-	-	
				-	-	-	-	
29		R ¹ = <i>t</i> -Bu; R ² = H; R ³ , R ⁴ = Me R ¹ = CMe ₂ OH; R ² , R ⁴ = H; R ³ = Me	IPA/Hex DMSO	70	-	50 ^h	27.1	97
				25	-	>0.8 ^h	25.1	
30		R ¹ = R ² = - R ¹ = O; R ² = - R ¹ , R ² = O	IPA/Hex IPA/Hex IPA/Hex	40	-	14 ^{b,h}	24.1	116
				17	-	70 ^{d,h}	20.6	
				50	-	6 ^h	25.5	

Table 1. continued

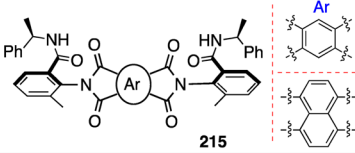
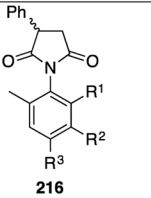
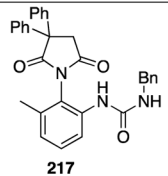
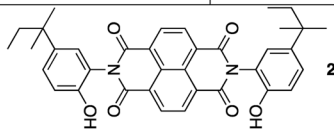
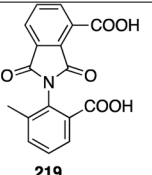
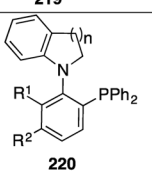
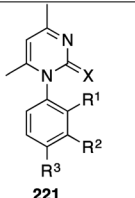
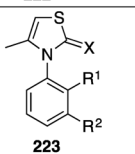
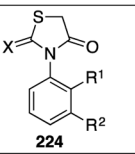
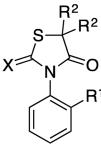
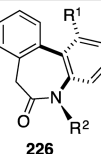
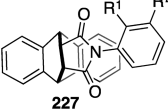
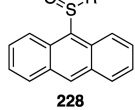
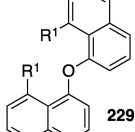
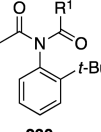
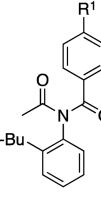
Ent.	Compound	Substituents	Solvent	<i>t</i> (°C)	Physical parameters			Ref
					<i>k</i> _{rac} (s ⁻¹)	$\tau_{1/2}$ (days)	$\Delta G^{\ddagger}_{rac}$ (kcal/mol)	
31		Ar		77	-	35 ^b	29.4	154
				152	-	4.1 ^b	34.0	
32		R ¹ = COOH; R ² = H; R ³ = H R ¹ , R ² =  ; R ³ = H R ¹ = PPh ₂ ; R ² = H; R ³ = Me	-	60	-	1.7	28.0	59
			- Toluene	106 110	-	-	7.9 >40.0	60
33		-	Xylene	130	9.9 × 10 ⁻⁵	-	31.7	155
34		-	DMSO	25	1.0 × 10 ⁻⁵	-	25.2	156
35		-	Neat	100	6.5 × 10 ⁻⁵	14 ^{h,i}	29.6	157
36		R ¹ , R ² = -C ₄ H ₉ -; n = 1 R ¹ = OMe; R ² = H; n = 1 R ¹ = Me; R ² = H; n = 1	Toluene	25	3.9 × 10 ⁻⁸ 6.8 × 10 ⁻⁶ 8.6 × 10 ⁻⁹	102 0.6 467	27.6 24.5 28.5	158
37		R ¹ = Me; R ² , R ³ = H; X = O R ¹ = Me; R ² = H; R ³ = Cl; X = O R ¹ , R ³ = Cl; R ² = H; X = O R ¹ , R ² = -(C ₂ H ₄)-; X = O R ¹ , R ² = -(C ₂ H ₄)-; X = S	Xylene	90 ^j	-	46 ^c	27.9	78,159
			Xylene	90	-	31 ^c	27.6	
			Xylene	50	-	24 ^c 27 ^c 4 ^c	27.4 27.5 23.1	
38		aR to aS epimerization	- ^g	- ^g	-	-	31.6	84
39		R ¹ = Me; R ² = H; X = S R ¹ = Me; R ² = H; X = O R ¹ = Cl; R ² = H; X = O R ¹ , R ² = Me; X = O R ¹ = Me; R ² = Cl; X = O	Diglyme	100	-	-	>32.0	161
			Diglyme	86	-	-	29.2	
			Diglyme	87	-	-	30.3	
			Diglyme	87	-	-	31.3	
			Diglyme	87	-	-	30.7	
40		R ¹ , R ⁴ = -(C ₂ H ₄)-; X = O R ¹ , R ⁴ = -(C ₂ H ₄)-; X = S R ¹ = Me; R ² = H; X = S	EtOH/Hex	50	5.0 × 10 ⁻⁵	-	25.3	162
			EtOH/Hex	78	2.0 × 10 ⁻⁴	-	26.6	163
			EtOH,	-	-	-	26.1	

Table 1. continued

Ent.	Compound	Substituents	Solvent	<i>t</i> (°C)	Physical parameters			Ref
					<i>k</i> _{rac} (s ⁻¹)	τ _{1/2} (days)	Δ <i>G</i> [‡] _{rac} (kcal/mol)	
41		R ¹ = Cl; R ² = Me; X = O	EtOH EtOH EtOH Toluene Toluene	70	5.0×10 ⁻⁵	-	26.9	164
		R ¹ = F; R ² = Me; X = S		7	1.0×10 ⁻⁴	-	21.5	
		R ¹ = Cl; R ² = Me; X = S		75	2.5×10 ⁻⁵	-	27.8	
		R ¹ = I; R ² = Me; X = S		105	3.0×10 ⁻⁵	-	30.6	
		R ¹ = I; R ² = H; X = S		110	2.0×10 ⁻⁵	-	30.8	
42		R ¹ , R ² = Me	Toluene Toluene DMF	110	-	-	29.3	165
		R ¹ = H; R ² = Me		37	-	-	23.4	
		R ¹ = H; R ² = <i>i</i> -Pr		150	-	-	32.7	
43		R ¹ = Me; R ² = H	NO ₂ -benzene	-	-	-	20.6 ^e	166
		R ¹ = OMe; R ² = H		-	-	-	19.6 ^e	
		R ¹ = Me; R ² = Cl		-	-	-	23.2 ^e	
44		R ¹ = Me	CD ₂ Cl ₂ CD ₂ Cl ₂ CD ₂ Cl ₂ TCE	-35 ^e	5.2×10 ²	-	10.9	112
		R ¹ = CH ₂ Ph		15 ^e	2.6×10 ²	-	13.7	
		R ¹ = <i>i</i> -Pr		28 ^e	4.8×10 ²	-	14.0	
		R ¹ = <i>t</i> -Bu		98 ^e	61	-	18.9	
45		R ¹ = C(Ph) ₂ OH	Toluene	111	-	3.8 ^b	30.2	96
46		R ¹ = <i>t</i> -Bu	Benzene Benzene Benzene Benzene	25	-	< 30 ^e	-	167,168
		R ¹ = <i>i</i> -Pr		40	1.2×10 ⁻⁶	-	26.8	
		R ¹ = Et		49	3.1×10 ⁻⁷	-	28.5	
		R ¹ = Ph		40	2.7×10 ⁻⁶	-	26.3	
47		R ¹ = NMe ₂	Benzene	40	9.1×10 ⁻⁶	-	25.4 ^k	169
		R ¹ = OMe			4.3×10 ⁻⁶	-	25.9 ^k	
		R ¹ = Me			2.9×10 ⁻⁶	-	26.2 ^k	
		R ¹ = H			2.7×10 ⁻⁶	-	26.2 ^k	
		R ¹ = F			2.2×10 ⁻⁶	-	26.3 ^k	
		R ¹ = Cl			1.8×10 ⁻⁶	-	26.6 ^k	
R ¹ = CF ₃	1.3×10 ⁻⁶	-	26.8 ^k					
48		R ¹ = Me; R ² = <i>p</i> -OMe-Ph	Benzene	80	-	2.4	24.9 ^l	121
		R ¹ = NO ₂ ; R ² = <i>p</i> -OMe-Ph			-	130 ^l	27.2	
		R ¹ = NO ₂ ; R ² = CHPh ₂			-	180 ^l	27.4	
		R ¹ = NO ₂ ; R ² = <i>i</i> -Pr			-	365 ^l	28.2	

^a*k*_{rac} (s⁻¹); τ_{1/2} (days); Δ*G*[‡]_{rac} (kcal·mol⁻¹). ^bτ_{1/2} in hours. ^cτ_{1/2} in minutes. ^dτ_{1/2} in seconds. ^eResults from VT-NMR. ^fτ_{1/2} reported for 20 °C. ^gEpimerization of atropisomers. ^hτ_{1/2} reported for 25 °C. ⁱτ_{1/2} in years. ^jBarrier to enantiomerization. ^kΔ*G*[‡]_{rac} at 27 °C. ^lΔ*G*[‡]_{rac} at 22 °C; TCE, deuterio-1,1,2,2-tetrachloroethane. Oct., octanol.

$$\tau_{1/2\text{rac}} = \frac{\ln 2}{2k_{\text{enat}}} \quad \text{or} \quad \frac{\ln 2}{k_{\text{rac}}} \quad (5)$$

The course of racemization or isomerization can be followed by various spectroscopic and analytical techniques. Depending on the time regime of the physical processes, one can choose the right tool. For example, ultrafast processes can be followed by flash photolysis, electron spin resonance spectroscopy (EPR), or nuclear magnetic resonance spectroscopy (NMR). Molecules whose energy barriers for isomerization are low (typically in the range 5–24 kcal·mol⁻¹) could be followed through variable

temperature NMR studies (VT-NMR). On the other hand, if the racemization barrier is greater than 24 kcal·mol⁻¹, then the individual isomers can be isolated and the isomerization processes can be followed through analytical techniques such as chiral chromatography and optical monitoring methods such as circular dichroism, optical rotatory dispersion, and polarimetry. Detailed experimental studies and concepts on these topics have already been discussed in various reports.^{125,126,128,131,132} Table 1 provides the physical parameters of the racemization for some of the commonly occurring atropisomeric scaffolds. It should be noted that some of the

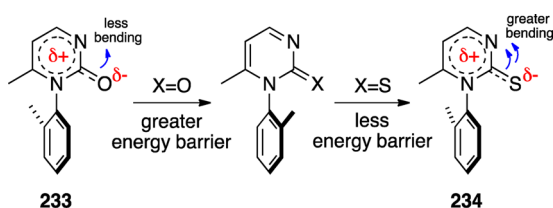
compounds listed in Table 1 are not atropisomeric, as they do not have high energy barriers to separation. However, these values are based on VT-NMR studies (refer to footnotes of Table 1) and are provided as additional information on these systems.

3.2. Various Mechanisms of Racemization

The major pathway for the racemization of axially chiral molecules is through the rotation of the chiral axis that is governed by several factors such as steric hindrance around the chiral axis, substituents, electronic factors, solvent, and temperature. However, other mechanisms were also proposed to substantiate the observed racemization process in atropisomeric systems. Mechanistic investigation on the racemization process of atropisomeric pyrimidine-2-thione **233** and thiazoline-2-thione **234** derivatives serves as an exemplar where more than one mechanism was put forward.

One of the important features that dictate the racemization barrier is the nature of the heteroatom that participates in the restricted bond rotations (vide infra). Depending on the type of C–X heteroatom involved (X = N, O or X = S, Si, P), the steric compression that is related to the bond length comes into prominence and impacts the barrier. One such example is atropisomeric pyrimidinethiones that are known to have lower racemization energy barriers compared to their oxygen analogues, pyrimidinones.¹⁶⁰ However, this seems contrary due to the nature of C=O and C=S bonds. The usual bond length of C=O is 1.22 Å, while the C=S bond length is 1.71 Å. Similarly, the van der Waals radius for oxygen is 1.52 Å and that of sulfur is 1.85 Å.¹⁵⁹ Several hypotheses were put forward to substantiate the observed lower energy barrier. Kashima and co-workers proposed a bending mechanism for the racemization process (Scheme 52). The C=S bond has more single bond

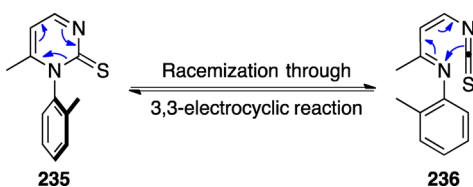
Scheme 52



character¹³¹ that allows the functionality to bend resulting in decreased repulsive interaction (decreased activation energy barrier toward racemization) between the sulfur atom and the *ortho* substituent of the aryl ring.

An alternative explanation was proposed by Roussel and co-workers, who invoked breaking and forming of the N–C=S bond through 3,3-electrocyclic reaction (Scheme 53).¹⁶¹ Support for such a process came from the insensitivity of the energy barrier to the bulk of the substituent at the *ortho* position (*o*-Me and *o*-Et had similar energy barriers). A recent mechanism for the racemization process in pyridinones **237** was proposed by

Scheme 53



Schirok and co-workers that involves the deformation of pyridinone ring (Scheme 54).¹⁷⁰ Experimental and computational analysis allowed them to propose that in the transition state the pyridinone loses its planarity significantly causing the phenyl ring to bend out of the plane accompanied by the coplanarity of the 1,3-amino carbonyl group in the opposite direction. Such a geared twisting reduces the energy barrier of N–C_{Aryl} bond rotation resulting in the facile racemization.

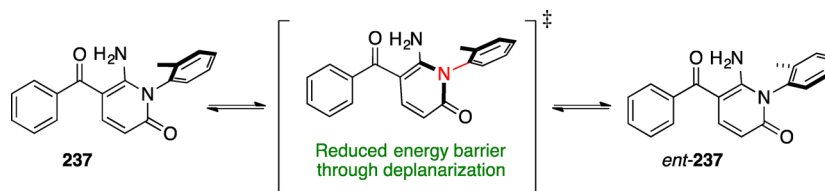
Clayden and co-workers carried out a comparative study between sulfide **238**, sulfoxide **239**, and sulfone **240** to estimate the energy barriers toward racemization (Figure 5).¹¹⁶ Their investigations revealed that the sulfoxide had a lower energy barrier to rotation (at least 3 orders of magnitude). The reason for this smaller barrier was attributed to longer C–S bond length and reduced steric hindrance. However, in sulfones, increased steric hindrance contributed toward higher energy barriers.

3.3. Racemization vs *E*–*Z* Isomerization vs Slow Rotation

As already mentioned, the physical analysis on atropisomers was initiated long before by Mannschreck, Ackerman, Pirkle, and others (atropisomers were not screened for atropselective reactions).^{115,134,149,171–173} In-depth investigations by them and others revealed several important insights into the activation energy for restricted bond rotation and the factors that impact the racemization process. Table 1 lists the physical parameters of some of the widely investigated systems in the literature. However, some of the terms and definitions that are involved in these physical processes are often misunderstood or used interchangeably, such as slow rotation, *E*/*Z* isomerization (*S*_{cis}/*S*_{trans} isomerization), and racemization. *E*–*Z* isomerization that occurs in certain atropisomeric molecules such as anilides does not racemize the molecule but can influence reactivity during chemical transformations. Our treatment in Scheme 55 is a simplified model, and not all amides and anilides fit into the generalization. Anilides prefer to be in *E*-rotamer form that is in contrast to an amide, which prefers to exist as a *Z*-rotamer (Scheme 55).¹⁴⁰ Curran explained such a preference toward minimization of electron–electron repulsion between the lone pair of oxygen and the electron cloud in the aromatic ring. The ratio of *E* vs *Z* rotamers is influenced by temperature and the solvent employed, while the magnitude of the preference depends on the nature of substituents on the anilide system.

Similarly in amides, the role of the geminal substituents on the nitrogen and its impact on rotamers was debated for a long time.^{131,174} NMR studies led to clear understanding of the diastereotopic nature of the geminal substituents. The studies revealed two types of dynamic processes as centered around C_{Aryl}–CO and C–N bond rotation that can be concerted in these systems (Scheme 56). The C_{Aryl}–CO bond rotations in amides (ArCONR₂) is responsible for the racemization of atropisomers (changes the configuration of *P* isomer to the *M* isomer), while the C–N bond rotation exchanges the substituents on the nitrogen with respect to the individual atropisomers and does not affect the configuration (*P* or *M* isomer). Depending on the steric bulk of the substituents on the nitrogen, the energy barrier for C–N rotation can be comparable to that of the energy barrier for the C_{Aryl}–CO bond rotation. Clayden and co-workers have contributed to a large extent to our understanding of the dynamics involved in atropisomeric amide derivatives such as 2-methyl-1-naphthamides (Scheme 57).¹⁷⁵ Kinetic analysis carried out on optically pure samples obtained through HPLC separations revealed the rate constants and activation energy (ΔG^\ddagger) for individual bond rotations. Due to steric demands, the

Scheme 54



	238 Sulfide	239 Sulfoxide	240 Sulfone
$\Delta G^{\ddagger}_{rac}$ (kcal.mol ⁻¹)	24.1	20.6	25.5
$\tau_{1/2rac}$ (25 °C)	14 h	70 s	6 days
C-S bond length [pm]	179.4	182.0	180.8

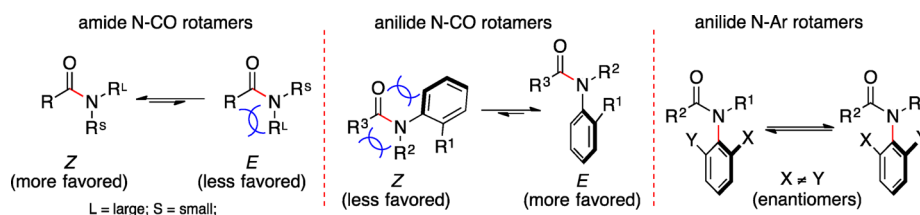
Figure 5. Comparison of racemization parameters between sulfide, sulfoxide, and sulfone.

concerted rotations ($C_{Ar}-CO$ rotation coupled with $C-N$ rotation or vice versa) occurred at a higher rate than the unconcerted individual $C_{Ar}-CO$ or $C-N$ bond rotations. The differences in the rates of concerted bond rotations (k_{endo} vs k_{exo}) were explained based on the differential steric barriers that had to be overcome for the isomerization process. The well-understood mechanism of bond rotations provides an avenue to employ them as molecular gears or storage devices that work based on the “gated” output.

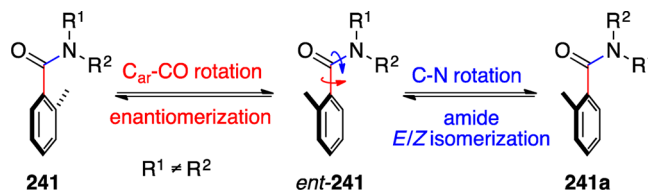
3.4. Importance of Physical Processes in Atropisomerism in Drug Discovery

Chirality plays an important role in drug development and as such impacts the pharmaceutical industry. Tremendous effort goes into introducing a single enantiomer as a therapeutic to the market (Figure 6). This process requires a good understanding of the differential biological activities, toxicities, and pharmacokinetics of individual enantiomers due to diastereomeric interaction in the biological environment. While classical compounds with central chirality were under intense scrutiny, atropisomers were overlooked for a long time. Just like central chiral molecules, atropisomeric compounds also interact differently in the biological milieu. In this regard, understanding the dynamics of atropisomers in rational drug design has become important.

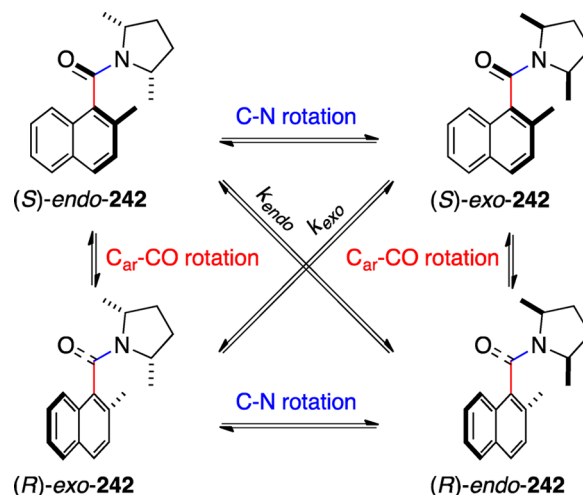
Scheme 55



Scheme 56



Scheme 57



$$\begin{aligned}
 k_{C-N}: & 3.9 \pm 0.8 \times 10^{-5} \text{ s}^{-1}; \Delta G^{\ddagger}: 24.1 \text{ kcal.mol}^{-1} \\
 k_{C-CO}: & 0.1 \pm 0.05 \times 10^{-5} \text{ s}^{-1}; \Delta G^{\ddagger}: 26.3 \text{ kcal.mol}^{-1} \\
 k_{exo}: & 1.0 \pm 0.1 \times 10^{-5} \text{ s}^{-1}; \Delta G^{\ddagger}: 24.9 \text{ kcal.mol}^{-1} \\
 k_{endo}: & 2.9 \pm 0.6 \times 10^{-5} \text{ s}^{-1}; \Delta G^{\ddagger}: 24.3 \text{ kcal.mol}^{-1}
 \end{aligned}$$

The analysis of kinetic parameters in axially chiral compounds provided some important information about time dependent chirality. Detailed information and techniques for analyzing and evaluating atropisomeric drug candidates have been reported.^{8,176,177} LaPlante, Clayden, and co-workers have written an excellent research article, perspective, and review on this subject, and readers are encouraged to refer to them for an in-depth understanding.^{8,176,177} For example, neuropeptide tachykinin **243**, a well-known NK_1 receptor antagonist used in the treatment of depression (Scheme 58), features restricted bond

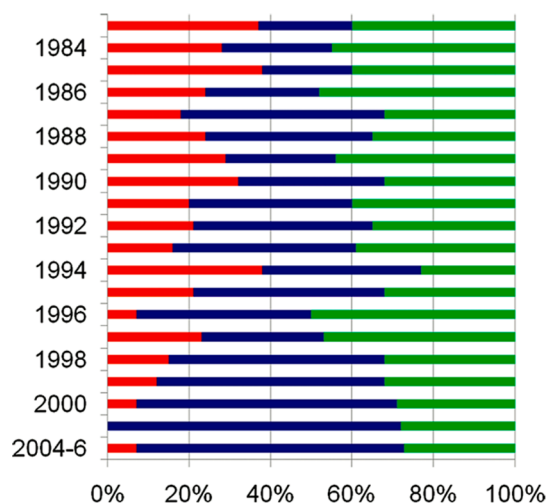


Figure 6. Data represents the percentage of new chemical entities (NCE) that were approved in recent years released by regulatory agencies. Red, blue, and green bars represent the percentage of racemates, single enantiomers, and achiral compounds, respectively. Reprinted from ref 176. Copyright 2011 American Chemical Society.

rotation around C_{Ar} -CO and N-CO.^{178–180} This led to the presence of multiple diastereomers that were observed in analytical methods causing complications during drug design and optimization.

This necessitated redesign of the NK_1 receptor antagonist to eliminate the complication that arose due to restricted bond rotations. Analysis of the individual rotamers (atropisomers had half-lives in days at 37 °C) allowed them to identify the atropisomer that had the best potency. Modifying the primary structure to eliminate such labile chiralities resulted in compound **244** that retained its biological potency both in vitro and in vivo. In another approach, Palani and co-workers used a symmetrization strategy to avoid atropisomers (Scheme 59).^{181,182} They were interested in the exploration of small molecule targets toward the treatment of HIV by inhibiting the viral entry (CCRS antagonists). They screened **245**, Sch-351125, a candidate that possessed axial chirality resulting in four diastereomers that differed in their antiviral activities (15-fold difference in some cases between stereoisomers). They overcame this bottleneck through symmetrization of the compound (as in **246**) eliminating the issue of axial chirality.

Just like central chiral compounds, scrutinizing the biologically active conformer in a particular atropisomeric substrate had to be carried out at early stages of drug design. To tackle the problem of conformers four main strategies are employed:¹⁷⁷

- symmetrization to eliminate the labile chirality
- reduction of the barrier to rotation to allow facile rotation along the chiral axis (making them rapidly interconverting conformers)
- increasing the energy barrier to rotation thus making the interconversion between the conformers less likely
- introducing chirality (central chirality) to bias the population of conformers to a desired conformation/diastereomer

4. APPLICATIONS

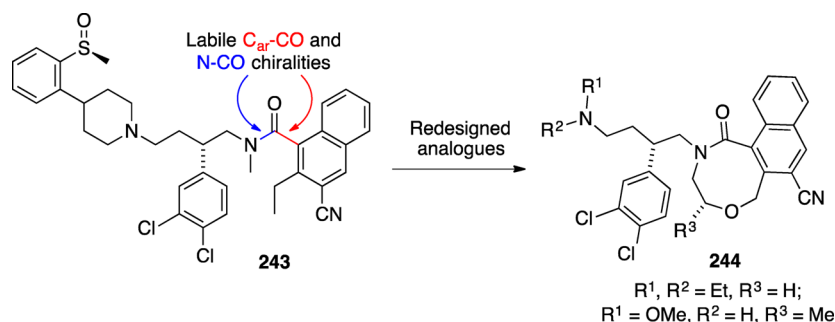
4.1. Atropselective Reactions

Biaryl atropisomers gained importance as ligands for a wide variety of metal catalysts that mediate important organic transformations.¹⁸³ In contrast, nonbiaryl atropisomers were viewed as chiral auxiliaries that can be employed as a stoichiometric chiral handle to stereodifferentiate a particular chemical transformation. Curran proposed a hybrid approach called “prochiral auxiliary approach” that possesses the advantage of a chiral catalyst and a chiral auxiliary (Scheme 60).¹⁴⁰

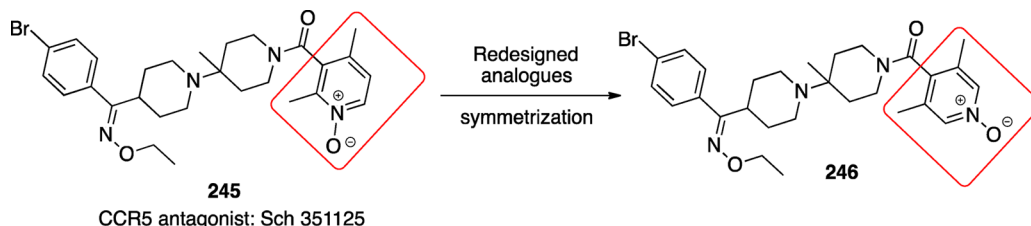
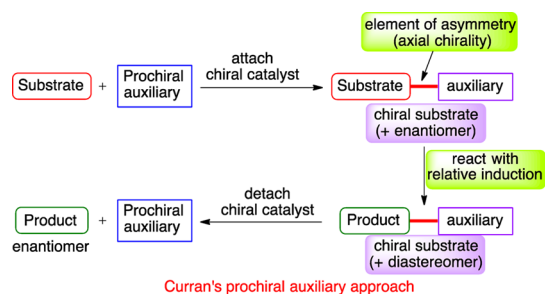
This approach utilizes two achiral molecules that on union results in an enantioenriched chiral adduct in the presence of a chiral catalyst or as separable enantiomers/atropisomers. This chiral framework can undergo atropselective reactions (not enantioselective) providing access to chirally enriched and synthetically useful building blocks (in principle the auxiliary can be removed and reused). In most cases, nonbiaryl atropisomers can be expected if the *ortho* substituents are bulky (e.g., *tert*-butyl substituent). However, the stability of atropisomers toward racemization depends on the size of the steric bulk and several other factors. Compounds possessing higher energy barrier for restricted bond rotations are desired for atropselective transformations as they provide multiple advantages. The first one is the ability to maintain the absolute configuration/axial chirality leading to an efficient axial to central chiral transformation. The second is the ease of operation/practicality in terms of separation and long-term storage without the erosion of its optical purity.

4.1.1. Cyclization Reactions. Right around the time when radical reactions of several axially twisted *o*-haloanilides were extensively investigated (to understand the origin of regioselectivity that gave rise to cyclization vs H-abstraction products),^{184,185} reports of atropisomeric anilides began to appear in the literature. Insights gained from *o*-haloanilides allowed scientists to take advantage of the inherent bias of amides and imides that possess noncoplanarity (to avoid steric congestion between *ortho* substituents of the phenyl group and carbonyl substituent on nitrogen) for atropselective transformations. Curran and co-workers documented the first report

Scheme 58



Scheme 59

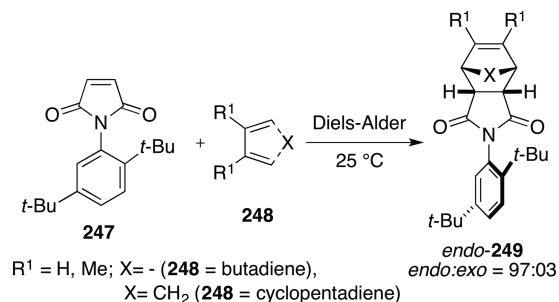
Scheme 60^a

^aReprinted with permission from ref 140. Copyright 1997 Elsevier.

of a series of atropselective reactions on nonbiaryl systems such as axially chiral imides and anilides.¹⁸⁵

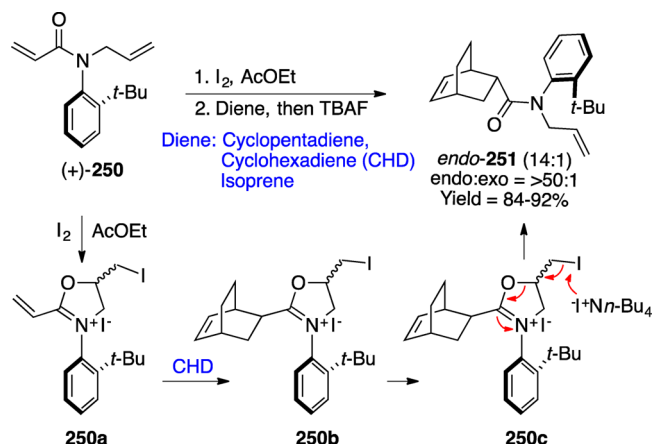
4.1.2. [4 + 2]-Cycloaddition. Axially twisted maleimides **247** underwent highly diastereoselective Diels–Alder reaction at ambient temperature to furnish the cycloadduct **249** (Scheme 61). The diene **248** attacked the maleimide **247** in an *endo* mode

Scheme 61



from the face opposite to the *t*-Bu group. The *t*-Bu group provided an excellent facial bias by forcing the diene to approach from the face away from the *t*-Bu group. Cycloaddition of dimethylbutadiene was sluggish at room temperature, but upon increasing the temperature to 80 °C the reaction accelerated with an *endo:exo* ratio of 93:7. A point to note is that the imides are not axially chiral as there is a plane of symmetry along the imide axis. Taguchi reported the chiral version of Diels–Alder reaction of optically pure maleimides accelerated by a Lewis acid, Et_2AlCl , with similar *endo* selectivity.²¹ The same group reported cycloaddition of enantioenriched axially chiral anilides **250** mediated by iodine (Scheme 62).^{20,21} In contrast to traditional chiral auxiliary substituted *N*-allylic enamides where the *endo/exo* ratio was 3–5, the axially chiral anilides **250** showed very high facial selectivity with *endo:exo* ratio >50:1. The selectivity was rationalized with the same facial differentiation argument where the diene attacked the cyclic imidate **250a** from a face opposite to the *t*-Bu group. The relative and absolute configurations of the

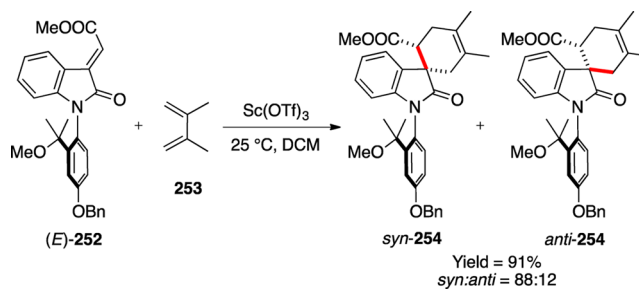
Scheme 62



products were verified by conversion of the adducts to known alcohols and performing Mosher's analysis.

Nakazaki reported highly diastereoselective [4 + 2]-cycloaddition of axially chiral oxindole derivative **252** with 2,3-dimethyl-1,3-butadiene (16 equiv) using $\text{Sc}(\text{OTf})_3$ as a Lewis acid (Scheme 63).¹⁸⁶ The reaction proceeded smoothly at

Scheme 63

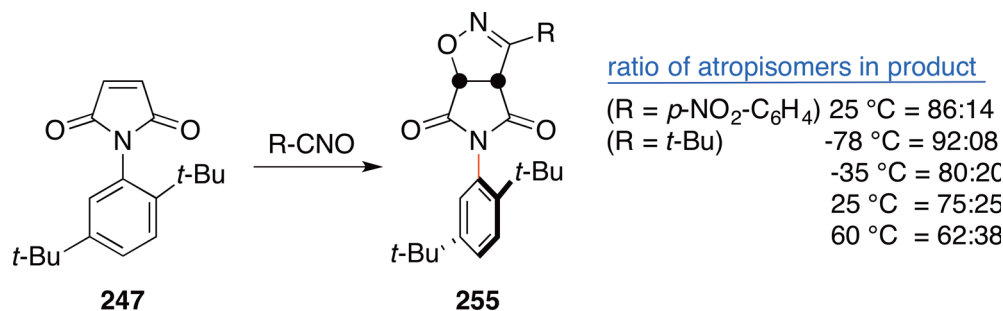


room temperature furnishing the Diels–Alder adduct **254** in excellent yield and selectivity (*syn:anti* of 88:12). Furthermore, the axial chirality was removed using $\text{PhI}(\text{OCOF}_3)_2$ to access a synthetically useful building block.

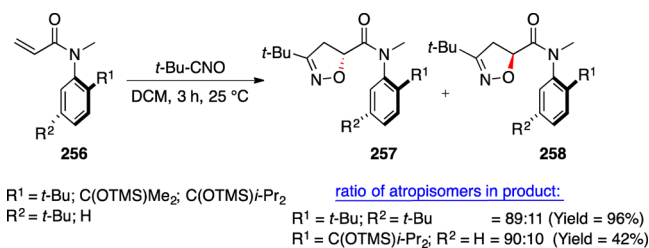
4.1.3. [3 + 2]-Cycloaddition. The first report of a series of reactions on atropisomers included [3 + 2]-cycloaddition of maleimides **247** with nitrile oxides (Scheme 64).¹⁸ The diastereoselectivity of the product **255** was highly dependent on the temperature at which the reaction was carried out. For example when $R = t\text{-Bu}$, the *dr* values at 60 and –78 °C were 62:38 and 92:8, respectively.

The [3 + 2]-cycloaddition reactions with acyclic amides are also highly stereoselective. For example, anilides such as **256** that feature a geometrical orientation dissimilar to cyclic imides undergo selective cycloaddition (Scheme 65). In cyclic imides, the alkene is *s-trans* to the carbonyl group, while the carbonyl

Scheme 64



Scheme 65

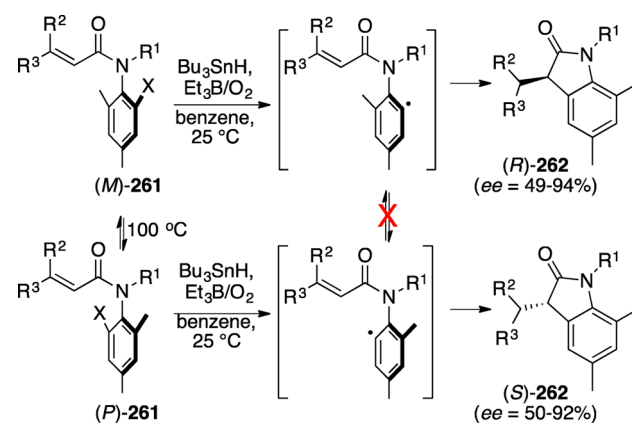


group and the *N*-phenyl substituents are in a *Z* configuration. However, the reverse is true in acyclic amides.¹⁴⁰ The cycloaddition of **256** proceeded with high stereoselectivity at 25 °C (dr = 89:11). Upon decreasing the temperature to -78 °C, the dr increased to 97:3 albeit with an increase in reaction time. When the product mixture was heated to 100 °C overnight, equilibration occurred resulting in a dr of 2:1. In addition, the major product had *N*-CO rotamers with *E/Z* ratios of 13:1 (R¹ = *t*-Bu) and 10:1 (R² = H).

Nakazaki reported [3 + 2]-cycloaddition of axially chiral oxindole derivatives with azomethine ylide (Scheme 66).¹⁸⁶ While the reaction proceeded smoothly, the diastereoselectivity was rather disappointing. In situ generation of ylide and steric size of the R-group in the ylide to increase selectivity in the reaction were unsuccessful.

4.1.4. Radical Cyclizations. Control of stereochemistry in radical reactions has remained a long-standing challenge. To address this issue, several strategies were attempted among which transfer of chirality proved to be very effective. Curran and co-workers took advantage of axial chirality in nonbiaryl systems and showcased several examples of radical reactions that proceeded smoothly with efficient chirality transfer. *o*-Haloacrylanilides **261** underwent 5-*exo* radical cyclization in the presence of radical chain reagent Bu₃SnH to yield enantioenriched oxindole

derivatives **262** (Scheme 67).¹⁴¹ While the (*M*)-**261** had very high energy barrier (30.8 kcal·mol⁻¹) and resisted racemization,

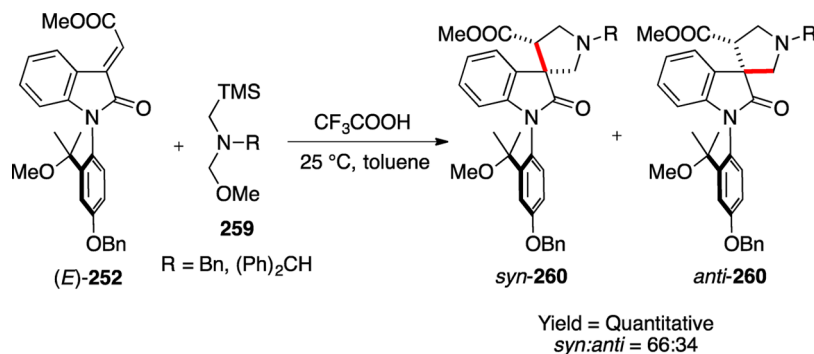
Scheme 67^a

X = I, Br; R¹ = Me, Et. R² = H, Me; R³ = Me, Ph

^aReprinted from ref 141. Copyright 1999 American Chemical Society.

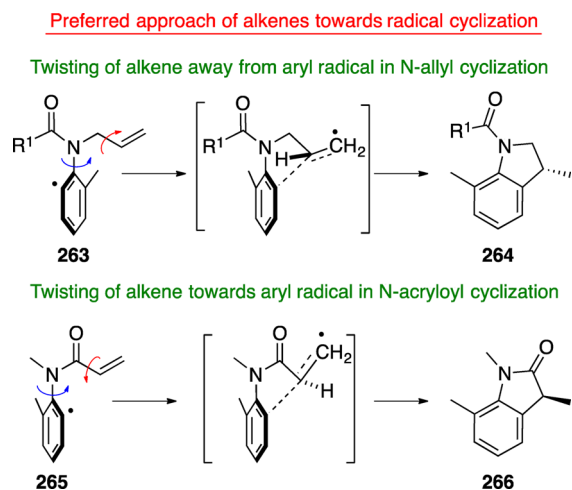
the radical intermediate generated possessed a much lower energy barrier toward racemization. However, as the rate of radical cyclization was faster than the rate of C-N_{aryl} bond rotation, it allowed for efficient axial to central chirality transfer yielding product **262** with high enantiomeric excess. In some cases, the selectivity in the product diminished either due to facile C-N_{aryl} bond rotation (racemization competing with cyclization) or due to unfavorable geometry of the alkene toward cyclization. If the *N*-substituent is an allyl group and a noncyclizable amide unit, then the cyclization occurred on the allyl substituent that resulted in 2,3-dihydroindole derivatives

Scheme 66



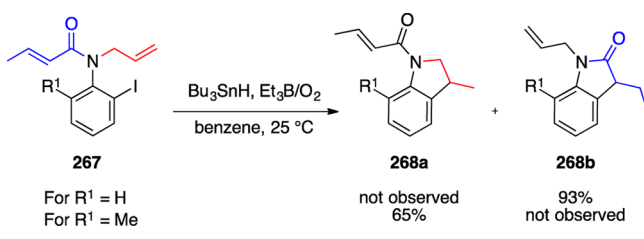
with very high axial chiral transfer.^{142,146,147} The approach of the aryl radical toward the alkene center and acryloyl center was quite different (*N*-acryloyl vs *N*-allyl, Scheme 68). In the case of *N*-allyl

Scheme 68



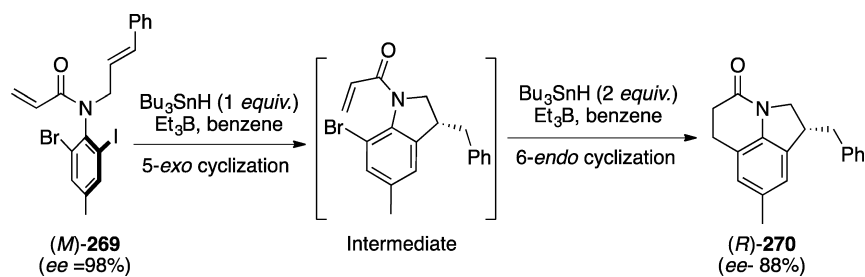
derivatives, the alkene swings away from the aryl radical exposing the internal carbon of the alkene. On the other hand, in substrate with *N*-acryloyl group, the alkene swings toward the aryl radical leading to the cyclized product. For substrates that contained both *N*-acryloyl and *N*-allyl groups (as in 267), competitive radical cyclization was observed and the chemoselectivity was dictated by the R¹ substituent at the *ortho* position (Scheme 69).¹⁴² When the R¹ was hydrogen, cyclization occurred

Scheme 69



exclusively on the *N*-acryloyl group leading to 268b.¹⁷⁸ However, if the R¹ substituent was a methyl group, cyclization occurred predominantly on the *N*-allyl substituent yielding 268a. Detailed kinetic study on the substrate that had *o*-methyl group revealed that the inherently fast *N*-acryloyl cyclization was retarded at least by 2 orders of magnitude. This retardation was due to unfavorable approach of the aryl radical toward the alkene of the

Scheme 70

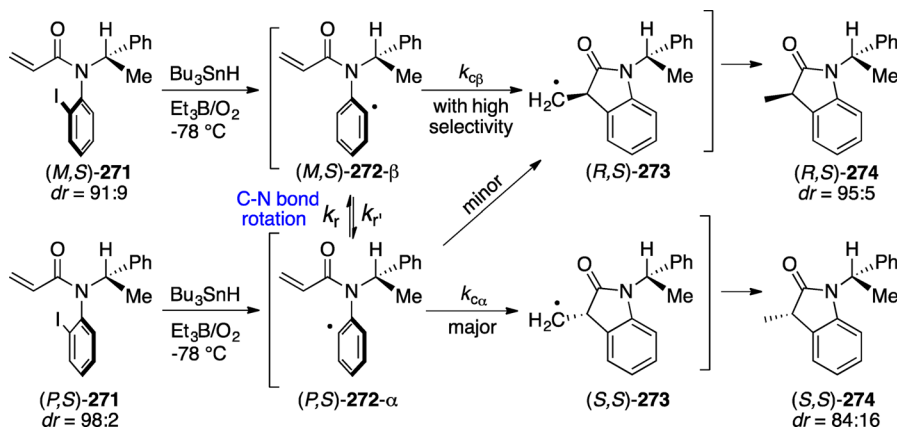


acryloyl group that in turn promoted the less favored cyclization on the *N*-allyl group.

When the methyl group at the *ortho* position was replaced by a radical precursor, double cyclization occurred (Scheme 70).¹⁴⁵ In a sequential reaction, the aryl iodide bond in (*M*)-269 reacted preferentially through a 5-*exo* radical cyclization to form indoline intermediate that subsequently underwent a 6-*endo* radical cyclization initiated through the homolytic cleavage of aryl bromide bond resulting in tricyclic product 270. This sequential double radical cyclization had a huge significance on the enantiopurity of the final product as the first cyclization occurred with efficient chirality transfer. The use of cleavable/modifiable substituents such as TMS and Br were explored that provided an avenue for traceless directing group or handle for further synthetic manipulation.

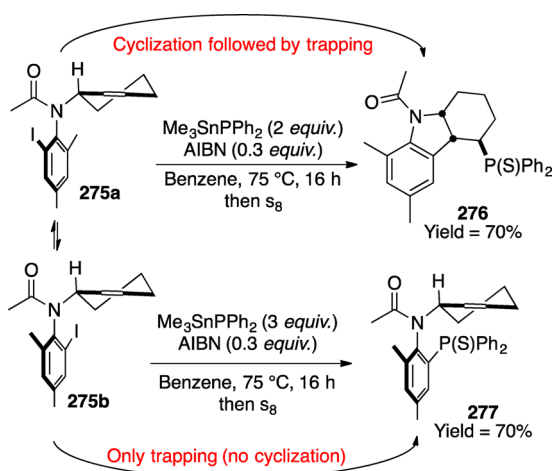
Curran and co-workers documented a novel way to access enantiomerically pure dihydroindoles through radical cyclization of acrylanilides containing an *N*-chiral substituent, viz., substrate with both axial and central chirality (Scheme 71).¹⁴³ Homolytic cleavage of aryl iodide bond in 271 resulted in a transient atropisomeric phenyl radical that cyclized to form the product 274. Interestingly, the stereoselectivity of the radical cyclization was temperature dependent (*dr* ratio at 20 and -78 °C were 78:22 and 84:16, respectively) and was higher than the rotamer ratio of the starting material ((*M,S*)-271/(*P,S*)-271 ratio was 68:32 at room temperature) leading to resolution. This was attributed to the different rates of interconversion of the transient atropisomeric radicals ((*M,S*)-272- β and (*P,S*)-272- α) through C–N bond rotation. At low temperature, interconversion (*k_i* vs *k_c*; Scheme 71) competed with cyclization. For example, (*M,S*)-272- β cyclized with high stereochemical integrity to give (*R,S*)-274. On the other hand, (*P,S*)-272- α cyclized with minor stereochemical leakage resulting in (*R,S*)-274 (minor) and (*S,S*)-274 (major).

Taking advantage of such a fast radical trapping, Curran and co-workers showed that the aryl radical generated from atropisomeric *o*-haloanilides can be trapped externally without the loss of stereochemical integrity (Scheme 72).¹⁸⁷ For example, they employed phosphonylation of an aryl radical that occurred with very high rate constants ($\approx 9 \times 10^8 \text{ M}^{-1} \text{ s}^{-1}$). Competitive radical reactions can occur for substrates featuring an intramolecular radical cyclization unit (e.g., as in 275a) and intermolecular radical trap (phosphonylation, 275b). The relative rates of the intra- and intermolecular radical reactions in substrates such as anilides were dictated by the position of the cyclization partner on the nitrogen substituent. For example, while radical generation occurred at similar rates for both 275a and 275b, radical cyclization was much faster than the radical trap by phosphonylation in 275a and the radical trap phosphonylation pathway dominated in the case of 275b. The reason for such

Scheme 71^a

^aReprinted from ref 143. Copyright 2005 American Chemical Society.

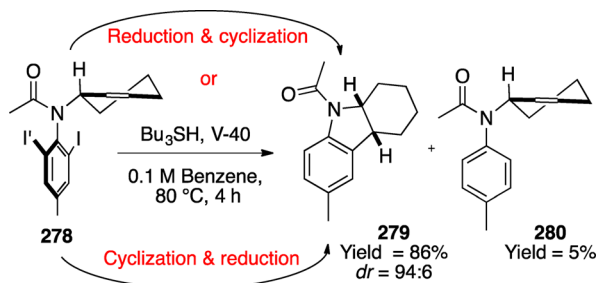
Scheme 72



an observation was bolstered by the fact that the high-energy 5-*exo* pathway for **275b** was shut down leading to a chemo-divergent process.

When an *o*-methyl substituent in **275** was replaced by an iodo substituent (as in **278**), regardless of the sequence of the steps (cyclization followed by reduction or reduction followed by cyclization), it led to **279** (Scheme 73).¹⁸⁸ The initial chemodivergent radical process underwent diastereotopic group selective transformation to yield a single product. Detailed kinetic and mechanistic analysis showed that the abstraction of iodine atom occurred in a nonselective fashion leading to isomeric intermediates. These intermediates underwent further transformation via nonintersecting pathways to yield a single

Scheme 73



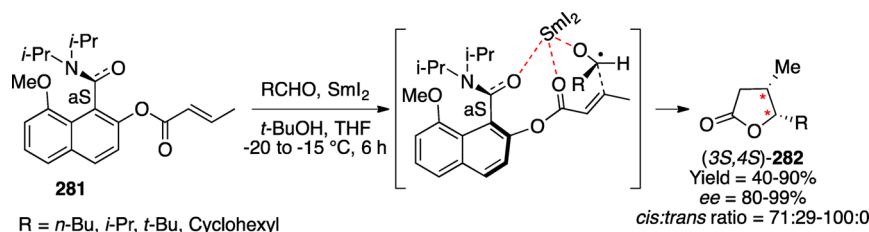
product **279**. The stereoselectivity of the divergent process was explained based on conformational preference in the product, X-ray analysis, and theoretical (DFT) calculations.

Dai and co-workers documented highly atropselective reductive cyclization of aldehydes **281** mediated by SmI₂ leading to highly enantioenriched *cis*- γ -butyrolactones **282** (Scheme 74).¹⁸⁹ The optically pure atropisomeric 8-methoxy naphthamides **281** obtained through chemical resolution served as a chiral auxiliary and provided excellent remote chirality transfer to the crotyl derivative in reductive cyclization process. The authors proposed a chelation model via an eight-membered transition state for the observed selectivity. The ketyl radical generated coordinated with the Sm(III) cation from the same face of the amide unit. Molecular modeling studies suggested *s-cis* conformation was energetically more favored over *s-trans* conformation. They also demonstrated that the reaction proceeded with the same level of axial to central chirality transfer in the solid phase reactions when the atropisomeric crotyl derivative was linked to Rink amide resin.

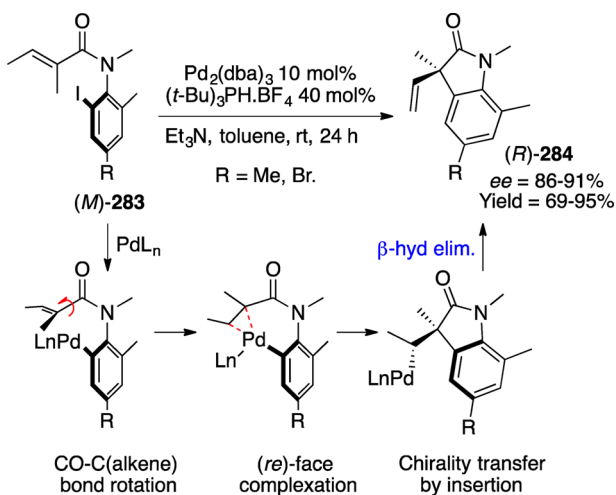
4.1.5. Heck Cyclization. Curran and co-workers reported highly efficient axial to central chiral Heck cyclization of axially chiral *o*-iodoacrylanilides **283** (Scheme 75).¹⁴⁴ The reaction was performed at room temperature to avoid racemization of axial chirality (a likely process at elevated temperatures) where oxidative addition of Pd to C_{Aryl}-iodine bond served as the stereocontrolling step. The CO-C(alkene) bond (existing as low energy conformers) rotated to form a complex with Pd[L_n] followed by Pd insertion. The final product (*R*)-**284** was obtained through β -hydride elimination.

As a comparison between radical and Heck cyclization, reaction with a compound containing both axial chirality and an additional stereogenic center such as *N*-(cyclohex-2-enyl)-*N*-(2-iodophenyl)acetamide **285**, the product outcome was contrasting and was dependent on the configuration of the substrates (Scheme 76).¹⁴⁸ Under radical conditions, the *syn*-**285** preferentially underwent cyclization to give the product **286** whereas the *anti*-**285** (not shown) underwent reduction to yield noncyclized product **288** with retention of chirality. However, in the Heck cyclization, only the *anti*-**287** isomer underwent cyclization. The observed pattern was explained based on transition state geometries. For radical reaction, only two atoms are involved in the bond forming process (aryl radical and alkene carbon that is attacked). However, in the Heck cyclization, four atoms have to come together for which *syn* geometry is not

Scheme 74



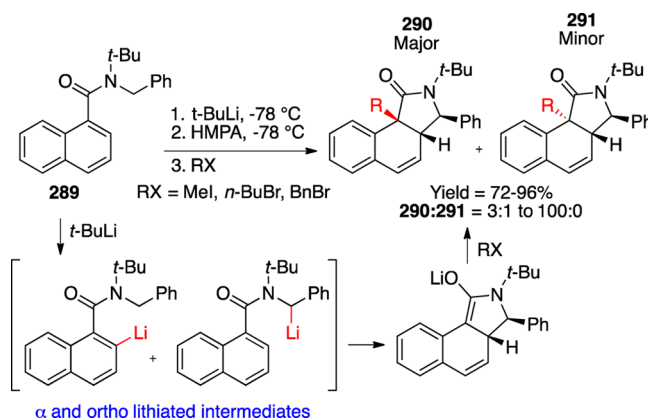
Scheme 75



suitable as it places the Pd atom right under the cyclohexene ring rather than near the alkene. In addition, in the Heck cyclization of allylic acetates, β -hydride elimination occurred if acetate was *trans* to palladium, whereas β -acetoxy elimination occurred if the acetate was *cis* to palladium. These results are in sharp contrast to the established *trans* relationship between the acetoxy group and palladium for β -elimination reaction (for compounds that do not have axial chirality). These results highlight the impact of axial chirality on the course of the reaction as well as the product outcomes that are different from established norms of mechanism and selectivity with achiral/nonatropisomeric substrates.

4.1.6. Anionic Cyclization. Clayden and co-workers reported an unusual anionic cyclization of axially chiral amide 289 to form tricyclic adducts 290/291 (Scheme 77).¹⁹⁰ The use of *t*-BuLi as a base resulted in a mixture of α - and *o*-lithiated species. These anions in the presence of HMPA, a stabilizing ligand, underwent cyclization leading to an enolate that was trapped by various electrophiles (RX) furnishing a mixture of

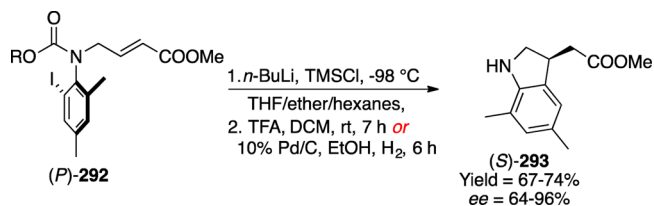
Scheme 77



diastereomeric tricyclic adducts 290/291. The enolate also underwent smooth aldol reaction, where the attack on the aldehyde took place from the less hindered face of the enolate.

Curran and co-workers reported an anionic cyclization of axially chiral carbamate derivatives 292 (Scheme 78).¹⁴⁶ The

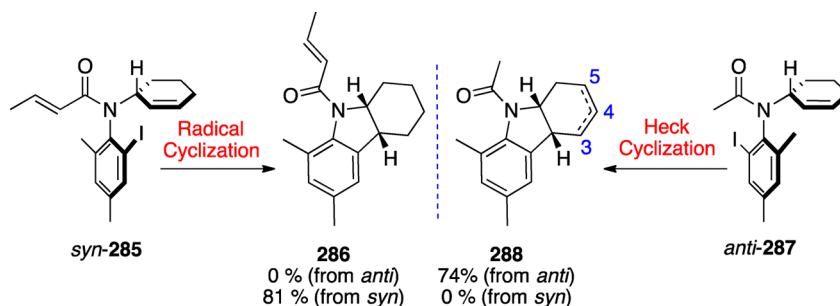
Scheme 78



reaction proceeded with excellent chirality transfer and the carbamate group in the resultant products could be easily removed after the reaction furnishing highly enantioenriched dihydroindole derivatives (*S*)-293.

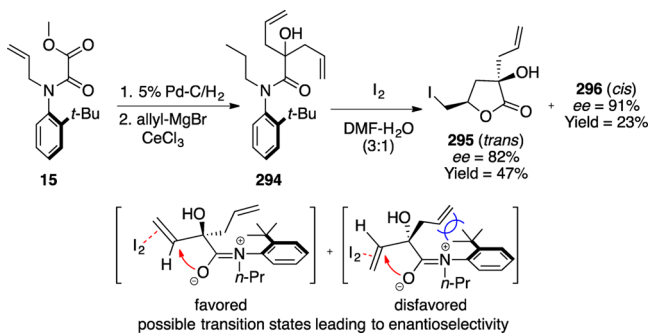
4.1.7. Iodolactonization. Taguchi and co-workers demonstrated the utility of atropisomeric acetanilide as a chiral auxiliary in a diastereoselective iodolactonization of diallylhydroxyaceta-

Scheme 76



nilide **294** (Scheme 79).²⁴ The origin of enantioselectivity was explained based on the favorable transition state that avoided the

Scheme 79

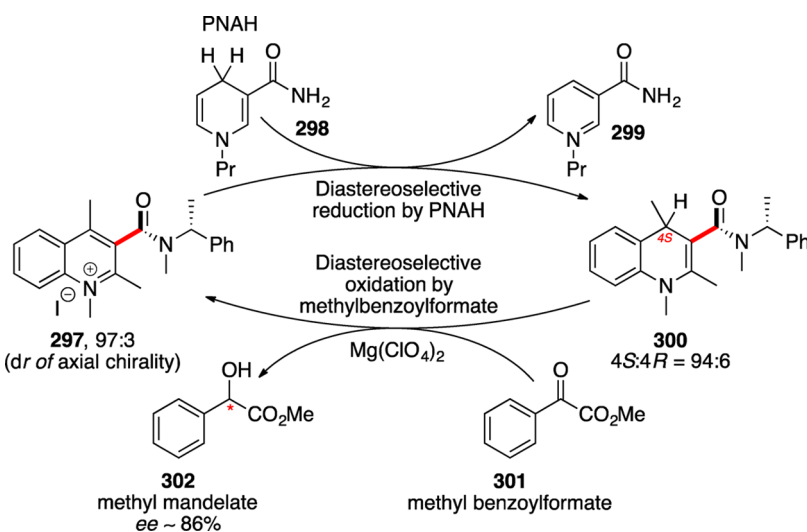


steric interaction of the allyl group with the *t*-Bu group. It is interesting to note that the chiral auxiliary was cleaved during the cyclization process resulting in lactone **295/296** in high ee and moderate dr (**295:296** was 2:1).

4.2. Addition of Nucleophiles

Atropselective nucleophilic addition in an atropisomeric system was reported a long time ago. For example, the stereochemistry of hydride transfer in NAD(P)/NAD(P)⁺ model systems was under intense scrutiny.¹⁹¹ When NADH or NADPH is reduced by alcohol dehydrogenase, depending on the type of coenzyme, the enantiotopic face (pro-*R* or pro-*S*) is differentiated by the coenzymes. Even model systems that have distant chirality show preferential hydride transfer pathways.¹⁹¹ Such interesting observations led to a series of investigations to understand the mechanism of hydride transfer reactions.^{39,192–197} One of the earliest reports on these systems was documented by Ohno and co-workers, who mimicked the stereoselective, reversible hydride transfer, in NAD⁺/NADH (nicotinamide adenine dinucleotide) coenzyme systems (Scheme 80).¹⁹¹ The methyl iodide salt **297** with dr of 97:3 (due to axial and central chirality) was reduced by neutral PNAH (**1-propyl-1,4-dihydropyridinamide**) to furnish dihydroquinoline **300**. The product **300** showed a diastereomeric ratio of 94:6 at the newly formed 4*S* chiral center. The reverse reaction, oxidation of the dihydroquinoline **300** by

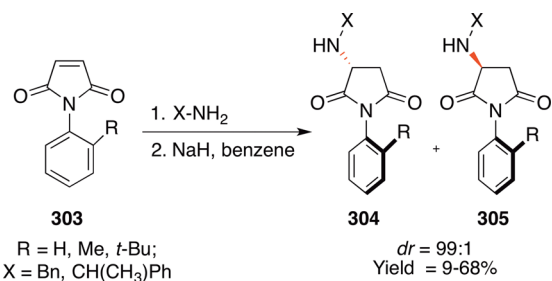
Scheme 80



methyl benzoylformate **301** in the presence of Mg(ClO₄)₂, gave the starting quinoline salt **297** with similar dr values at the axial chiral center and enantioenriched methyl mandelate **302** (ee ~ 86%). While the absolute configuration of atropisomeric **297** was not determined, the chirality of **300** and methyl mandelate **302** reversed with equal magnitude if the other axially chiral diastereomer of **297** was employed. Thus, the axial chirality influenced both the oxidation and reduction reactions.

Kishikawa and co-workers reported conjugate amine addition to maleimides **303** (Scheme 81).¹⁹⁸ In this reaction, both the R

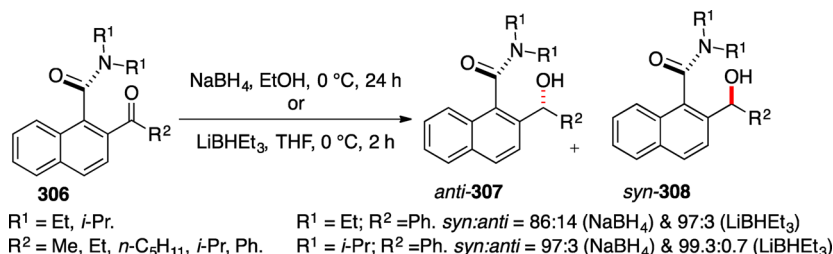
Scheme 81



group and the amine impacted the selectivity. A combination of bulky *t*-Bu and phenethylamine gave optimal results with dr up to 99:1. Rotational barrier studies in product **304** revealed a fairly high energy barrier for rotation (~28 kcal·mol⁻¹). The aminated maleimides **304** were further subjected to methylation (that occurred at the CH₂ position of the succinimide) in which the newly formed methyl group was oriented *anti* to the *t*-Bu (*cis* to amine substituent) group.

Clayden and co-workers have made several interesting observations on nucleophilic (hydride, organometallic reagents) addition to axially chiral naphthamides.^{199,200} During hydride addition, use of a more bulky reducing agent such as LiBHET₃ increased the *anti* selectivity (97:3) in comparison to reaction with sodium borohydride (86:14) as shown in Scheme 82. The observed selectivity was rationalized based on nucleophilic attack from the less hindered face of the ketone **306** (*anti* to N(R)₂ substituents). This was bolstered by an increase in selectivity when more bulky amide substituent was employed. The selectivity in the reduction further increased when more bulky

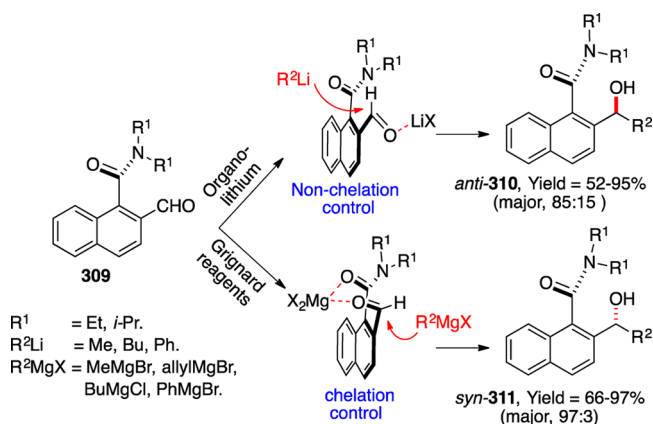
Scheme 82



reducing agent was employed or when the temperature was lowered.

Interestingly, for atropisomeric naphthamides **309** when subjected to nucleophilic attack by organometallic reagents, depending on the type of metal, a reversal in selectivity was observed (Scheme 83). For example, when organolithium

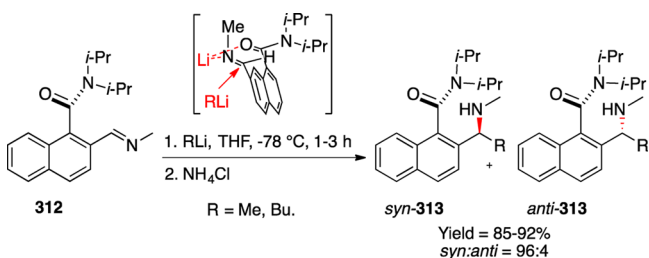
Scheme 83



reagents were employed, *anti*-**310** was obtained as the major product. However, if Grignard reagents were employed, *syn*-**311** was the dominant product. This reversal in selectivity was attributed to the differential ability of the metal to coordinate an aldehyde. Alkyl lithium coordinates only to aldehyde carbonyl leading to “non chelation controlled” transition state. However, more Lewis acidic magnesium coordinates simultaneously to both the amide and aldehyde carbonyl groups with reaction occurring through a “chelation controlled” transition state. This hypothesis was further supported by the addition of HMPA to the Grignard reaction resulting in *syn* selective product (*syn:anti* = 62:38) due to disruption of chelation.

When atropisomeric naphthimine **312** was subjected to nucleophilic attack by alkylolithiums, *syn* product **313** dominated (Scheme 84).^{200,201} This unexpected *syn* selectivity was explained by the twisting of $\text{CH}=\text{NMe}$ away from the $\text{N}(i-$

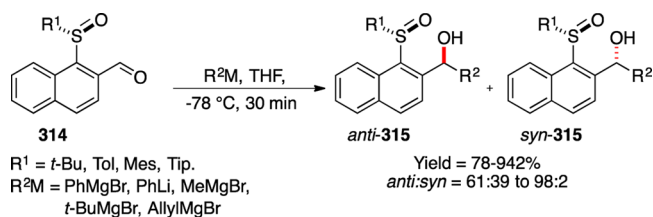
Scheme 84



$\text{Pr})_2$ group either by coordination of N and O to Lewis acid or to avoid steric crowding. The major reason provided for the high level of thermodynamic *syn* preference was hydrogen bonding between secondary N–H and amide carbonyl in the product rather than steric crowding.

In contrast to naphthamides, 1-sulfinyl-2-naphthaldehyde **314** underwent nucleophilic addition with RMgX and RLi reagents from a nonchelated transition state (Scheme 85).²⁰² Although

Scheme 85

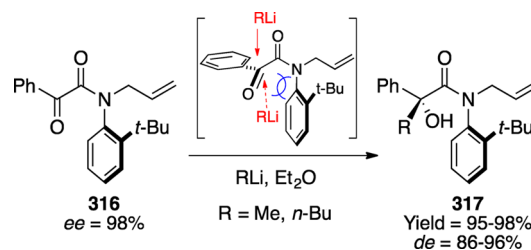


314 is not an atropisomer, room temperature NMR studies showed the presence of restricted rotation about the $\text{C}_{\text{nap}}\text{—S}$ bond and the ratio of the conformers dictated the *anti:syn* ratio in the product **315**. When the reaction was carried out in the presence of a chelating Lewis acid such as $\text{Yb}(\text{OTf})_3$, reversal in product selectivity was observed (*anti:syn* = 30:70). This was explained based on the chelated transition state between the sulfinyl oxygen and formyl oxygen. The steric bulk of the nucleophile and the R^1 substituent dictated the dr in the product.

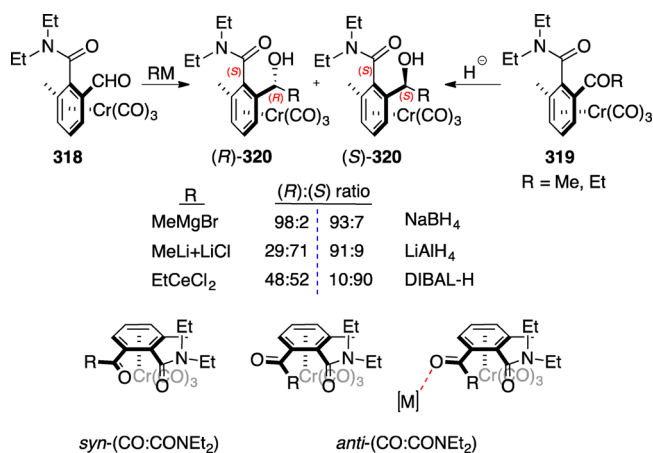
Taguchi and co-workers documented a highly diastereoselective addition of alkylolithiums to an atropisomeric α -oxoamide **316** without the addition of any external Lewis acid (Scheme 86).²⁴ X-ray structure of the α -oxoamide revealed that the *si*-face was more open to attack by the organolithium RLi whereas the *re*-face was hindered by the sterics from *t*-Bu group.

Uemura and co-workers demonstrated diastereoselective nucleophilic addition of organometallic reagents to atropisomeric chromium complexed benzamides **318/319** (Scheme 87).²⁰³ In all cases, the nucleophile attacked from the side opposite to the bulky chromium tricarbonyl functionality. However, depending on the conformation of the aldehyde

Scheme 86



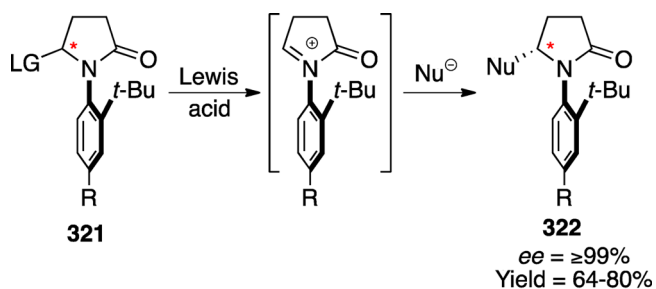
Scheme 87



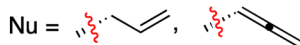
carbonyl with respect to the amide carbonyl, the stereochemical outcome in the product was different. Addition of Lewis acid also impacted the stereoselectivity of the product. Generally, the nucleophiles (regardless of the carbanions) attacked the carbonyl group of the chromium complexes in an *anti* conformation as observed in the case of *o*-alkoxy and *o*-methylbenzaldehyde chromium complexes.²⁰⁴ However, in the chromium complex **318**–**319**, the mode of nucleophile attack depended on its ability to coordinate with the aldehyde (**318**) or ketone (**319**). Noncoordinating nucleophiles such as alkyl lithium species preferred to attack the chromium complex in a *syn* conformation giving rise to (*S*)-**320** product. However, for a coordinating nucleophile such as MeMgBr, the metal coordinating step happens rapidly leading to equilibrium between a coordinated *anti* conformer and noncoordinated *syn* conformer (Lewis acid coordination in a *syn* conformation would be sterically demanding). Here the rate-determining step was the addition of nucleophile where the addition to coordinated *anti* conformer was preferred resulting in (*R*)-**320**.

Simpkins and co-workers demonstrated the nucleophilic trapping of an atropisomeric *N*-acyliminium intermediate with high stereocontrol (Scheme 88).^{136,205} The enantiomerically

Scheme 88



LG = L-menthol; Lewis acid = Me₃SiOTf; R = H, OMe.

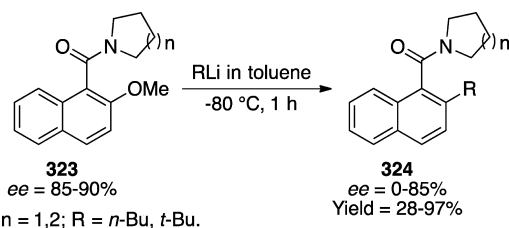


enriched starting material **321** was obtained by attaching optically pure L-menthol (chiral auxiliary approach) and separating the resulting diastereomers by chromatography. While reactions proceeded smoothly, the resulting product **322** did not possess a configurationally stable C–N chiral axis. This necessitated a post reaction modification for analytical purposes.

The analysis revealed very high stereoselection ($\geq 99\%$). The attempted removal of chiral auxiliary (when R = OMe) using ceric ammonium nitrate (CAN) was successful albeit with modest chemical yield.

Sakamoto and co-workers have reported an enantiospecific asymmetric S_NAr reaction of naphthamide derivatives (Scheme 89).¹⁵³ These chiral naphthamides **323** generated through

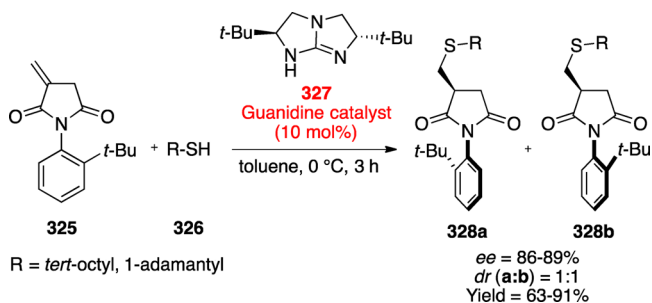
Scheme 89



amplification by spontaneous crystallization by seeding with desired enantiomer had very low energy barriers to rotation ($\tau_{1/2}$ of 26 min at 10 °C) at room temperature, but were sufficiently stable at lower temperature for asymmetric reactions. The energy barrier of the resulting product **324** depended on the bulkiness of the R group and the ring size ($n = 1, 2$). Though the reaction proceeded with very high selectivity, the ee of the product eroded over time at ambient temperatures due to racemization (observed in the case of R = *n*-Bu substrate). However, product with a bulky *t*-Bu group was stable and did not racemize at room temperature. The same authors have also reported highly enantioselective nucleophilic addition reactions of axially chiral amides that were generated through spontaneous crystallization.²⁰⁶

Tan and co-workers reported an enantioselective tandem conjugate addition–protonation of axially chiral itaconimide **325** with thiols **326** in the presence of a chiral bicyclic guanidine based organocatalyst **327** (Scheme 90).²⁰⁷ The reaction proceeded with high enantioselectivity to yield **328**; however, there was no diastereocontrol in the reaction resulting in 1:1 diastereomeric mixture.

Scheme 90

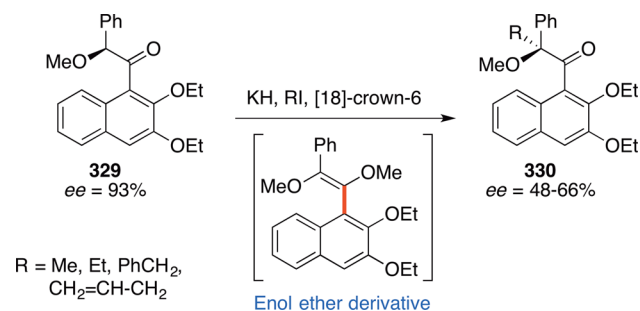


4.3. Reactions with Electrophiles

4.3.1. Enolate Chemistry. Anionic reactive intermediates derived from atropisomeric substrates react with electrophiles with good control over atropselectivity. Most of the reactions involve the generation of a transient enolate, which then reacts with a variety of electrophiles to produce products with new chiral center(s).

Fuji showcased atropselective alkylation of an optically active ketone **329** (Scheme 91). Deprotonation of the α -hydrogen to

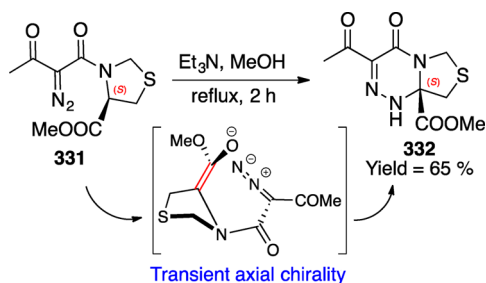
Scheme 91



the carbonyl group in **329** using potassium hydride as a base furnished an enolate that had transient axial chirality. During electrophilic quenching of the enolate, the axial chirality was effectively transferred to product **330** with high specificity. The formation of a transient enolate with retention of chirality was further substantiated based on the isolated intermediate as an enol ether derivative and with a half-life of ~60 min at room temperature.

Stoodley and co-workers put forward a similar explanation to account for the observed stereoselectivity in the intramolecular cyclization reaction of thiazolidine derivative **331** that proceeded with retention of configuration (Scheme 92).²⁰⁸ The ester

Scheme 92

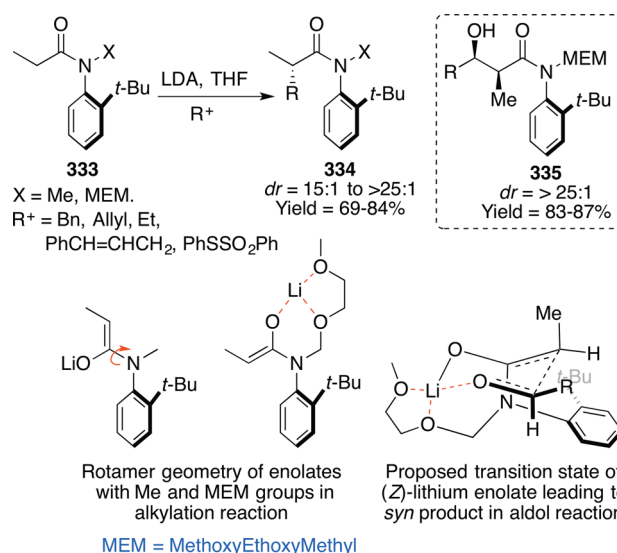


enolate generated during the course of the reaction had transient axial chirality and was trapped by the internal electrophile. In this process, electrophile quenching was much faster than racemization resulting in retention of configuration in the cyclized product **332**. A racemic product would be furnished from a planar enolate in the absence of axial chirality.

Since these early investigations, several examples of memory of chirality have been reported in the literature. Excellent review and research articles on this topic have appeared in the literature, and readers are encouraged to refer to them for an in-depth analysis.²⁰⁹⁻²¹¹ However, the extension of this concept to enolates derived from nonbiaryl isomers was slow.

Simpkins and co-workers documented highly diastereoselective alkylation and aldol reactions of atropisomeric amide derivatives **333** (Scheme 93).^{19,22} In this work, the N-X substituent had a huge impact on the diastereoselectivity of the product. A noncoordinating X group allows for a facile rotation of the C-N bond resulting in a poor dr value (2.4:1) for the product **334**. However, if the X group was a coordinating group such as MEM (methoxyethoxymethyl), the axial chirality was stabilized and the reaction proceeded with excellent dr ($\geq 25:1$). The major product **334** was assumed to have the R group away from the bulky *t*-Bu group and the minor diastereomer was confirmed by thermal atropisomerization. The (*Z*)-enolates generated from **333** also underwent smooth aldol reaction with

Scheme 93



various aldehydes and furnished the *syn* adduct **335** with very high diastereoselectivity. Simpkins and co-workers also attempted nonoptimized kinetic resolution of these amides by treatment with chiral lithium amide bases followed by quenching with MeI. This process gave enantiomerically enriched amides with an ee value of 88%.

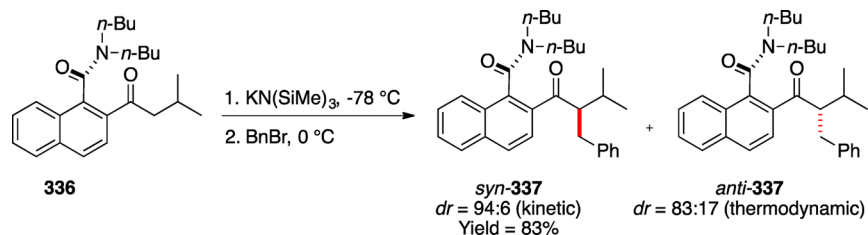
Clayden and co-workers reported the highly diastereoselective aldol reaction of atropisomeric amide derivative **336** (Scheme 94).²¹² The reaction proceeded under kinetic control giving rise to *syn*-**337** as the major diastereomer in a 94:6 ratio. Thermal equilibration (2 weeks) of *syn*-**337** (major diastereomer) occurred at ambient conditions resulting in *anti*-**337** (minor diastereomer) with a dr of 83:17.

Kitagawa and co-workers documented the synthesis of optically pure lactam **338** and its atropselective reactions with various electrophiles (Scheme 95).^{74,213} The reaction proceeded with modest to high diastereoselectivity. The choice of the base and the substituent at the C-5 position of the lactam **338** was critical for a successful outcome. Lithium tetramethylpiperidide (Li-TMP) was the optimal base and gave the products in modest to good selectivity. The approach of the electrophile was from the face opposite to the *t*-Bu group resulting in *cis*-**339** product. Bases such as LDA, *n*-BuLi, and NaHMDS gave low dr for the product. This was attributed to the inability of these bases to prevent N-C_{Aryl} bond rotation. If the substituent at the C-5 position was replaced by an OBn group (instead of OMe), the *cis:trans* ratio dropped to 3:1 from 10:1.

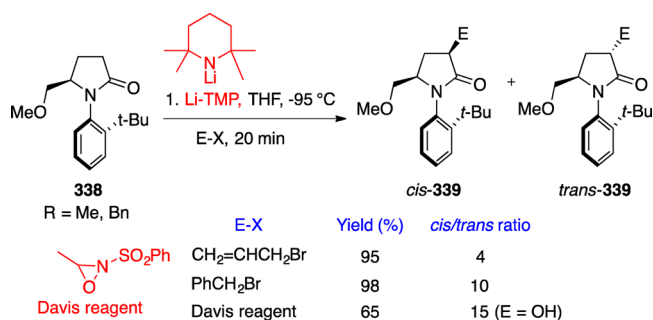
Simpkins and co-workers reported diastereoselective alkylation reactions of cyclic enamide derivatives **187** (Scheme 96).¹³⁶ While the atropselective reaction proceeded with modest dr (*anti:syn* = 6:1), the low energy barrier around the N-C_{Aryl} chiral axis (27.0 kcal·mol⁻¹ at 65 °C in CHCl₃) led to equilibration of the product **340**. They also attempted kinetic resolution of the enamide **187** using a chiral lithium amide base and partial alkylation of the enolate species. At 53-74% conversion, they were able to recover the unreacted (*M*)-**187** isomer with 62-74% ee and the alkylated product (*P,3R*)-**341** (alkylated product of *P*-**187**).

The same group extended the asymmetric deprotonation method to desymmetrize *pro*-atropisomeric maleimide **342** and synthesize natural product (+)-hinokinin **345** (Scheme 97).²¹⁴

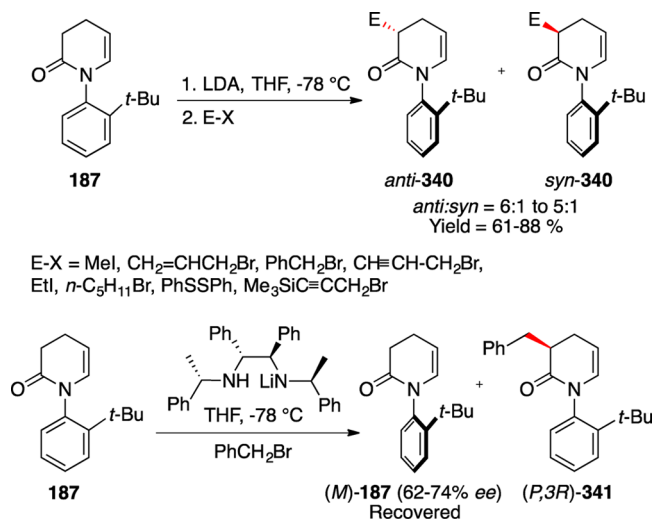
Scheme 94



Scheme 95



Scheme 96



Initial reaction optimization with a chiral bis-lithium amide base resulted in homodialkylated product where two groups were *anti* to each other (monoalkylated product dictated the second alkylation rather than the *t*-Bu group) resulting in a *meso* product. In contrast, the use of monolithiated amide base gave the monoalkylated compound **343** as the major product along with a trace of the dialkylated product. Using the monoalkylated maleimide **343**, the synthesis of (+)-hinokinin **345** was accomplished in three steps in moderate overall yields.

Kawabata and co-workers reported a highly enantioselective cyclization of alkyl aryl ethers **346** by generating a short-lived axially chiral enolate at the C–O axis (Scheme 98).²¹⁵ In this transformation, the substituent R played a critical role in effective asymmetric induction as it dictated the stability of the C–O chiral axis (the half-life of racemization at -78°C was estimated to be ~ 1 s). After several optimization studies involving various bases and solvents, a combination of NaHMDS and THF gave the best yield and selectivity for product **347**. Several control studies revealed that the five-membered cyclization proceeded

with retention of configuration. The extension of this condition to access six-membered rings met with a new set of challenges (Scheme 99). One of the major problems was that the rate of cyclization for the formation of the six-membered ring was slower than in the case of five-membered ring leading to poor selectivity (as a consequence of racemization). To stabilize the axial chirality, two bulky substituents were introduced (R^1 and R^2) in **348** that slowed down the rate of racemization and allowed for stereoselective cyclization resulting in **349** with enhanced ee values (e.g., when R^1 and R^2 were *t*-Bu and Me an ee of 91% was observed). Use of nonbulky bases such as NaHMDS resulted in styrene-type products due to β -elimination of hydrogen iodide. This was circumvented by the use of a bulky base such as TMS(*t*-Bu)NLi.

4.3.2. Ortho and Lateral Lithiation. Reactions of *ortho* lithiated amide and carbamate derivatives (DoM = Directed *ortho* Metalation) with various electrophiles serves as a powerful methodology to synthesize *ortho* functionalized aromatic rings in a highly regioselective fashion.^{216–218} Conformational preferences present in amides and carbamates have been exploited in the synthesis of axially chiral compounds³⁹ and have been employed in atropselective reactions.

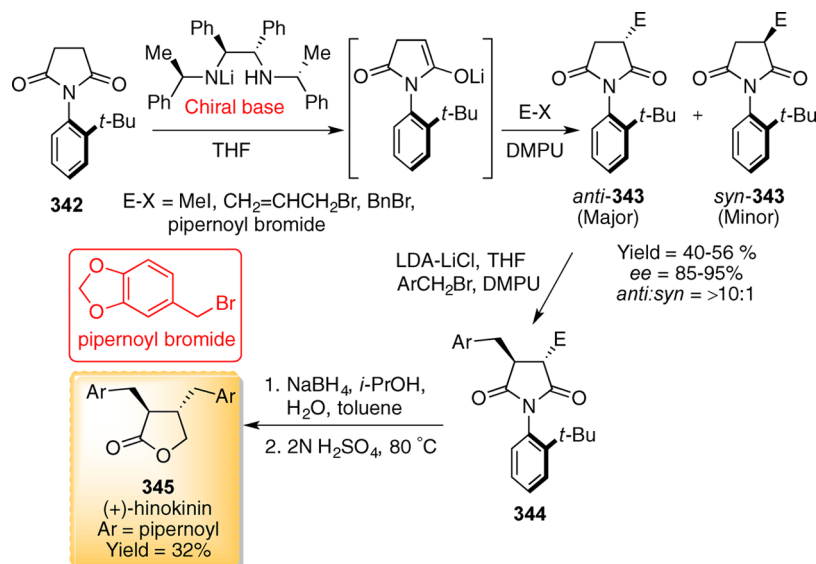
Clayden and co-workers were the first to exploit the conformational features of tertiary aromatic amide for stereoselective reactions. For example, reactions of naphthamides **350** with various electrophiles proceeded with moderate to high diastereoselectivity (Scheme 100).^{37,38} While **350** itself is not atropisomeric at room temperature, the products are separable diastereomers that equilibrate at room temperature on standing for a long time. The observed selectivity was rationalized based on the approach of the aldehyde R^2 substituent away from the $\text{N}(\text{R}^1)_2$ substituent in the transition state resulting in *syn-351* as the major product.

Clayden and co-workers also demonstrated that atropisomeric tertiary amides **352** exert higher influence over lateral lithiation followed by electrophilic quenching resulting in high *dr* values $>98:2$ in the resulting product **353** (Scheme 101).^{219,220}

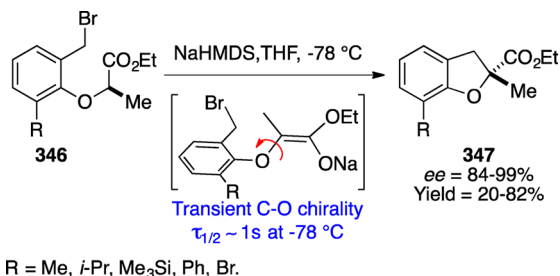
To understand if the lithiation or electrophilic quenching step was the stereodetermining step, reactions with a “stereochemical marker” were carried out with substrate **355** (Scheme 102). Reaction of atropisomeric stannane derivatives **355** revealed that the tin–lithium exchange was nonstereospecific, which is contrary to the usual stereospecific tin–lithium exchange.^{220,221} Also, the electrophilic quench was not selective (product **357**), which made interpretation of stereochemical outcome a challenging task. The same group also reported the addition of laterally lithiated 2-alkylnaphthamides and 2,6-benzamide to imine electrophiles resulting in amine derivatives with very high 1,5-asymmetric induction.^{212,222}

Clayden and co-workers demonstrated that an (–)-ephedrine derived atropisomeric ketoamide **359** showed high diastereoselectivity during nucleophilic addition using Grignard reagents

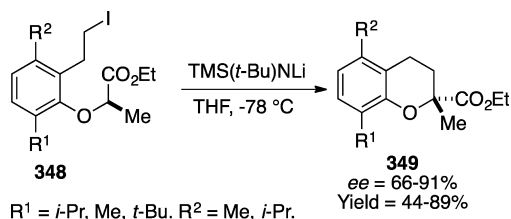
Scheme 97



Scheme 98



Scheme 99



(Scheme 103).²²³ The remote oxazolidine auxiliary in 359 dictated the conformation of the amide axis that is otherwise achiral. This amide orientation translated the chiral influence from the oxazolidine motif during the nucleophilic addition of Grignard reagents (1,5-stereocontrol) with excellent diastereoselectivity in the product 360.

Metzner and co-workers documented the first atropselective reactions of metalated thiobenzamides 361 (Scheme 104).²²⁴ They also compared the diastereoselectivity in the addition of the laterally metalated species to carbonyls in the amide and thioamide series. The results revealed that both metalated benzamides and naphthamides reacted efficiently with aldehydes leading to high selectivity in the product. In the case of thioamides, the reaction with aldehydes resulted in poor selectivity while the reaction with ketone resulted in higher selectivity.

Beak and co-workers reported stereoretentive reactions of atropisomeric silyl derivative 363 with various carbonyl and allyl halide electrophiles to form products 364 and 365 respectively

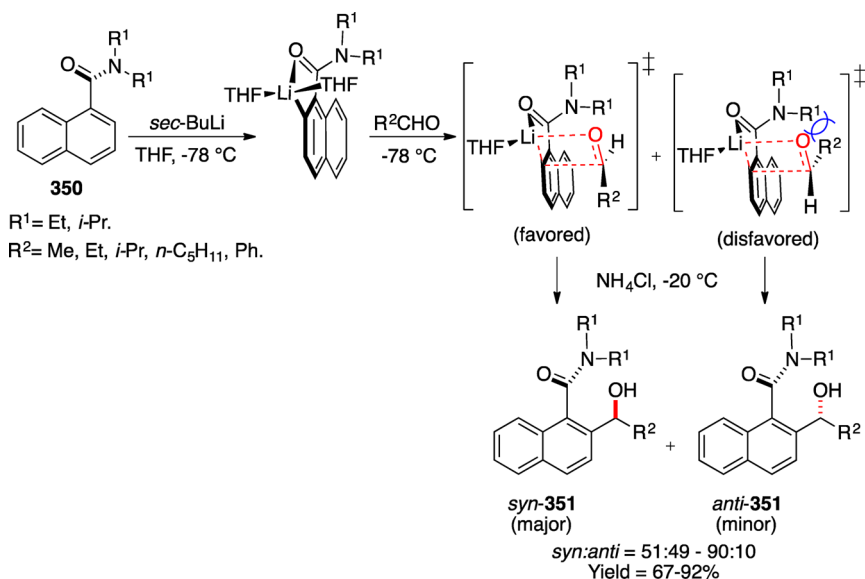
(Scheme 105).²²⁵ The fluoride activated chirality transfer proceeded well at ambient temperatures with moderate *er* and poor *dr* in the products. The enantiomeric ratio of the 1,4 chiral center (red) was slightly higher than the 1,5 chiral center (green) and the temperature had very little influence on the enantioinduction but had considerable influence on the rate of the reaction (room temperature reaction proceeds with higher conversion).

Taking advantage of well probed and understood conformational preference of tertiary amides, Clayden and co-workers demonstrated several reactions that relay stereochemical information propagated from the amide chiral axis. In one of the earliest examples, they were able to show that the silyl substituent in 366 controlled the conformation of the amide that in turn influenced the new chiral center that is being formed in the product 368 resulting in excellent 1,5 diastereoselectivity (Scheme 106).^{151,226} With additional work on these systems, Clayden and co-workers were able to show that the axial chirality can influence the conformations of more than one chiral axis.^{212,227,228} When a laterally lithiated 369 was added to atropisomeric imine 370, two diastereomers (*syn*- and *anti*-371) were formed with no kinetic preference leading to a 1:1 mixture. However, due to unequal energies of these isomers, they equilibrate to thermodynamically stable *anti*-371 diastereomer as the only product.

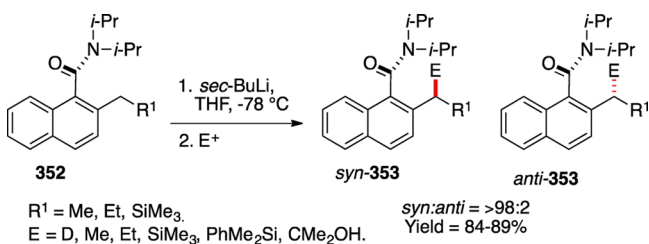
The chiral axis A (Scheme 107) influenced the chiral axis B that propagated through the central chiral stereogenic center. A similar observation of conformational influence was also observed in other systems such as xanthene derivatives that resulted in C₂-symmetric products (with respect to the two amide chiral axes).²²⁹ In addition, studies on biphenyl-1,1'-dicarboxamide scaffolds^{230,231} showed that C₂-symmetric product (kinetic product) was preferred over achiral S₂-symmetric scaffold (thermodynamic product) extending 1,10-stereocontrol in such systems.

Clayden and co-workers documented regioselective alkylation of unsymmetrical diarylureas 372 at the more substituted sterically crowded nitrogen atom, which further underwent selective functionalization through *ortho* metalation and electrophilic quenching sequence (Scheme 108).^{232,233} Several important conformational requirements for the origin of the

Scheme 100



Scheme 101



regioselectivity were put forward. The presence of an X-substituent twisted the N–Ar bond and inhibited the delocalization of the anion making it more nucleophilic, which overpowered the steric congestion of the X-substituent itself.

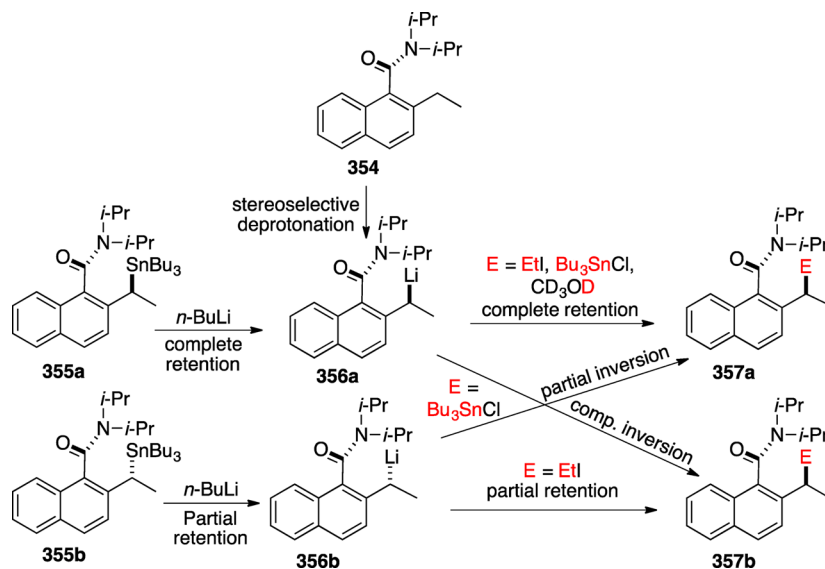
Subjection of the N-alkylated 373 to *ortho* lithiation followed by electrophilic quenching resulted in diarylureas 374 (Scheme 109) that are regioselectively functionalized at the ring that held

the alkylated nitrogen. Several control studies revealed that the N-alkylation was the governing factor that directed the *ortho* lithiation. They proposed two factors, namely “complex-induced proximity” by an electron rich center that placed alkyl lithium next to a C–H bond and acidification of *o*-hydrogen by inductive electron withdrawal by electronegative atoms. The *o*-aromatic hydrogen on the unsubstituted nitrogen was deactivated through higher electron density and failed to undergo deprotonation. These new classes of diarylureas displayed high diastereoselectivity toward synthetic manipulations.²³³

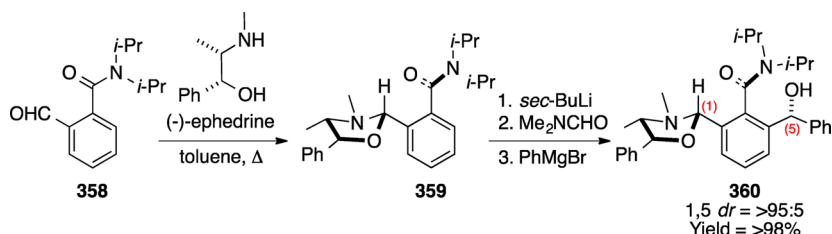
4.4. Rearrangements

Clayden and co-workers reported one of the first uses of atropisomeric amides as a chiral auxiliary for [3,3]-sigmatropic rearrangement (Scheme 110).^{234,235} Diastereomerically pure ketene acetal 376 obtained from *peri*-substituted 2-formyl naphthamides underwent atropselective Johnson–Claisen rearrangement to result in ester 377 as a single diastereomer. Similarly, the dimethylacetamide dimethoxy acetal 378 under-

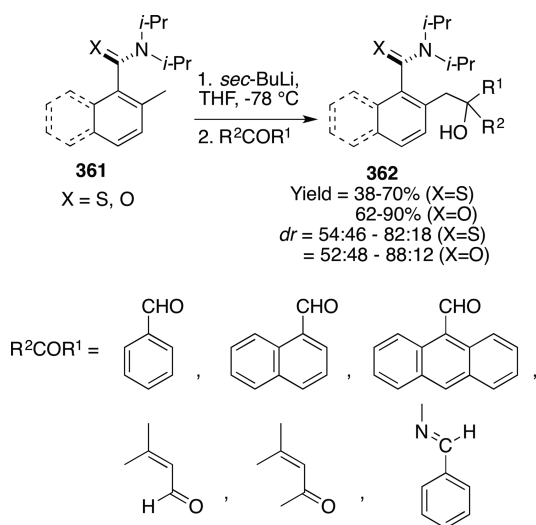
Scheme 102



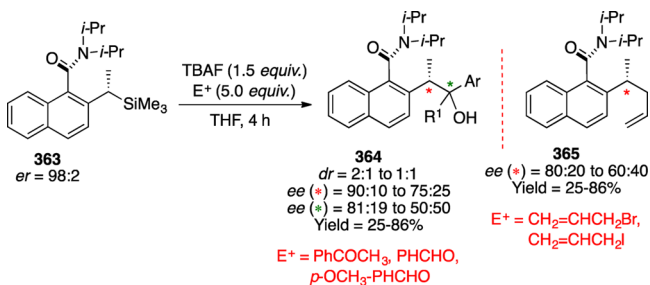
Scheme 103



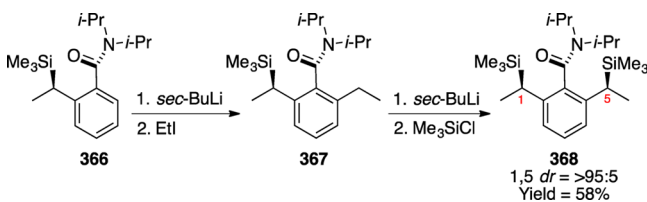
Scheme 104



Scheme 105



Scheme 106



went smooth Eschenmoser–Claisen rearrangement but gave a mixture of 1:1 epimeric products **379**. The higher reaction temperature likely caused the equilibration of the epimers resulting in lower selectivity.

The product **379** was subjected to ozonolysis to provide an alcohol that had (*R*)-configuration based on Mosher ester analysis confirming the atropselectivity of the [3,3]-sigmatropic rearrangement. Unfortunately, the chiral auxiliary could not be recovered due to the oxidation of electron rich naphthalene ring during ozonolysis.

Metzner and co-workers documented asymmetric thio-Claisen rearrangement of substituted *S*-allylketene thioacetals (Scheme 111).²³⁶ The atropisomeric thioanilides **380** preferred the *E*-geometry along the N–C_{Aryl} bond as observed by NMR spectroscopy. Treatment of thioanilides with LDA followed by quenching with allyl halides resulted in thioacetals that underwent smooth Claisen rearrangement to yield γ -substituted thioanilides **381** and **382** in good yields and dr values. Based on the stereochemistry of the product, they proposed a pseudochair transition state model for the observed selectivity, where the *S*-allyl group approached the enolate from the backside that avoids the steric hindrance from the *t*-Bu group.

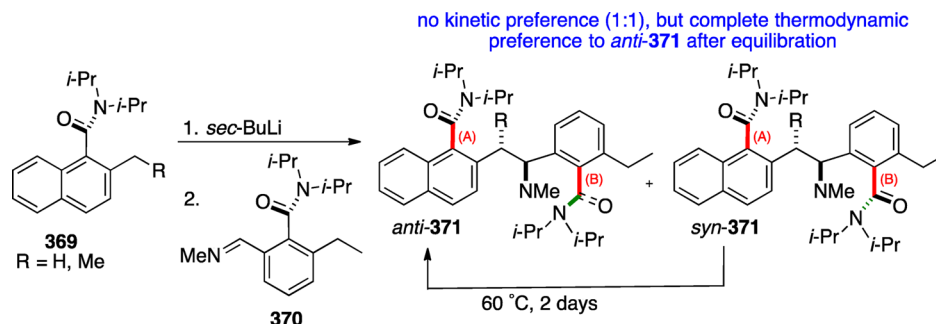
4.5. Catalysis

During the period when nonbiaryl atropisomeric systems were being investigated as a chiral scaffold to induce or transfer of chirality in a desired reaction, their use as a chiral catalyst was also progressing on a parallel platform. This progress was due to the success of biaryl systems in chiral catalysis.¹⁸³ The initial attempt was reported by Virgil and Clayden simultaneously, who employed different nonbiaryl scaffolds for the asymmetric allylic alkylation (AAA) reaction.^{151,237,238} So far, palladium catalyzed AAA has remained as the yardstick to rigorously evaluate nonbiaryl systems as chiral catalysts/ligands (Chart 2). Compilations of these results are provided in Table 2. Other than dimethyl malonate, few other nucleophiles were also examined and they also gave very high stereoselectivities in the product.

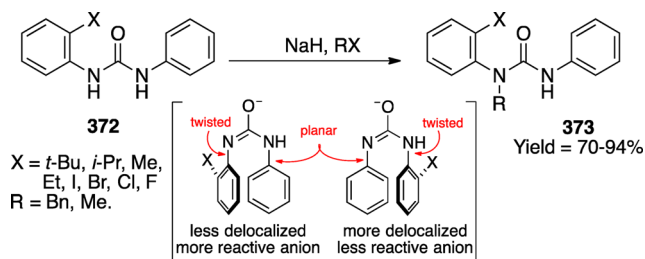
Wang and co-workers used palladium-derived nonbiaryl complex **400** for the asymmetric allylic arylation of racemic **399** to yield resolved Morita–Baylis–Hillman adducts **401** and chirally enriched **399** (Scheme 112).²⁴⁶ The reaction proceeded under kinetic control yielding 99% ee in the arylated product **401** and up to 92% ee in the recovered alcohol **399**. The reaction proceeded smoothly below room temperature to yield (*E*)-product with k_{rel} as high as 42 in some cases. They proposed that the new stereogenic center formed was of *R*-configuration that was controlled by the axially chiral catalyst via 1,4-addition followed by the destruction of the initial chiral center through Pd–OH elimination pathway. In another report, Mino and co-workers employed indole as a nucleophile in AAA reaction that resulted in very high enantioselectivity.²⁴⁷ The same group also successfully demonstrated a resolution technique in an asymmetric allylic alkylation reaction using atropisomeric ligand **394**.

4.5.1. Desymmetrization. Dai and co-workers reported desymmetrization of cyclic *meso*-anhydrides **403** using an atropisomeric naphthamide ligand **402** under basic conditions (Scheme 113).²⁴⁸ Nonbulky bases such as KH and NaH gave high yields of the product (*n*-BuLi as a base deprotonates the acidic hydrogen resulting in enolates). The observed high *syn* selectivity (*syn*-**404**) was supported by the formation of a chelation complex assisted by metal ions (Na⁺ and K⁺) with the

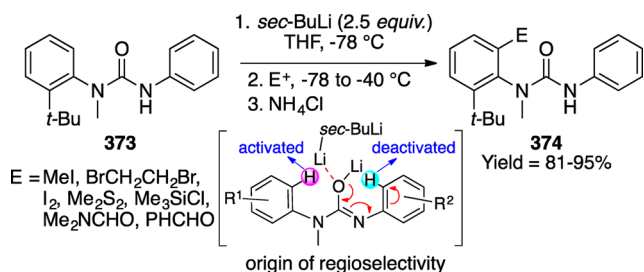
Scheme 107



Scheme 108



Scheme 109



amide carbonyl. The axial chirality at the amide underwent epimerization at elevated temperatures resulting in the formation of *anti* product.

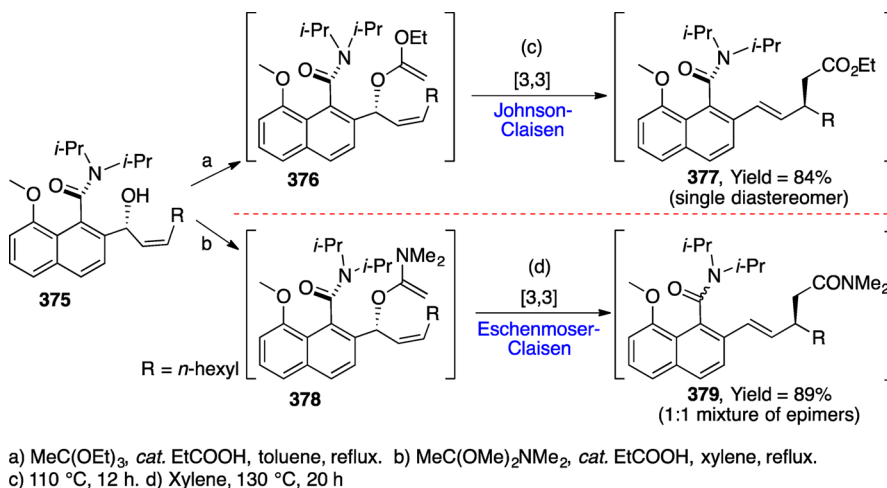
4.5.2. Grignard Coupling. Kondo and co-workers reported asymmetric cross coupling of β -bromostyrene **405** with Grignard reagents (Scheme 114).²⁴⁹ The rate of the reaction was

dependent on the nature of the X substituent on the catalyst **407**. For example, the reaction proceeded at a faster rate if X = oxygen (e.g., OBn) than if X = nitrogen (pyrrolidinyl). This difference in reaction rate was attributed to the strong coordination of nitrogen to the palladium metal, affecting the catalysis. However, changing the N skeleton to piperidinyl ($n = 2$), the reaction rate improved due to diminished coordination of nitrogen to Pd. The reaction was tolerant to several substituents except electron donating groups at the *para* position (substrate with a *p*-OMe gave no reaction).

4.5.3. Asymmetric Heck Reaction. Dai and co-workers demonstrated asymmetric Heck reaction of dihydrofuran **409** with a variety of aryltriflates **410** using atropisomeric amide-derived P,O ligands **411** (Scheme 115).²⁵⁰ The reaction resulted in two regioisomeric products **412** and **413** with moderate ee. However, the reaction failed in the case of electron deficient aryltriflates (*p*-Cl, *p*-Br, *p*-CN, *p*-Ph, and *p*-COOMe). The distribution of the regioisomeric products differed significantly and presented a complementary reaction to that of P,P and P,N ligands.

4.5.4. Suzuki–Miyaura Cross Coupling. Dai and co-workers documented highly efficient Suzuki–Miyaura cross coupling of aryl halides **414** and aryl boronic acids **415** catalyzed by atropisomeric amide derived P,O ligands, APhos **416** (Scheme 116).²⁵¹ They synthesized a library of APhos ligands through the self-assisted molecular editing (SAME) approach where both the substrate and product catalyzed the product formation. They screened these ligands for cross coupling with a variety of substrates under both microwave and thermal

Scheme 110



Scheme 111

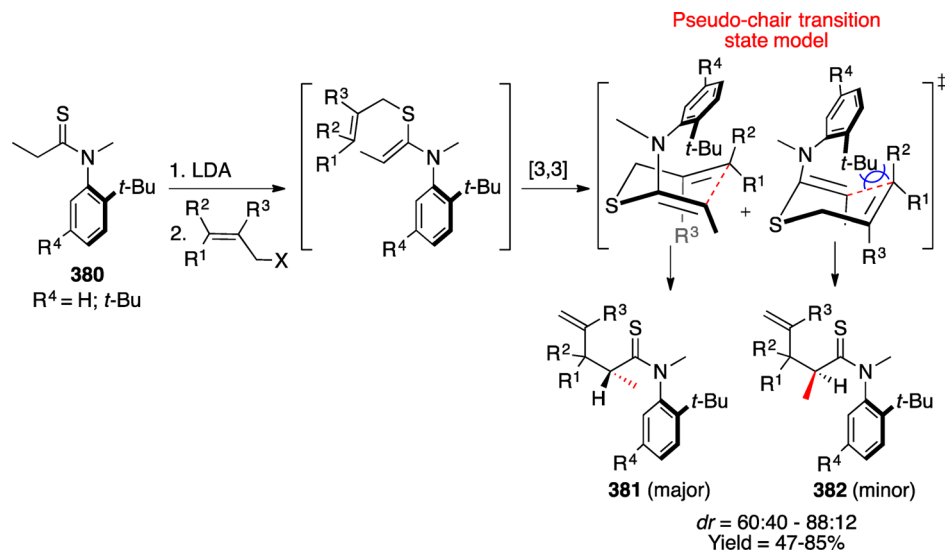
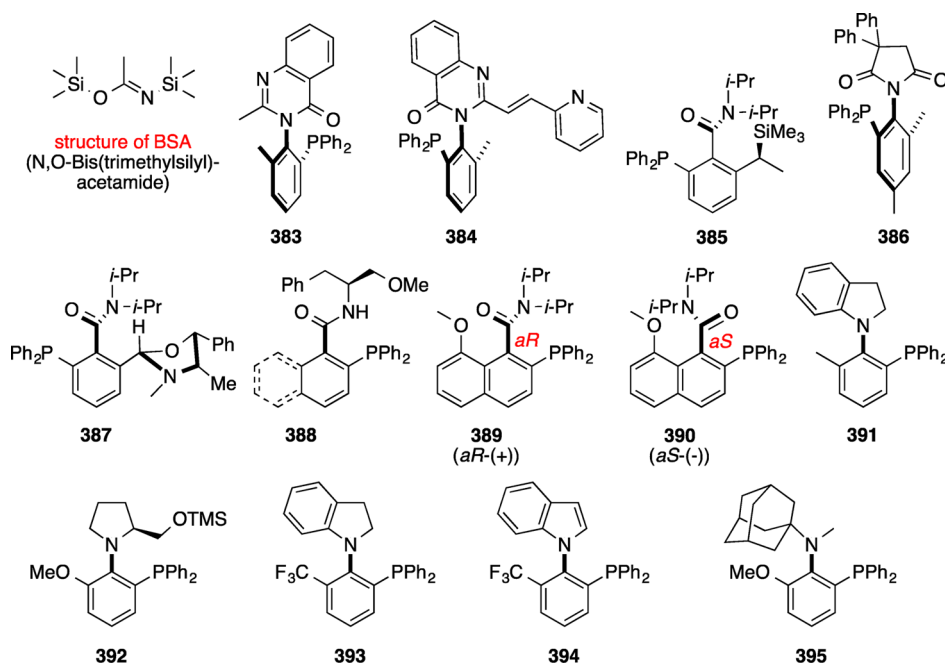


Chart 2. Nonbiaryl Atropisomeric Ligands for Asymmetric Allylic Alkylation Reactions



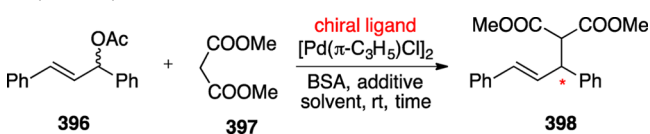
conditions. The reaction was tolerant to bulky and highly substituted aryl halides and arylboronic acids. The reaction proceeded smoothly with APhos: Pd ratio as high as 25:1 at 80–100 °C.

4.5.5. Benzoin and Stetter Reaction. Bach and co-workers reported a new class of atropisomeric catalysts based on imidazolium and thiazolium that were efficient in promoting Stetter and benzoin reaction with moderate enantioselectivity (Scheme 117).²⁵² Screening experiments revealed that the thiazolium salts **419** were superior for the intramolecular Stetter reaction of α,β -unsaturated ester **421** and benzoin condensation of benzaldehyde **418**. While the reaction proceeded smoothly, the chiral induction suffered. The authors suggested that the intermediate carbene that was generated suffers from racemization. This was evident from a decrease in diastereomeric purity of the catalyst analyzed after the reaction. They substantiated this observation by independently performing racemization/isomer-

ization of diastereomerically pure catalyst **419** in the presence of Et_3N in THF or NaHCO_3 leading to four new diastereomers in a ratio 60:20:15:5.

Jørgenson and co-workers documented α -fluorination of α -substituted aldehydes **423** using atropisomeric 8-amino-2-naphthol **425** as an organocatalyst (Scheme 118).²⁵³ The reaction proceeded smoothly in all the solvents screened except for methanol. Also, the reaction had significant limitation to the substrates employed. Substantial reduction in the ee was observed for aliphatic substituents ($\text{R}^1, \text{R}^2 = \text{alkyl}$), while linear aldehydes and ketones such as cyclohexanone/acetone failed to react. The origin of enantioselectivity was attributed to preferential shielding of one of the faces of the enamine intermediate by the organocatalyst **425**. Aliphatic enamines suffered from *E/Z* isomerization leading to erosion in the enantioselectivities of the product.

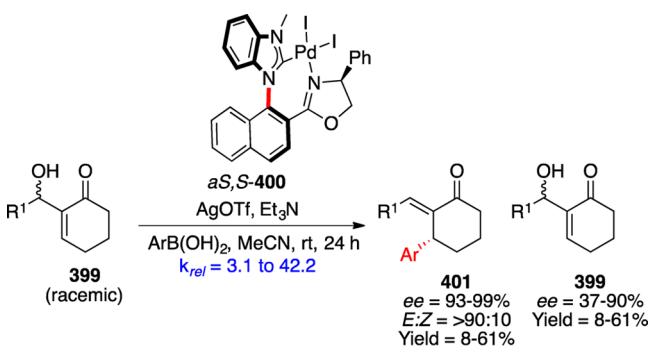
Table 2. Nonbiaryl Atropisomeric Systems in Asymmetric Allylic Alkylation Reaction



entry	ligand	solvent	t (h)	additive	yield (%)	% ee	ref
1	383	DCM	96	15-crown-5	30 ^a	52 (S)	238
2	384	DCM	36	15-crown-5	65 ^a	87 (R)	238
3	385	DCM	72	KOAc	60	90 –	151
4	386	DCM	24	–	23 ^b	52 –	60
5	387	–	24	–	93	82 (S)	223
6	388	Et ₂ O	24	LiOAc	95 ^c	85 –	239
7	389	DCM	4	NaOAc	89	94 (S)	240
8	390	DCM	4	LiOAc	97	93 (R)	240
9	391	PhMe	72	LiOAc	63 ^d	91 (S)	158
10	392	PhMe	24	LiOAc	97 ^e	95 (S)	241
11	393	PhMe	24	LiOAc	93	93 (S)	242, 243
12	394	Et ₂ O	24	LiOAc	99	99 (R)	244
13	395	MeCN	48	LiOAc	98 ^d	88 (S)	245

^aNaH used as a base. ^bCatalyst was Pd₂(dba)₃. ^cTemperature was 4 °C. ^dTemperature was 0 °C. ^eTemperature was –10 °C.

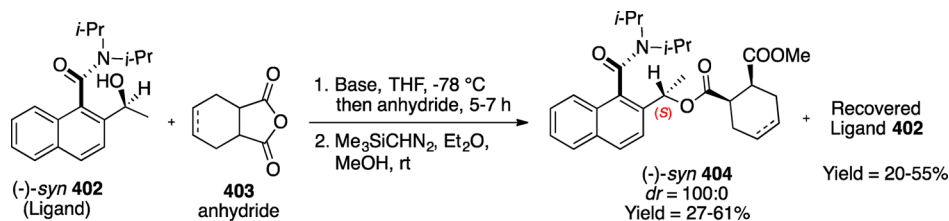
Scheme 112



R¹ = Ph, *p*-CNPh, *p*-CH₃Ph, *p*-OMePh, *m*-ClPh, *o*-ClPh, *p*-NO₂Ph, CH₃, cyclohexyl, 2,4-*d*ClPh.
Ar = Ph, *o*-CH₃Ph, *m*-CH₃Ph, *p*-CH₃Ph, *o*-CH₃Ph, *o*-ClPh, *p*-ClPh, *o*-OMePh, 2-Naphthyl, *p*-C₆H₅Ph

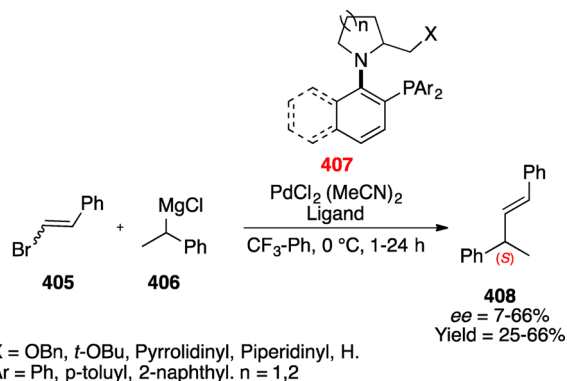
4.5.6. Michael Addition. Jørgenson and co-workers also reported an enantioselective Michael addition reaction of ethyl-2-oxocycloalkenone carboxylate **427** to acrolein and methyl vinyl ketone **428** mediated by cinchona-based atropisomeric organocatalyst **429** (Scheme 119). Reaction optimization revealed that iodobenzene was an excellent solvent for the reaction and the reaction proceeded smoothly to furnish the Michael addition

Scheme 113



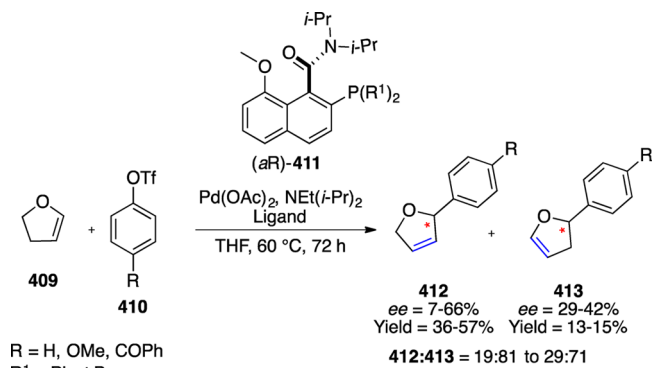
Base: *n*-BuLi, NaH, KH

Scheme 114



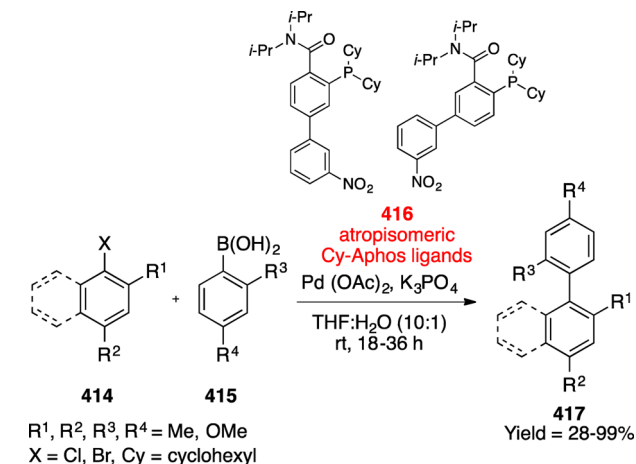
X = OBn, *t*-OBu, Pyrrolidinyl, Piperidinyl, H.
Ar = Ph, *p*-toluyl, 2-naphthyl. n = 1,2

Scheme 115



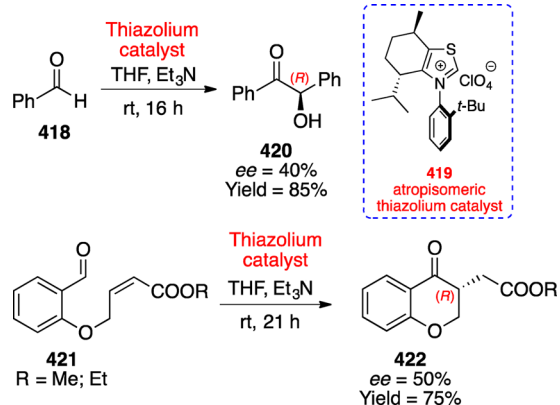
R = H, OMe, COPh
R¹ = Ph, *t*-Bu

Scheme 116

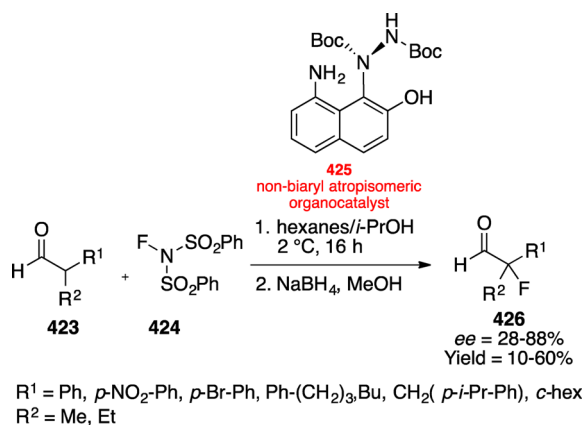


R¹, R², R³, R⁴ = Me, OMe
X = Cl, Br, Cy = cyclohexyl

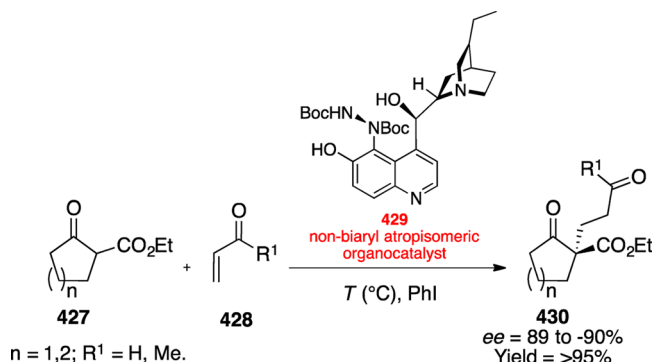
Scheme 117



Scheme 118



Scheme 119



product **430** in excellent yield and enantioselectivity. Interestingly, on lowering the temperature from 25 to 0 °C, the sense of stereoinduction was reversed (ee at 25 °C was -90% and at 0 °C was 89%). In general, cyclopentanone derivatives yielded products with higher ee than their six-membered analogues (cyclohexanones).

4.5.7. [3 + 2]-Cycloaddition. Xu, Xia, and co-workers reported a highly efficient and selective catalytic asymmetric cycloaddition reaction using atropisomeric P,O ligands.²⁵⁴ The atropisomeric aromatic amide *syn*-(*R,R*)-**433** serves as the ligand in silver catalyzed [3 + 2]-cycloaddition of aldiminoesters with nitroalkenes leading to nitrosubstituted pyrrolidines **434** in excellent ee (>99:1) and dr (95–99%). While the ligand **433** suffered racemization at the axial chirality at room temperature, under their reaction condition (-20 °C) it was stable enough to

promote the reaction efficiently. Interestingly, without the addition of ligand the cycloaddition yielded *endo*-selective product, but in the presence of the ligand complete reversal in the selectivity was observed leading to *exo*-**434** (Scheme 120). The single crystal X-ray analysis of Ag-ligand complex revealed that the two oxygen atoms (amide carbonyl and S=O) with the phosphine atom coordinate to provide the chiral environment, which also explains the dependence of ee on the epimerization of the axial chirality.

Recently, Faigl, Mátravölgyi, and co-workers reported an efficient amino alcohol derived atropisomeric pyrrole as a chiral ligand to promote for the enantioselective addition of diethylzinc to aldehydes.²⁵⁵ The ligand **436** is an improvement to their previously reported atropisomeric pyrrole ligand.^{256–259} The reaction proceeded smoothly to result in alcohol **437** (Scheme 121) with excellent yield and enantioselectivity. The substitution on the aromatic ring of the aldehyde had little influence on the outcome of the yield or ee. The reaction was hypothesized to occur via a nine-membered cyclic adduct in which the coordinated diethylzinc attacks the *Si*-face of the aldehyde leading to enantioenriched alcohol. The axial chirality on the atropisomeric pyrrole and the substituents (phenyl and pyrrolidine) ensures proper orientation of the organometallic species and aldehyde and provides necessary facial discrimination.

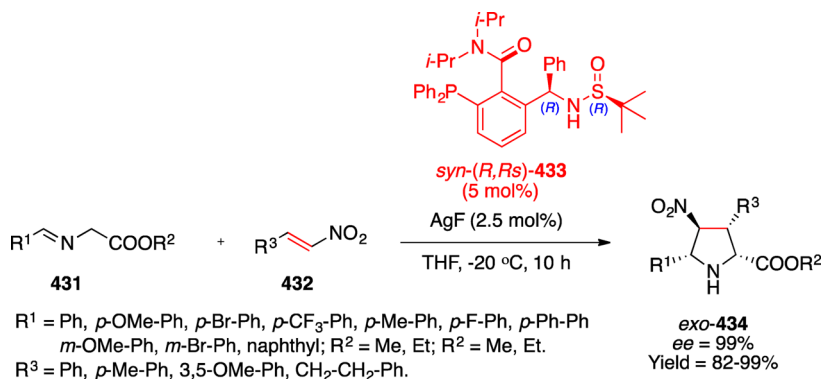
4.6. Atropselective Photoreactions

For a long time, investigations on the use of nonbiaryl atropisomers in stereoselective/atropselective reactions focused mostly on reactions under thermal conditions. In contrast, very few of these reactions explored alternate activation methods, especially photochemical activation. Bach and co-workers carried out early attempts on photoreactions in which they employed atropisomeric enamides **438** as ground state reactive partners to an excited aldehyde (Scheme 122).²⁶⁰ The diastereoselectivity in the oxetane products **439** and **440** was only modest, but provided a strong indication that face shielding dictated by axial chirality was feasible.²⁶¹

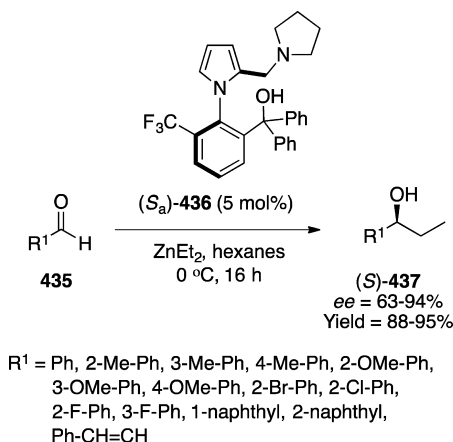
Nevertheless, this did not lure the photochemical community to adopt atropisomers to perform atropselective phototransformations. A probable reason might have been concern over controlling the short-lived excited state species to provide meaningful chiral induction. While photochemistry of compounds obtained by spontaneous crystallization was slowly developing, photoreaction in solution remained dormant for almost a decade, until research from Sivaguru and co-workers revealed the importance of axial chirality in atropisomers for imparting chiral induction in several photochemical transformations. They showed that photoexcited atropisomers are excellent scaffolds for controlling excited state reactivity and demonstrated this by employing them for various photochemical transformations. They also demonstrated that the photochemical and photophysical properties of atropisomers are different from their achiral counterparts (vide infra).

4.6.1. 6 π -Photocyclization. Sivaguru and co-workers reported photochemical reactions involving excited atropisomeric acrylanilides **441** that underwent enantioselective 6 π -photocyclization leading to 3,4-dihydro-quinoline-2-one photo-products **442/443** (Scheme 123).^{262–264} They observed the regiochemistry of photocyclization was dependent on the substitution on the anilide nitrogen. If the nitrogen was unsubstituted (NH), photocyclization occurred at the unsubstituted *o*-carbon of the acrylanilide. On the other hand, if the

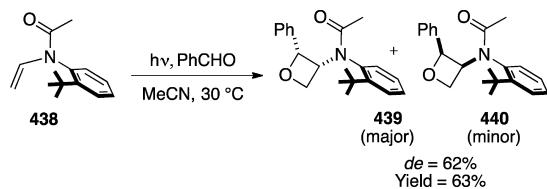
Scheme 120



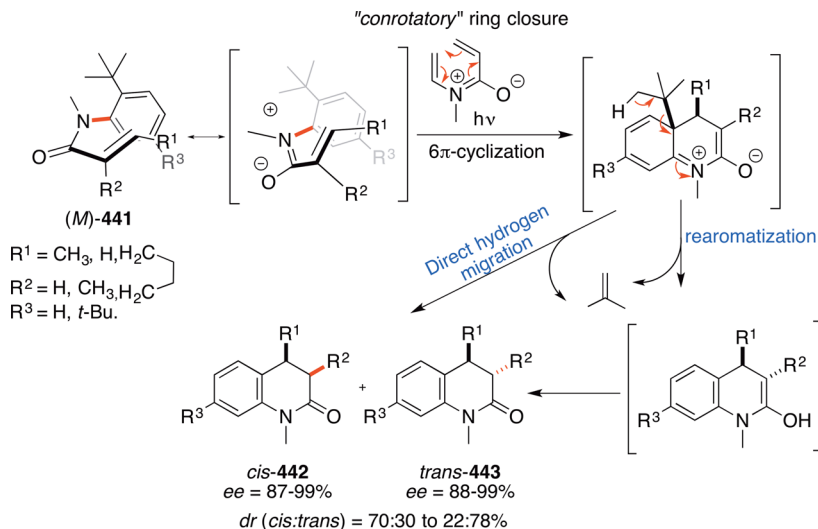
Scheme 121



Scheme 122



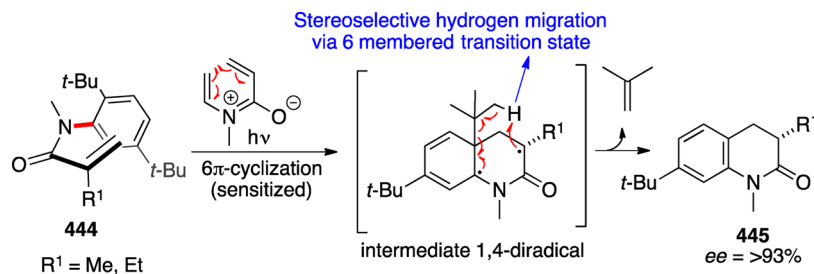
Scheme 123



anilide nitrogen was substituted (e.g., N-alkyl), the *conrotatory* 6π -photocyclization occurred exclusively on the carbon bearing the *t*-Bu group on the phenyl ring. Expulsion of 2-methylpropene occurred during the rearomatization process. This outcome was attributed to relief of strain caused by *t*-Bu group in the photoproduct.

The atropisomeric acrylanilides **441** had fairly high energy barriers for racemization allowing them to be separated and stored without the loss of absolute configuration. The enantioselective photocyclization carried out on individual atropisomers revealed some critical information about the importance of the substitution on the acrylanilides. The atropisomers do not interconvert at ambient temperature even in the excited state (obeying the NEER principle),^{265–267} and the presence of a β -substituent on the alkene (R^1) was crucial in order to obtain high atropselectivity in the photoreaction that occurred from the singlet excited state (direct irradiation). Under direct irradiation conditions, the *conrotatory* ring closure proceeded via a singlet excited state leading to a zwitterionic intermediate. For substrates possessing β -substituents, the axial to central chiral transfer occurred at the newly formed benzylic position. Subsequent aromatization with the loss of an 2-methylpropene unit followed by protonation of the enolate created the second chiral center leading to *cis*-**442** and *trans*-**443** photoproducts with identical enantiomeric excess (the first cyclization step dictating the stereochemistry in the photo-

Scheme 124

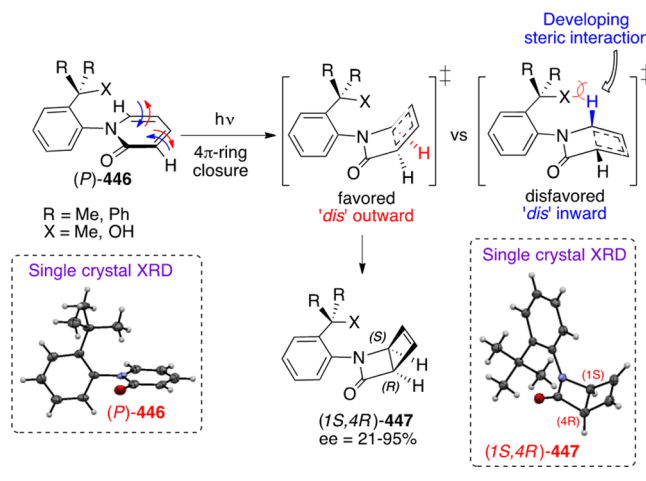


product). The mechanistic rationale was further bolstered by the reaction of α -substituted atropisomeric acrylanilides that gave racemic products due to the nonstereospecific second step. To improve the enantioselectivity in the photoproduct from α -substituted atropisomeric acrylanilides, triplet sensitized irradiations were carried out in acetone serving as a solvent and sensitizer. Triplet sensitized reaction of α -substituted atropisomeric acrylanilides **444** gave photoproduct **445** with high enantiomeric excess (direct irradiation in trifluoroethanol resulted in racemic photoproducts; Scheme 124).²⁶⁸ Under sensitized condition, the reaction proceeded via a diradical pathway (rather than a zwitterionic pathway that was observed during direct irradiation) leading to a 1,4-diradical. The 1,4-diradical abstracted a hydrogen atom from the *t*-Bu group via a six-membered transition state leading to highly enantioenriched photoproduct **445**.

Similar levels of enantioenrichment were also observed when acrylanilides lacking β -substitution were subjected to direct irradiation in a crystalline matrix (optically pure crystal of acrylanilide)²⁶⁹ and in the presence of heavy alkali metal ions (Cs⁺).²⁷⁰ High selectivity was observed in the crystalline media due to molecular confinement that enabled atropselective migration of *tert*-butyl hydrogen followed by elimination of 2-methylpropene. In the presence of heavy cations, the enhanced intersystem crossing from the singlet excited state enabled the reaction to proceed from the triplet manifold in spite of direct irradiation of the substrate leading to higher enantioselectivity in the photoproduct (via a diradical intermediate; similar to the one proposed for sensitized reaction in Scheme 124).

4.6.2. 4 π -Photocyclization. 2-Pyridones are one of the well-studied chromophores that undergo either intramolecular 4 π -ring closure or intermolecular [4 + 4]-photocycloaddition depending on the concentration employed.^{271–275} Axial to central chiral strategy on 4 π -ring closure of 2-pyridones revealed the effectiveness of steric biasing in achieving high enantioselectivity in the photoproduct (Scheme 125).¹³³ 4 π -Ring closure occurs through *disrotatory* ring closure on either face of the ring (inward face or outward face) leading to racemic photoproducts. Sivaguru and co-workers reported atropselective 4 π -ring closure of atropisomeric 2-pyridones **446**.¹³³ The presence of a bulky group at the *ortho*-position shielded one of the enantiotopic faces forcing the ring closure to occur away from the steric bulk leading to enantioenriched β -lactam photoproducts **447**. Depending on the type of facial shielding (*viz.*, compounds with pure sterics (*t*-Bu) or compounds having a blend of sterics and H-bonding unit) and the solvent employed, the enantiomeric excess varied significantly in the photoproduct **447**. The enantiomeric excess in the photoproduct showed greater temperature and solvent dependency for pyridones with the ability to form intra- and intermolecular H-bonding (R, X = Me, OH or Ph, OH), whereas compounds lacking them (R, X = Me) showed only minimal

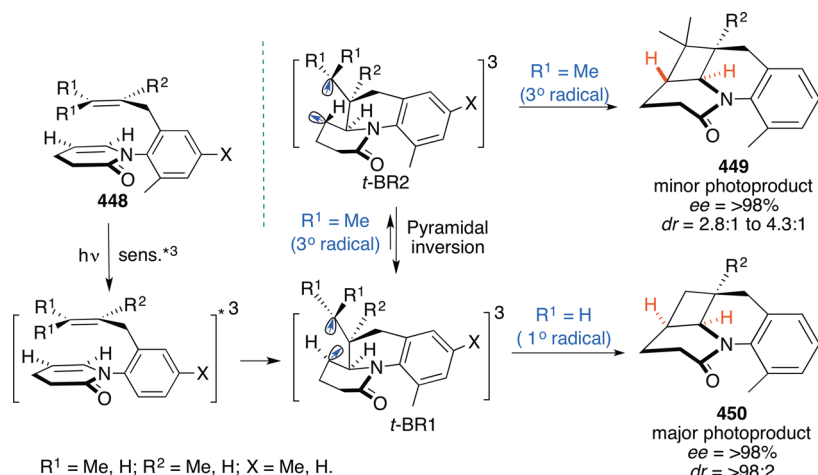
Scheme 125



temperature and solvent dependencies. Analysis of Eyring parameters and deciphering the mechanistic pathway through absolute crystal structure of reactants and their photoproducts enabled determination of the mode of photocyclization for a given atropisomer. The result aligned well with the hypothesis that the steric bias indeed operates very effectively. If atropisomerism is due to pure sterics such as an *ortho tert*-butyl group, the differential activation entropic contribution ($\Delta\Delta S^\ddagger$) was less significant than the differential activation enthalpic contributions ($\Delta\Delta H^\ddagger$). On the other hand, for the atropisomeric compounds that are influenced by H-bonding, both ($\Delta\Delta S^\ddagger$) and ($\Delta\Delta H^\ddagger$) played a significant role contributing to the observed temperature and solvent dependency during 4 π -ring closure.

4.6.3. [2 + 2]-Photocycloaddition. Four-membered ring forming reactions via a photochemical process is one of the widely utilized strategies in organic synthesis.^{276–278} But only recently the [2 + 2]-photocycloaddition reactions involving atropisomers were documented by Sivaguru and co-workers using atropisomeric dihydropyridones (Scheme 126).¹³⁵ Photocycloaddition of dihydropyridones **448** proceeded well under sensitized irradiation with very high enantioselectivity. The diastereomeric ratio of the products depended on the substituents on the alkenyl tether. Dihydropyridones **448** with unsubstituted terminal carbon (R¹ = H) gave very high dr values (>98:2), whereas the dihydropyridones with disubstituted alkenyl tether (R¹ = Me) gave poor dr values (2.8:1 in acetone and 4.3:1 in MeOH). Mechanistically, the reaction proceeded via a triplet pathway leading to a 1,4-biradical (*t*-BR1) at the carbon bearing R¹ substituent. If R¹ = H, the resulting short-lived primary radical center rapidly intersystem crossed and cyclized to product with good ee and dr values. However, if R¹ = Me the resultant 3° radical (*t*-BR2) lived long enough for the β -carbon of

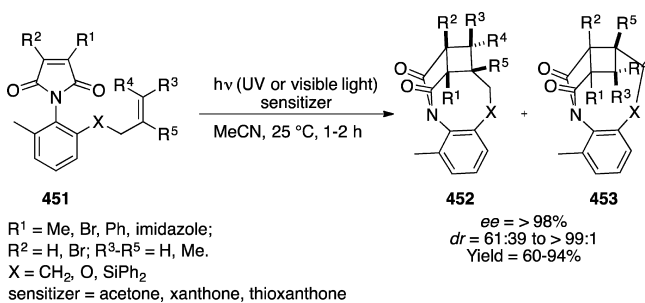
Scheme 126



the lactam ring to undergo pyramidal inversion leading to poor dr in the photoproduct.

Similarly, Sivaguru and co-workers also investigated UV/visible light mediated [2 + 2]-photocycloaddition of atropisomeric maleimides that led to several interesting observations (Scheme 127).²⁷⁹ *N*-Alkyl maleimides are known to undergo

Scheme 127

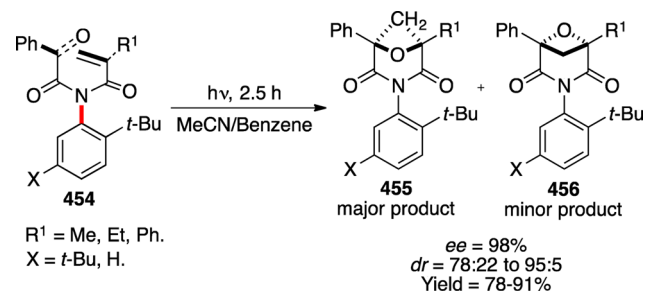


both [2 + 2]- and [5 + 2]-photocycloaddition reactions depending on the irradiation conditions (direct irradiation favoring [5 + 2] and sensitized irradiation favoring [2 + 2] products).^{280,281} On the other hand, in case of atropisomeric *N*-aryl maleimides **451**, the chemoselectivity ([2 + 2] vs [5 + 2]) depended on the chain length of the alkenyl tether. For example, maleimide with allyl tether gave the [5 + 2] product exclusively, whereas the butenyl counterpart gave the [2 + 2] product.²⁷⁹

The ee value in the [2 + 2]-photocycloaddition was very high (>98%), while the dr depended on the type of R (R^1 – R^5) substituent. The substituent at the maleimide double bond exerted greater influence than the substituent on the alkenyl tether. Detailed photophysical and mechanistic studies revealed that the triplet lifetime of the maleimide was short-lived. However, energy transfer from external sensitizers such as xanthone and thioxanthone occurred at a diffusion controlled rate to promote the photoreaction.

A variation in the [2 + 2]-photocycloaddition between an alkene and an excited carbonyl compound termed as Paternò–Büchi is a synthetically useful strategy to access oxetane photoproducts (see Scheme 122).^{282,283} Sivaguru and co-workers reported atropselective intramolecular Paternò–Büchi reaction of α -oxoamides **454** resulting in oxetane product with excellent ee and dr (Scheme 128).¹³⁸ The photoreaction of

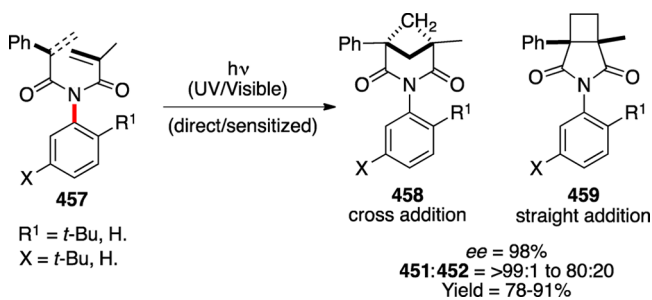
Scheme 128



atropisomeric oxoamides **454** proceeded effectively than the achiral analogues, where the axial chirality exerted conformational control in the solution and forced reaction partners to be in the vicinity to undergo desired photocycloaddition in a facile manner. The diastereomeric ratio in the cross cycloaddition product (**455**:**456**) was higher ranging from 78:22 to 95:5 depending on the R^1 substituent. Interestingly, when optically pure crystal of α -oxoamide **454** (for substrate $R^1 = \text{Et}$) was subjected to photolysis in the solid state, a reversal in the dr was observed **455**:**456** (15:85). The reversal in the product selectivity suggested that conformational preference of α -oxoamides **454** was different in solution and in the solid state.

Similarly, photochemistry of atropisomeric acrylamides (as in **457**) was quite different when compared to nonatropisomeric acrylamides.²⁸⁴ The acrylamide **457** underwent highly regioselective [2 + 2]-photocycloaddition to furnish cross cycloadduct **458** with excellent ee and de (Scheme 129). On the contrary, the nonatropisomeric analogue (lacking *t*-Bu group at the *ortho* position) yielded a mixture of straight and cross addition product

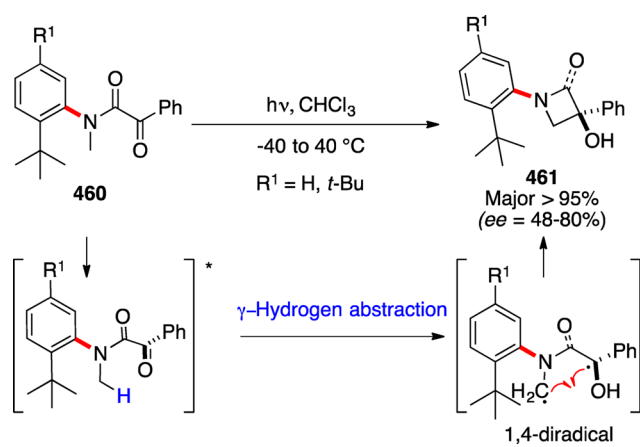
Scheme 129



(458:459 was 80:20). This clearly indicates the impact of axial chirality in influencing the conformations of chromophores thus affecting the selectivity in a given photoreaction.

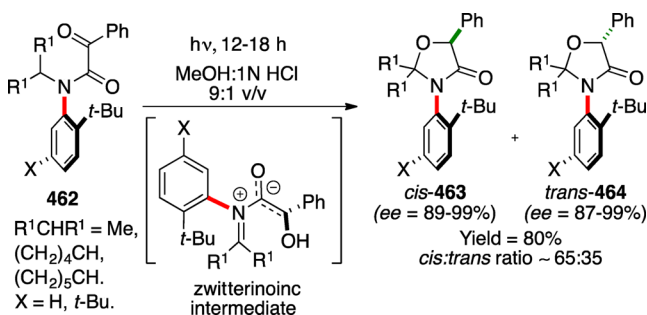
4.6.4. Hydrogen Abstraction. One of the well-known reactions of the excited state carbonyl compounds is H-abstraction reaction termed as Norrish/Yang type-II reaction. Sivaguru and co-workers reported an atropselective Norrish/Yang type-II reaction of atropisomeric α -oxoamides **460** in solution (Scheme 130).²⁸⁵ The reaction proceeded from an $n\pi^*$

Scheme 130



excited state of the carbonyl compound that initiated γ -hydrogen abstraction from the N–Me substituent resulting in a 1,4-diradical. This diradical subsequently cyclized leading to chirally enriched β -lactam photoproduct **461**. Since the 1,4-diradical was free to rotate in solution, competition between bond rotation and cyclization played a crucial role in determining the enantiomeric excess in the photoproduct. This manifested as temperature dependent axial central chiral transfer in which lower temperature resulted in higher selectivity in the β -lactam photoproduct (ee at 40 and -40 °C was 48 and 80% respectively). A slight change in the reaction conditions (replacing chloroform with MeOH:1 N HCl) changed the chemoselectivity of the reaction leading to enantioenriched oxazolidinone products **463/464** (Scheme 131).¹³⁹ The reaction proceeded through a zwitterionic

Scheme 131

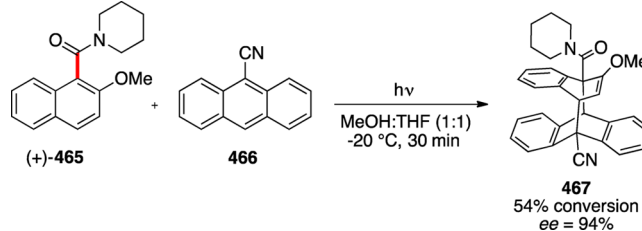


intermediate (both diradical or zwitterionic pathways are feasible) that cyclized to form *cis*-**463** and *trans*-**464** products in a 65:35 ratio. The absolute configuration of the axial chirality was preserved during the reaction resulting in the same configuration being observed in the product. Subjection of *trans*-**464** to higher temperature (120 °C for 5 h) led to isomerization resulting in thermodynamic equilibrium (65:35 *cis*-

463:trans-464) without compromising the optical purity of the stereogenic center providing an avenue for resolution of the photoproducts.

4.6.5. Photochemistry of Chiral Crystals. Photochemistry of homochiral crystals of achiral molecules obtained through spontaneous crystallization or chiral crystallization is well-studied and holds a basis for absolute asymmetric synthesis.^{286–290} In addition, memory of chirality in photoreactions have been explored.^{139,289} Sakamoto and co-workers reported asymmetric photocycloaddition of axially chiral naphthamides with 9-CN anthracene in solution (Scheme 132).¹⁵² The

Scheme 132

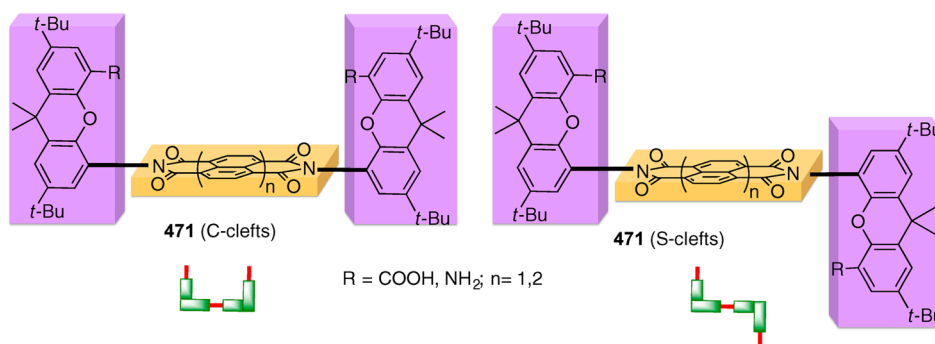
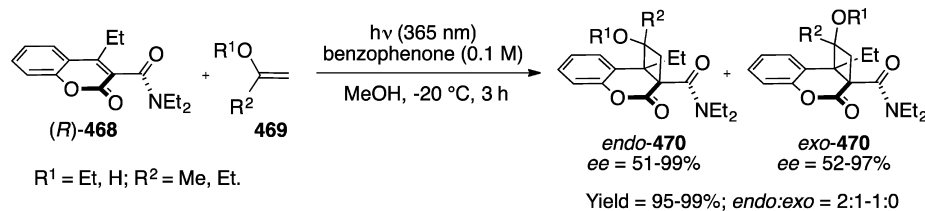


optically pure naphthamides **465** were acquired through spontaneous crystallization of the melt. Large-scale enantiomerically pure crystals were obtained by seeding the melt with the desired enantiomer of the naphthamide. The C–CO rotation barrier of naphthamides **465** in solution was low at room temperature and slightly increased at lower temperatures (half-life of enantiomerization ~ 2 h in 1:1 MeOH:THF mixture at 15 °C). Similarly, L-proline derived naphthamides were crystallized as a single diastereomer using the melt approach even though multiple diastereomers existed in solution due to axial chirality and *E,Z*-isomerization. The optically pure crystals of **465** were dissolved in THF, and diastereoselective photocycloaddition with 9-CN anthracene **466** was performed at low temperature yielding stereoselective photocycloadducts.²⁹¹ The same group also reported highly stereoselective reactions of several homochiral photosubstrates that were acquired through a spontaneous crystallization technique that includes intramolecular Paternò–Büchi reactions of tetrahydronaphthyl imide derivatives,²⁹² intramolecular [2 + 2]-photocycloaddition of *N,N*-diallyl-2-quinolone-3-carboxamides,²⁹³ and intermolecular [2 + 2]-photocycloaddition of naphthamides with dienes.²⁹⁴

In further investigation along this vein, Sakamoto and co-workers reported a unique photosensitized asymmetric reaction involving a homochiral molecule **468** that was generated by spontaneous crystallization (Scheme 133).²⁹⁵ A methanolic solution of optically pure *N,N*-diethyl carboxamide **468** underwent [2 + 2]-photocycloaddition with alkenes **469** resulting in cyclobutane photoproducts **470**. The reaction proceeded from both the singlet and the triplet excited states. However, the singlet state reaction was slow and it competed with racemization of atropisomers, thus leading to poor selectivity in the photoproducts. On the other hand, if the reaction was carried out under benzophenone sensitized conditions, the reaction proceeded smoothly at low temperature where racemization occurred much more slowly compared to the photoreaction yielding *endo*-**470** and *exo*-**470** cyclobutane adduct in very high selectivity.

4.6.6. Photochemistry of Atropisomeric Compounds under Elevated Pressures. The atropisomeric compounds with stable chiral axes are observed to undergo photoreaction

Scheme 133

Figure 7. Molecular clefts derived from diimides **471**.

under ambient conditions with excellent stereocontrol. On the other hand, if the compounds have labile chiral axes (compounds with low energy barriers for racemization), the photoreaction suffers from poor stereocontrol due to loss of absolute configuration in the atropisomers. Lowering reaction temperature can be used to control racemization. However, this approach fails when one requires higher temperatures for successful outcome of a reaction. To address this bottleneck, Sivaguru and co-workers evaluated pressure as a remedy to arrest racemization and increase the stereoselectivity in photoreactions.²⁹⁶ Atropisomeric acrylanilide **441**, 2-pyridone **446**, and α -oxoamide **460** were evaluated for their racemization kinetics under elevated pressures. By a slight increase in pressure, the rate of racemization was significantly reduced increasing the half-life of racemization (even at higher temperatures). The enantioselective phototransformations carried out on 2-pyridones **446** and α -oxoamides **460** at high temperature (acetonitrile, $70\text{ }^\circ\text{C}$) and pressure (0.1, 20, and 100 MPa) revealed a discernible increase in the enantiomeric excess in the resulting products. For example, the enantioselectivity in the photoproduct during photoreaction of 2-pyridones **446** at $70\text{ }^\circ\text{C}$ was 4, 18, and 27% at 0.1, 20, and 100 MPa, respectively. This is the result of an increased racemization barrier where the atropisomeric molecules were able to maintain their absolute configuration for an efficient axial to central chiral transfer. This investigation provided a simple proof of principle that can be extended to other asymmetric reactions involving atropisomeric compounds.

4.7. Molecular Machines and Gears

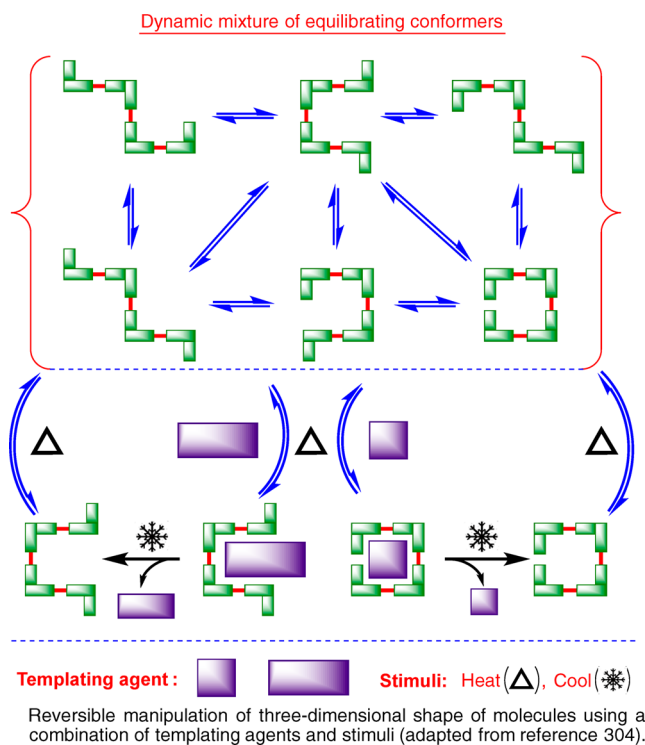
Axially chiral moieties with sufficient bulk around the chiral axis and high energy barriers for racemization provide molecular cleft like structures that are rigid. These molecular clefts are appealing in terms of their potential application in molecular recognition, as chiral catalysts for host–guest chemistry (molecular clefts acting as a host) and as molecular machines that can perform an action for a given stimulus.^{297,298} In 1984, Rebek and co-workers introduced Kemp's triacid based molecular cleft like structures that showed preferential epoxidation of *cis*-alkenes over *trans*-

alkenes and made clefts more attractive and promising for selective reactions.²⁹⁹ Ease of synthesis and structural diversity that can lead to molecules of various sizes and shapes were also appealing.

Rebek and co-workers reported a new family of molecular clefts that showed restricted rotation around the N_{aryl} –imide bond **471** (C-clefts) and **471** (S-clefts) with energy barriers for racemization higher than $28\text{ kcal}\cdot\text{mol}^{-1}$ (Figure 7).^{300,301} These molecules are highly preorganized, where the R groups are held firmly (restricted rotation) by H-bonding from the internal hydrogens. Thermodynamic binding analysis with various guest molecules such as quinoxalinedione showed strong 1:1 complexation demonstrating the affinity of these binding pockets. The same group also demonstrated the formation of metal complexes (Pd(II), Ag(I), and Au(I)) with C-shaped clefts with exclusive *trans* conformation and highly controlled coordination geometry and stoichiometry.³⁰²

In 2000, Shimizu and co-workers documented similar atropisomeric diacids (e.g., **472**) based on a N_{aryl} –imide bond that are stable atropisomers with a racemization barrier of $29.4\text{ kcal}\cdot\text{mol}^{-1}$ ($\tau_{1/2} = 35\text{ h}$ at $77\text{ }^\circ\text{C}$).¹⁵⁴ Further work along these lines in Shimizu's group involving *N*-aryl atropisomers led to the development of several molecular/nanodevices such as molecular switches and rotors that had chiral memory and shape persistency (Scheme 134).³⁰³ By employing suitable templating agents, they achieved controllable and programmable three-dimensional shapes at the molecular level. These shapes can be preserved or erased by providing suitable stimuli (such as temperature) even after the removal of the templating agents.

Axially chiral moieties were the perfect choice for molecular receptors that have read and write capability, as the chiral center rested on the single bond (chiral axis) was dynamic and can be controlled by temperature and sterics. Shimizu and co-workers demonstrated the recognition properties of these molecular clefts including the “write–save–erase” combination in the diacid derivative (e.g., **472**) involving guest molecule ethyl adenine-9-acetate (purple) as a templating agent (Figure 8).³⁰⁵ The diacid preferentially formed a 1:1 *syn* complex **472** ($K_a = 1100\text{ M}^{-1}$). Similarly, chelation ability of bis(pyridine) appended

Scheme 134^a

^aAdapted with permission from ref 304. Copyright 2009 Royal Society of Chemistry.

cleft (green, 473) toward metals such as Pd was also demonstrated by Shimizu and co-workers.³⁰⁶ The cleft could chelate with Pd in a *trans*-spinning geometry resulting in *syn*-473 quantitatively (*syn:anti* ratio = 100:0); this demonstrated the “writing” ability of the system. On removing the templating agent Pd (by the addition of TMEDA ligand), they could retain the geometry of the host (save), and upon increasing the temperature, the host system reached equilibrium state demonstrating the “erasing” ability. The reversible switching behavior can also be utilized as an ON and OFF recognition process.³⁰⁷ This process can be repeated several times through multiple cycles without appreciable reduction in the amplitude of switching. One of the distinguishing advantages of employing atropisomers for molecular switches was its ability to retain the switching mode (ON vs OFF) even after the removal of external

stimuli, whereas other supramolecular switches need the constant presence of their stimuli (guest molecules) to maintain their switching modes.³⁰⁸

Shimizu and co-workers also reported a method based on high-throughput screening of guest molecules with the aid of receptors 474 (Scheme 135).³⁰⁹ The process involved heating a 1:1 mixture of *syn:anti* receptor 474 in the presence of various guests (basic guest ranging from nucleoside, mono- and diamines) and analyzing the *syn/anti* ratio in the host–guest complex. The ratio reflected the affinity of the guest for a given atropisomeric receptor 474 (binding affinity was separately calculated by ¹H NMR titration studies). The advantage of this method was that the shape of the receptor was maintained even after the removal of the guest due to the presence of stable axial chirality. The same group further improved the versatility of their molecular clefts by introducing a resolution technique by employing a chiral guest molecule (chiral alkaloid), thus opening up new avenues for chiral switches.¹⁵⁷

The equilibrium ratio of *syn*-476 vs *anti*-476 (that are typically 1:1 at the equilibrium) can be affected by connecting the two *ortho* substituents by a linker attributing a “molecular spring” like behavior (Scheme 136).^{310,311} While the energetically preferable *syn*-476 is achiral, the chiral *anti*-476 that has the strained architecture (twisted spring) can be separated and preserved without erosion of the conformation due to the stabilization from axial chirality.

The studies on guest-induced conformational change of molecular receptors or molecular clefts have mostly been limited to atropisomeric imide derivatives. However, this principle can be applied to other systems that feature dynamic chirality. Clayden and co-workers demonstrated this concept by employing a new class of molecular receptors involving atropisomeric aromatic amide derivatives.³¹² The *N*-substituted xanthene-1,8-dicarboxamide 477 has a thermodynamic preference for *anti* conformer that is dictated by dipole repulsion. However, in the presence of a strong coordinating or chelating guest such as a Lewis acid (TiCl₄ or SnCl₄), this preference is switched to result in *syn*-477 conformer. However, in these systems the barrier to rotation is not high enough to retain the *syn*-477 conformation upon the removal of chelating metal. This issue was solved in a related system such as biphenyl-2,2'-dicarboxamide 478 (Scheme 137), where the energy barrier to rotation was significantly higher (26.2 kcal·mol⁻¹). The biphenyl dicarboxamide derivative 478 has only a weak preference to *anti* conformation and can be affected by the solvent (nonpolar solvent favoring *anti* conformation). *anti*-478 in toluene treated

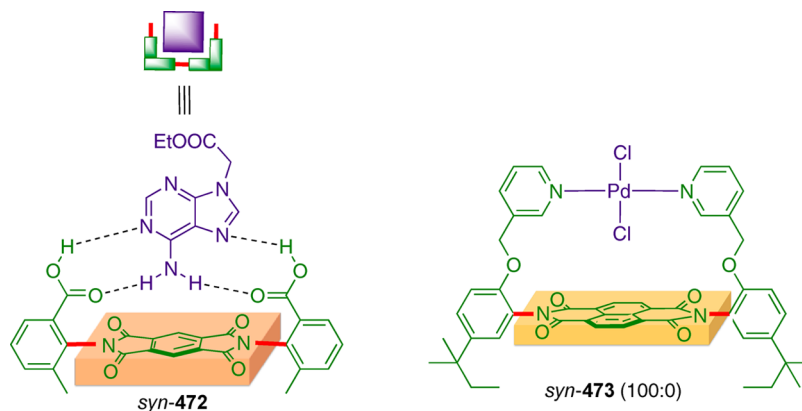
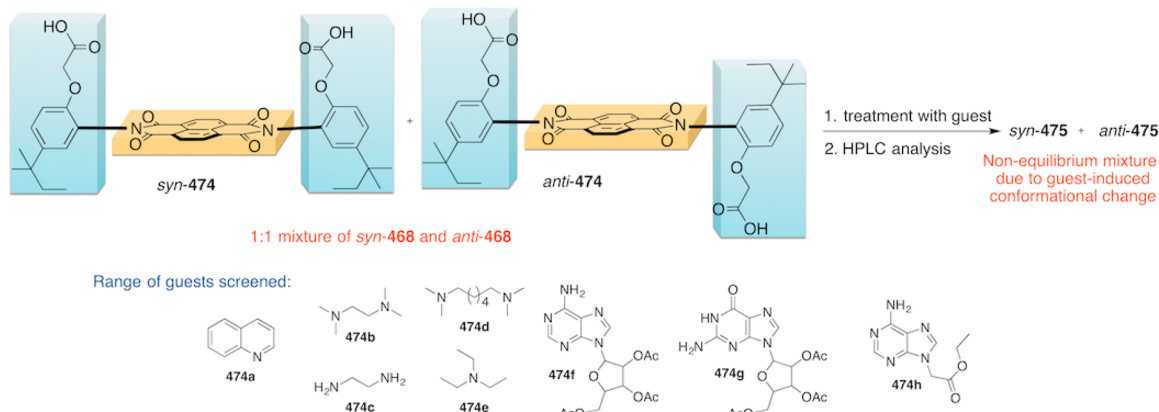
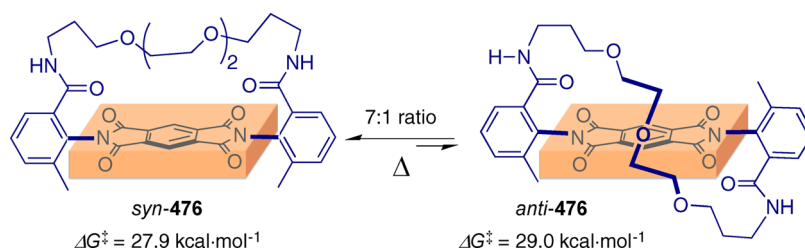


Figure 8. Molecular receptors.

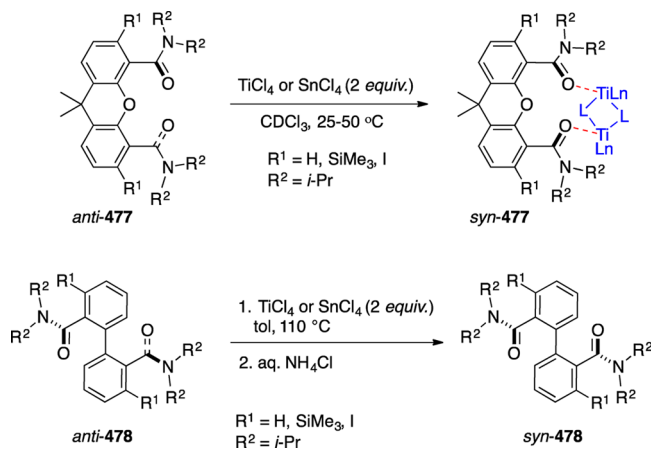
Scheme 135



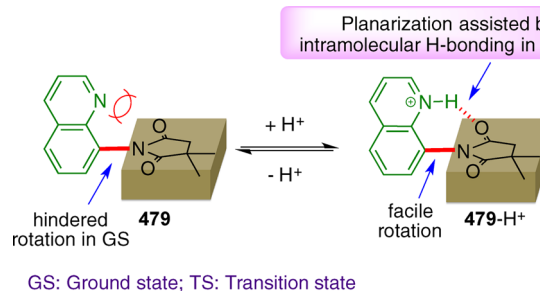
Scheme 136



Scheme 137



Scheme 138



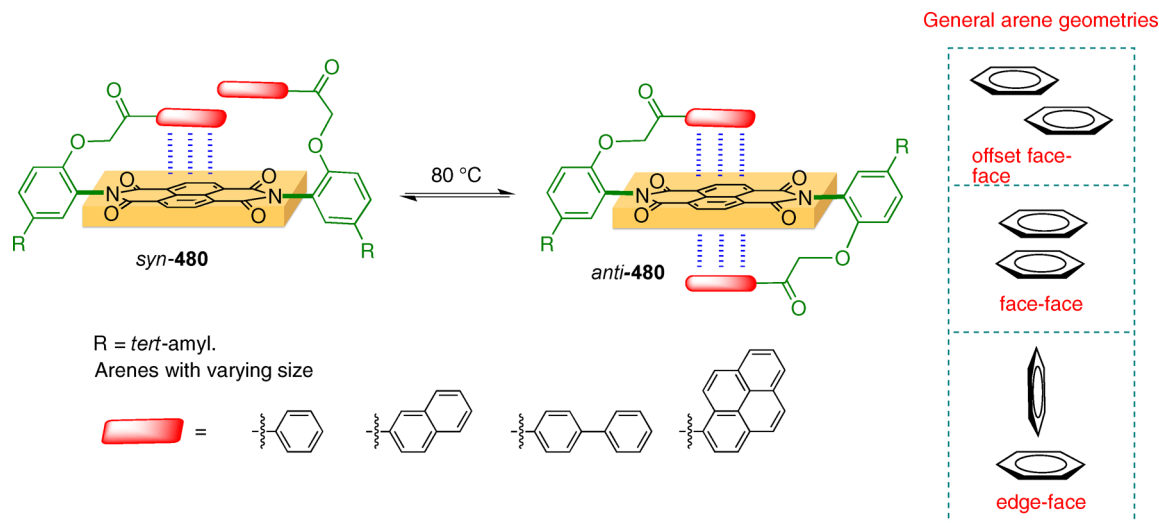
with 2 equiv of Lewis acid at higher temperature resulted in exclusive formation of *syn*-478. Upon decomplexation of the Lewis acid by aqueous NH_4Cl workup, the *syn* conformation is preserved due to the presence of stable chiral axis.

The energy barrier to racemization of an axially chiral molecule can be influenced by external stimuli. While most application involves the use of steric bulk and/or the complexation of guest to receptors to slow/arrest racemization, stimuli that accelerate the racemization process are not common.³¹³ The challenge of finding suitable stimuli that accelerate the racemization process was critical and has been addressed albeit at a slow pace compared to arresting racemization through stimuli. Shimizu and co-workers designed a novel atropisomeric molecular rotor **479** that rotated 10^7 times faster on protonation (Scheme 138).³¹⁴ The protonated form had a rotational barrier of $9.3 \text{ kcal}\cdot\text{mol}^{-1}$, while the unprotonated form had a rotational barrier of $\sim 20.2 \text{ kcal}\cdot\text{mol}^{-1}$. Analysis of the crystal structures of the protonated

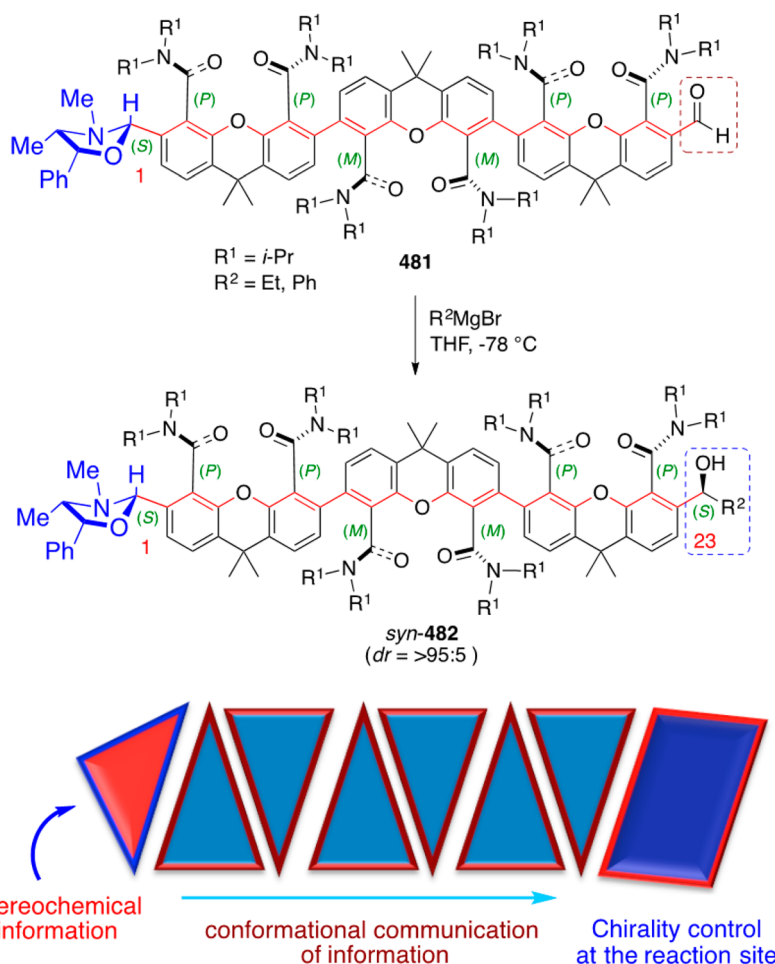
and unprotonated **479** showed that the ground state was not stabilized (crystal structures were isostructural and the dihedral angles were 87.9° and 80.0° for the unprotonated and protonated forms, respectively). This led the authors to conclude that the transition state was dramatically affected upon protonation that was responsible for the decreased rotational barrier. A similar system was also reported based on a guest accelerated molecular rotor by the same group where the complexation of the guest molecule (acetate ion) reduced the energy barrier to rotation by $2\text{--}4 \text{ kcal}\cdot\text{mol}^{-1}$.¹⁵⁵

Shimizu and co-workers also reported an atropisomeric substrate **480** that acted as a “molecular balance” for measuring face–face and arene–arene interaction both in solid state and in solution state (Scheme 139).^{315,316} The design was cleverly planned to avoid other modes of interactions, viz., slipped face–face and edge–arene interaction. Small model systems were chosen (compared to protein or peptides) to avoid other noncovalent interactions. The systems with larger arene surfaces preferred *anti*-**480** orientation (e.g. *anti*:*syn* ratios of 47:53 and 80:20 were observed for phenyl and pyrene derivatives in DMSO, respectively), and the ratio was solvent dependent. The results revealed a strong nonlinear free-energy trend, where

Scheme 139



Scheme 140



larger arene surfaces (pyrene and biphenyl) had a better arene–arene interaction than the smaller arene surfaces (phenyl and naphthyl) due to their greater polarizability. The observed nonlinear trend was attributed to conformational constraints and electrostatic impact of the acyl tether. Isotopic study carried out on similar systems to evaluate the CH– π vs CD– π interaction revealed that the interaction was not affected by the presence of

deuterium.³¹⁷ The experimental observation was bolstered by computational studies that also revealed the absence of isotopic effect in the CH– π interaction.

4.8. Stereochemical Relay through Conformation Control

Traditional methods to carry out asymmetric reactions involve the use of a chiral information source such as chiral catalysts or receptors to exert a certain influence over the substrate that

primarily targets the reaction site. This requirement of direct communication of the chiral source to the reaction site puts severe limitations on the stereochemical relay that might happen several bonds or distance away. To overcome this bottleneck, a completely new strategy was envisioned such that the stereochemical relay can be initiated at a remote place and transferred to the reaction without the loss of stereochemical information. One such system was elegantly designed by Clayden and co-workers taking advantage of the atropisomeric amide system (Scheme 140).^{229,230,318} In this system, three main interactions were reliably designed and controlled, viz., (a) interaction between the chiral perturber (ephedrine derived chiral oxazolidine unit) and the flexible unit (xanthene derived aromatic amide), (b) interaction between the flexible unit that communicated the information, and (c) flexible unit influencing the reaction site, e.g., nucleophilic addition to an aldehyde to yield diastereomerically enriched alcohol. Employing this system, they were able to achieve stereocontrol at the reaction site that was more than 20 bond lengths away corresponding to a linear distance of about 2.5 nm (*dr* > 95:5% in *syn*-482). The limitation to further extend this concept to control stereochemistry over longer distances was only hindered by the synthetic challenges involved in obtaining these substrates rather than the efficiency of information relay through the flexible units. This study clearly showed the potential of flexible chirality (especially in the atropisomeric aromatic amides) that can be tuned to design molecular devices and architectures that can relay and process information.

5. CONCLUSION AND OUTLOOK

Nonbiaryl atropisomeric systems have received significant attention in recent times due to their importance in the atropselective transformations and their applications in molecular devices. The presence of axial chirality in atropisomers imparts some unique reactivity that is not generally observed in central chiral molecules. The high level of enantio- and diastereoselectivity observed in both thermal and photochemical reactions of atropisomeric compounds makes them an attractive choice to access enantioenriched building blocks. Although some of the nonbiaryl atropisomeric compounds discussed in this review are not used as frequently as biaryl scaffolds for asymmetric synthesis and catalysis, their presence and performance were realized in some of the well-tested reactions, e.g., asymmetric allylic alkylation reactions. Further, the presence of axial chirality in natural products has made a strong impact on drug discovery and design strategy that necessitates careful attention to this dynamic chirality.

The emerging importance of these molecules as molecular recognition motifs, nanomachines, molecular clefts, etc. highlights the versatility of these nonbiaryl atropisomeric compounds in several other applications. While the current investigations are steered toward evaluating these compounds in the area where biaryl compounds dominate (as ligands in metal catalyzed reactions), more efforts are needed to extend the scope of these compounds in other areas of chemistry as well. The ability to switch the chirality by simple bond isomerization in these molecules provides an enticing opportunity and a challenge to employ them for novel applications in chemical systems.

AUTHOR INFORMATION

Corresponding Authors

*E-mail: sivaguru.jayaraman@ndsu.edu.

*E-mail: Mukund.Sibi@ndsu.edu.

Notes

The authors declare no competing financial interest.

Biographies



Elango Kumarasamy obtained his bachelor's degree from St. Joseph's College, Trichy, India, in 2004 and master's degree from Madras Christian College, Chennai, India, in 2006. After working in a pharmaceutical company for few years, he moved to North Dakota State University in the spring of 2010 for his doctoral studies under the guidance of Prof. Jayaraman Sivaguru. His doctoral thesis focused on stereospecific photochemical transformations of atropisomeric chromophores. He is the recipient of the prestigious NSF ND-EPSCoR doctoral dissertation fellowship and Closs award. He is currently a postdoctoral researcher in the Campos group, Columbia University.



Ramya Raghunathan obtained her bachelor's degree from S. D. N. B. Vaishnav College for Women, Chennai, India, in 2004 and master's degree from Madras Christian College, Chennai, India, in 2006. She then worked in a fast-moving consumer goods company before she moved to North Dakota State University for her doctoral studies in 2011. She is presently a fifth year graduate student performing her doctoral investigation under the mentorship of Prof. Jayaraman Sivaguru and Prof. Mukund P. Sibi. Her doctoral thesis is focused on stereospecific photochemical transformations of atropisomeric chromophores and photodegradation of oligomer/polymer derived from renewable bioresources.



Mukund P. Sibi was born in Bangalore, India. He received his early education from Bangalore University. He received his Ph.D. degree from the City University of New York under the mentorship of Prof. Robert Lichter. After postdoctoral studies in the laboratories of Profs. Gordon Gribble and Victor Snieckus, he started his independent academic career in 1987 at North Dakota State University (NDSU). He is currently the James A. Meier Professor and a University Distinguished Professor and serves as the project director for the Center for Protease Research at NDSU. His research interests include asymmetric synthesis, radical chemistry, total synthesis, medicinal chemistry, organocatalysis, and the use of biomass to prepare commodity chemicals. Prof. Sibi has received several awards in recognition of his scientific achievements that include the Fargo Chamber of Commerce Professorship, Arthur C. Cope Scholar Award, University Distinguished Professor, Japanese Society for Promotion of Science Fellow, James A. Meier Professorship, Dale Hogboom Professorship, and Jordan Engberg Professorship.



Jayaraman Sivaguru (Siva) is the James A. Meier Jr. Professor at the Department of Chemistry and Biochemistry, North Dakota State University. He completed his bachelor's (1996) and master's (1998) degrees from St. Joseph's College, Trichy, Tamil Nadu, India, and Indian Institute of Technology, Madras, Tamil Nadu, India, respectively. He came to the United States in 1998 to pursue his doctoral degree and worked with Prof. V. Ramamurthy at Tulane University, New Orleans, LA, USA. After receiving his Ph.D. in 2003, he did his postdoctoral studies with Prof. Nicholas J. Turro at Columbia University, NY, USA, from 2003 to 2006. Siva began his independent career as an assistant professor at NDSU in 2006 and was promoted as an associate professor in 2011 and as a full professor in 2014. He is a recipient of a 2008 NSF CAREER award, 2010 Grammaticakis-Neumann Prize from the Swiss Chemical Society for outstanding independent research by a young faculty under the age of 40 in the fields of photochemistry or photophysics or molecular photobiology, 2011 young-investigator award from the Inter-American Photochemical Society (I-APS), and

2012-young investigator award from Sigma-Xi. At NDSU, Siva has been honoured with the 2010 Excellence in Research award and 2011 Excellence in Teaching award, both from the College of Science and Mathematics, and the 2012 Peltier Award for Innovation in Teaching. He was a 2011 Global Centre for Excellence visiting young professor at Osaka University, Suita Campus, Osaka, Japan. In 2013, he was named the American editor for the *Journal of Photochemistry and Photobiology A: Chemistry*, published by Elsevier. In 2014, he was named as the James A. Meier Jr. Professor at NDSU. His research interests on light induced processes span the areas of supramolecular photochemistry, asymmetric photochemistry, organo-photocatalysis, supramolecular photocatalysis, and molecular recognition in chemical and biological systems. Currently his research program is investigating (a) light induced axial to central chiral transfer in atropisomeric systems, (b) atropisomeric templates for asymmetric organo-photocatalysis, (c) supramolecular photocatalysis with water-soluble nanocontainers, and (d) light responsive materials derived from biomass.

ACKNOWLEDGMENTS

J.S. thanks the National Science Foundation for generous support for his research (CHE-1465075, CHE-1213880 and CAREER CHE-0748525). E.K. and J.S. thank the NSF ND-EPSCoR for generous funding for student fellowships for E.K. (EPS-0814442 and IIA-1355466). R.R., J.S., and M.P.S. thank the NDSU for the doctoral dissertation fellowship for R.R. The authors thank Dr. Rethesh Krishnan and Nandini Vallavoju for their contributions in the preparation of the manuscript.

ABBREVIATIONS

TLC thin layer chromatography
 dr diastereomeric ratio
 ee enantioselectivity
 er enantiomeric ratio

REFERENCES

- (1) Cahn, R. S.; Ingold, C.; Prelog, V. Specification of Molecular Chirality. *Angew. Chem., Int. Ed. Engl.* **1966**, *5*, 385–415.
- (2) Christie, G. H.; Kenner, J. The Molecular Configurations of Polynuclear Aromatic Compounds. *J. Chem. Soc., Trans.* **1922**, *121*, 614–620.
- (3) Kuhn, R. Molekulare Asymmetrie. In *Stereochemie*; Freudenberg, K., Ed.; Franz Deuticke: Leipzig, 1933, p 803.
- (4) Oki, M. Recent Advances in Atropisomerism. *Top. Stereochem.* **1983**, *14*, 1–81.
- (5) Miyashita, A.; Yasuda, A.; Takaya, H.; Toriumi, K.; Ito, T.; Souchi, T.; Noyori, R. Synthesis of 2,2'-bis(diphenylphosphino)-1,1'-binaphthyl (BINAP), an atropisomeric chiral bis(triaryl)phosphine, and its use in the rhodium(I)-catalyzed asymmetric hydrogenation of α -(acylamino)-acrylic acids. *J. Am. Chem. Soc.* **1980**, *102*, 7932–7934.
- (6) Bringmann, G.; Menche, D. Stereoselective Total Synthesis of Axially Chiral Natural Products via Biaryl Lactones. *Acc. Chem. Res.* **2001**, *34*, 615–624.
- (7) Bringmann, G.; Gulder, T.; Gulder, T. A. M.; Breuning, M. Atroposelective Total Synthesis of Axially Chiral Biaryl Natural Products. *Chem. Rev.* **2011**, *111*, 563–639.
- (8) LaPlante, S. R.; Edwards, P. J.; Fader, L. D.; Jakalian, A.; Hucke, O. Cover Picture: Revealing Atropisomer Axial Chirality in Drug Discovery. *ChemMedChem* **2011**, *6*, 381–381.
- (9) Rosini, C.; Franzini, L.; Raffaelli, A.; Salvadori, P. Synthesis and Applications of Binaphthyl C2-Symmetry Derivatives as Chiral Auxiliaries in Enantioselective Reactions. *Synthesis* **1992**, *1992*, 503–517.
- (10) Wencel-Delord, J.; Panossian, A.; Leroux, F. R.; Colobert, F. Recent Advances and New Concepts for the Synthesis of Axially Stereoenriched Biaryls. *Chem. Soc. Rev.* **2015**, *44*, 3418–3430.

- (11) Mikami, K.; Aikawa, K.; Yusa, Y.; Jodry, J. J.; Yamanaka, M. Tropos or Atropos? That is the Question! *Synlett* **2002**, 1561–1578.
- (12) Clayden, J. Non-Biaryl Atropisomers: New Classes of Chiral Reagents, Auxiliaries, and Ligands? *Angew. Chem., Int. Ed. Engl.* **1997**, *36*, 949–951.
- (13) Clayden, J. Stereocontrol with Rotationally Restricted Amides. *Synlett* **1998**, 1998, 810–816.
- (14) Clayden, J.: Non-Biaryl Atropisomers: New Classes of Chiral Reagents, Auxiliaries and Ligands? In *Organic Synthesis Highlights IV*; Wiley-VCH Verlag GmbH: Weinheim, Germany, 2000; pp 48–52.
- (15) Clayden, J. Atropisomers and Near-Atropisomers: Achieving Stereoselectivity by Exploiting the Conformational Preferences of Aromatic Amides. *Chem. Commun.* **2004**, 127–135.
- (16) Campolo, D.; Gastaldi, S.; Roussel, C.; Bertrand, M. P.; Nechab, M. Axial-to-Central Chirality Transfer in Cyclization Processes. *Chem. Soc. Rev.* **2013**, *42*, 8434–8466.
- (17) Clayden, J.; Vassiliou, N. Stereochemical Relays: Communication via Conformation. *Org. Biomol. Chem.* **2006**, *4*, 2667–2678.
- (18) Curran, D. P.; Qi, H.; Geib, S. J.; DeMello, N. C. Atroposelective Thermal Reactions of Axially Twisted Amides and Imides. *J. Am. Chem. Soc.* **1994**, *116*, 3131–3132.
- (19) Hughes, A. D.; Price, D. A.; Shishkin, O.; Simpkins, N. S. Diastereoselective Enolate Chemistry Using Atropisomeric Amide. *Tetrahedron Lett.* **1996**, *37*, 7607–7610.
- (20) Kitagawa, O.; Izawa, H.; Taguchi, T.; Shiro, M. An Efficient Synthesis of Optically Active Axially Chiral Anilide and its Application to Iodine-Mediated Asymmetric Diels-Alder Reaction. *Tetrahedron Lett.* **1997**, *38*, 4447–4450.
- (21) Kitagawa, O.; Izawa, H.; Sato, K.; Dobashi, A.; Taguchi, T.; Shiro, M. Optically Active Axially Chiral Anilide and Maleimide Derivatives as New Chiral Reagents: Synthesis and Application to Asymmetric Diels-Alder Reaction. *J. Org. Chem.* **1998**, *63*, 2634–2640.
- (22) Hughes, A. D.; Price, D. A.; Simpkins, N. S. Atropisomeric Amides: Stereoselective Enolate Chemistry and Enantioselective Synthesis via a New SmI₂-Mediated Reduction. *J. Chem. Soc., Perkin Trans. 1* **1999**, 1295–1304.
- (23) Hughes, A. D.; Simpkins, N. S. SmI₂-Mediated Reduction of α -Functionalised Amides: Highly Enantiospecific Access to an Atropisomeric Amide. *Synlett* **1998**, 1998, 967–968.
- (24) Kitagawa, O.; Momose, S.-i.; Fushimi, Y.; Taguchi, T. Efficient Synthesis of Various Atropisomeric Amides in Optically Pure Forms and Their Application to Asymmetric Reactions. *Tetrahedron Lett.* **1999**, *40*, 8827–8831.
- (25) Hata, T.; Koide, H.; Taniguchi, N.; Uemura, M. Asymmetric Synthesis of Axially Chiral Anilides by Enantiotopic Lithiation of Tricarbonyl(N-methyl-N-acyl-2,6-dimethylanilide)chromium Complex. *Org. Lett.* **2000**, *2*, 1907–1910.
- (26) Koide, H.; Hata, T.; Uemura, M. Asymmetric Synthesis of Axially Chiral Benzamides and Anilides by Enantiotopic Lithiation of Prochiral Arene Chromium Complexes. *J. Org. Chem.* **2002**, *67*, 1929–1935.
- (27) Kitagawa, O.; Kohriyama, M.; Taguchi, T. Catalytic Asymmetric Synthesis of Optically Active Atropisomeric Anilides through Enantioselective N-Allylation with Chiral Pd-tol-BINAP Catalyst. *J. Org. Chem.* **2002**, *67*, 8682–8684.
- (28) Terauchi, J.; Curran, D. P. N-Allylation of Anilides with Chiral Palladium Catalysts: The First Catalytic Asymmetric Synthesis of Axially Chiral Anilides. *Tetrahedron: Asymmetry* **2003**, *14*, 587–592.
- (29) Kitagawa, O.; Takahashi, M.; Yoshikawa, M.; Taguchi, T. Efficient Synthesis of Optically Active Atropisomeric Anilides through Catalytic Asymmetric N-Arylation Reaction. *J. Am. Chem. Soc.* **2005**, *127*, 3676–3677.
- (30) Kitagawa, O.; Yoshikawa, M.; Tanabe, H.; Morita, T.; Takahashi, M.; Dobashi, Y.; Taguchi, T. Highly Enantioselective Synthesis of Atropisomeric Anilide Derivatives through Catalytic Asymmetric N-Arylation: Conformational Analysis and Application to Asymmetric Enolate Chemistry. *J. Am. Chem. Soc.* **2006**, *128*, 12923–12931.
- (31) Kitagawa, O.; Kurihara, D.; Tanabe, H.; Shibuya, T.; Taguchi, T. Catalytic Enantioselective Synthesis of Key Intermediates for NET Inhibitors Using Atropisomeric Lactam Chemistry. *Tetrahedron Lett.* **2008**, *49*, 471–474.
- (32) Tanaka, K.; Takeishi, K.; Noguchi, K. Enantioselective Synthesis of Axially Chiral Anilides through Rhodium-Catalyzed [2 + 2 + 2] Cycloaddition of 1,6-Diynes with Trimethylsilylynamides. *J. Am. Chem. Soc.* **2006**, *128*, 4586–4587.
- (33) Oppenheimer, J.; Hsung, R. P.; Figueroa, R.; Johnson, W. L. Stereochemical Control of Both C–C and C–N Axial Chirality in the Synthesis of Chiral N,O-Biaryls. *Org. Lett.* **2007**, *9*, 3969–3972.
- (34) Shirakawa, S.; Liu, K.; Maruoka, K. Catalytic Asymmetric Synthesis of Axially Chiral o-Iodoanilides by Phase-Transfer Catalyzed Alkylations. *J. Am. Chem. Soc.* **2012**, *134*, 916–919.
- (35) Liu, K.; Wu, X.; Kan, S. B. J.; Shirakawa, S.; Maruoka, K. Phase-Transfer-Catalyzed Asymmetric Synthesis of Axially Chiral Anilides. *Chem. - Asian J.* **2013**, *8*, 3214–3221.
- (36) Ates, A.; Curran, D. P. Synthesis of Enantioenriched Axially Chiral Anilides from Atropisomerically Enriched Tartarate Ortho-Anilides. *J. Am. Chem. Soc.* **2001**, *123*, 5130–5131.
- (37) Bowles, P.; Clayden, J.; Tomkinson, M. Diastereoisomeric Atropisomers from the Addition of Lithiated N,N-Dialkyl-L-Naphthamides to Aldehydes. *Tetrahedron Lett.* **1995**, *36*, 9219–9222.
- (38) Bowles, P.; Clayden, J.; Helliwell, M.; McCarthy, C.; Tomkinson, M.; Westlund, N. Atroposelectivity in the Reactions of Ortholithiated Aromatic Tertiary Amides with Aldehydes. *J. Chem. Soc., Perkin Trans. 1* **1997**, 2607–2616.
- (39) Thayumanavan, S.; Beak, P.; Curran, D. P. Asymmetric Deprotonation of N,N-Dihexyl-1-Naphthamides to Provide Atropisomers of N,N-Dihexyl-2-Alkyl-1-Naphthamides. *Tetrahedron Lett.* **1996**, *37*, 2899–2902.
- (40) Beak, P.; Basu, A.; Gallagher, D. J.; Park, Y. S.; Thayumanavan, S. Regioselective, Diastereoselective, and Enantioselective Lithiation–Substitution Sequences: Reaction Pathways and Synthetic Applications. *Acc. Chem. Res.* **1996**, *29*, 552–560.
- (41) Clayden, J.; Johnson, P.; Pink, J. H. Asymmetric Synthesis of Enantiomerically Enriched Atropisomeric Amides by Desymmetrisation of N,N-Dialkylmesitamidates. *J. Chem. Soc., Perkin Trans. 1* **2001**, 371–375.
- (42) Ikeura, Y.; Doi, T.; Fujishima, A.; Natsugari, H. Enantioselective Synthesis of an Axially Chiral 1,7-Naphthyridine-6-Carboxamide Derivative Having Potent Antagonist Activity at the NK1 Receptor. *Chem. Commun.* **1998**, 2141–2142.
- (43) Natsugari, H.; Ikeura, Y.; Kamo, I.; Ishimaru, T.; Ishichi, Y.; Fujishima, A.; Tanaka, T.; Kasahara, F.; Kawada, M.; Doi, T. Axially Chiral 1,7-Naphthyridine-6-carboxamide Derivatives as Orally Active Tachykinin NK1 Receptor Antagonists: Synthesis, Antagonistic Activity, and Effects on Bladder Functions. *J. Med. Chem.* **1999**, *42*, 3982–3993.
- (44) Ikeura, Y.; Ishichi, Y.; Tanaka, T.; Fujishima, A.; Murabayashi, M.; Kawada, M.; Ishimaru, T.; Kamo, I.; Doi, T.; Natsugari, H. Axially Chiral N-Benzyl-N,7-dimethyl-5-phenyl-1,7-naphthyridine-6-carboxamide Derivatives as Tachykinin NK1 Receptor Antagonists: Determination of the Absolute Stereochemical Requirements. *J. Med. Chem.* **1998**, *41*, 4232–4239.
- (45) Koide, H.; Uemura, M. Synthesis of Axially Chiral N,N-Diethyl 2,6-Disubstituted Benzamides Utilizing Planar Chiral (Arene)Chromium Complexes. *Chem. Commun.* **1998**, 2483–2484.
- (46) Clayden, J. P.; Lai, L. W. Enantioselective Synthesis of Atropisomeric Amides by Dynamic Resolution: Thermodynamic Control with a Proline-Derived Diamine Resolving Agent. *Angew. Chem., Int. Ed.* **1999**, *38*, 2556–2558.
- (47) Clayden, J.; Lai, L. W. (–)-Ephedrine as an Auxiliary for the Asymmetric Synthesis of Atropisomeric Amides by Dynamic Resolution Under Thermodynamic Control. *Tetrahedron Lett.* **2001**, *42*, 3163–3166.
- (48) Clayden, J.; Lai, L. W.; Helliwell, M. Dynamic Resolution of Atropisomeric Amides Using Proline-Derived Imidazolines and Ephedrine-Derived Oxazolidines. *Tetrahedron* **2004**, *60*, 4399–4412.

- (49) Clayden, J.; Mitjans, D.; Youssef, L. H. Lithium–Sulfoxide–Lithium Exchange for the Asymmetric Synthesis of Atropisomers under Thermodynamic Control. *J. Am. Chem. Soc.* **2002**, *124*, 5266–5267.
- (50) Rios, R.; Jimeno, C.; Carroll, P. J.; Walsh, P. J. Kinetic Resolution of Atropisomeric Amides. *J. Am. Chem. Soc.* **2002**, *124*, 10272–10273.
- (51) Dai, W.-M.; Zhang, Y.; Zhang, Y. Synthesis of Atropisomeric 2,8-Dioxygenated N,N-Diisopropyl-1-Naphthamides via Kinetic Resolution Under Sharpless Asymmetric Dihydroxylation Conditions. *Tetrahedron: Asymmetry* **2004**, *15*, 525–535.
- (52) Brandes, S.; Bella, M.; Kjærsgaard, A.; Jørgensen, K. A. Chirally Aminated 2-Naphthols—Organocatalytic Synthesis of Non-Biaryl Atropisomers by Asymmetric Friedel–Crafts Amination. *Angew. Chem., Int. Ed.* **2006**, *45*, 1147–1151.
- (53) Suda, T.; Noguchi, K.; Hirano, M.; Tanaka, K. Highly Enantioselective Synthesis of N,N-Dialkylbenzamides with Aryl–Carbonyl Axial Chirality by Rhodium-Catalyzed [2 + 2 + 2] Cycloaddition. *Chem. - Eur. J.* **2008**, *14*, 6593–6596.
- (54) Tanaka, K.; Takahashi, Y.; Suda, T.; Hirano, M. Synthesis of Enantioenriched N-Aryl-2-pyridones with Chiral C–N Axes by Rhodium-Catalyzed [2 + 2 + 2] Cycloaddition of Alkynes with Isocyanates. *Synlett* **2008**, *2008*, 1724–1728.
- (55) Barrett, K. T.; Miller, S. J. Enantioselective Synthesis of Atropisomeric Benzamides through Peptide-Catalyzed Bromination. *J. Am. Chem. Soc.* **2013**, *135*, 2963–2966.
- (56) Takahashi, H.; Wakamatsu, S.; Tabata, H.; Oshitari, T.; Harada, A.; Inoue, K.; Natsugari, H. Atropisomerism Observed in Indometacin Derivatives. *Org. Lett.* **2011**, *13*, 760–763.
- (57) Porter, J.; Payne, A.; Whitcombe, I.; de Candole, B.; Ford, D.; Garlish, R.; Hold, A.; Hutchinson, B.; Trevitt, G.; Turner, J.; Edwards, C.; Watkins, C.; Davis, J.; Stubberfield, C. Atropisomeric Small Molecule Bcl-2 Ligands: Determination of Bioactive Conformation. *Bioorg. Med. Chem. Lett.* **2009**, *19*, 1767–1772.
- (58) Chauhan, P.; Kaur, J.; Chinni, S. S. Asymmetric Organocatalytic Addition Reactions of Maleimides: A Promising Approach Towards the Synthesis of Chiral Succinimide Derivatives. *Chem. - Asian J.* **2013**, *8*, 328–346.
- (59) Shimizu, K. D.; Freyer, H. O.; Adams, R. D. Synthesis, Resolution and Structure of Axially Chiral Atropisomeric N-Arylimides. *Tetrahedron Lett.* **2000**, *41*, 5431–5434.
- (60) Chen, Y.; Smith, M. D.; Shimizu, K. D. An Axially Chiral Phosphine Ligand Based on Restricted Rotation in N-Arylimides. *Tetrahedron Lett.* **2001**, *42*, 7185–7187.
- (61) Duan, W.-L.; Imazaki, Y.; Shintani, R.; Hayashi, T. Asymmetric Construction of Chiral C–N Axes Through Rhodium-Catalyzed 1,4-Addition. *Tetrahedron* **2007**, *63*, 8529–8536.
- (62) Di Iorio, N.; Righi, P.; Mazzanti, A.; Mancinelli, M.; Ciogli, A.; Bencivenni, G. Remote Control of Axial Chirality: Aminocatalytic Desymmetrization of N-Arylmaleimides via Vinylogous Michael Addition. *J. Am. Chem. Soc.* **2014**, *136*, 10250–10253.
- (63) Eudier, F.; Righi, P.; Mazzanti, A.; Ciogli, A.; Bencivenni, G. Organocatalytic Atroposelective Formal Diels–Alder Desymmetrization of N-Arylmaleimides. *Org. Lett.* **2015**, *17*, 1728–1731.
- (64) Bringmann, G.; Tasler, S.; Endress, H.; Peters, K.; Peters, E.-M. Synthesis of Mukonine and Seven Further 1-Oxygenated Carbazole Alkaloids. *Synthesis* **1998**, *1998*, 1501–1505.
- (65) Bringmann, G.; Tasler, S.; Endress, H.; Kraus, J.; Messer, K.; Wohlfarth, M.; Lobin, W. Murrastifoline-F: First Total Synthesis, Atropo-Enantiomer Resolution, and Stereoanalysis of an Axially Chiral N,C-Coupled Biaryl Alkaloid. *J. Am. Chem. Soc.* **2001**, *123*, 2703–2711.
- (66) Kamikawa, K.; Kinoshita, S.; Matsuzaka, H.; Uemura, M. Stereoselective Synthesis of Axially Chiral N–C Bonds in N-Aryl Indoles. *Org. Lett.* **2006**, *8*, 1097–1100.
- (67) Kamikawa, K.; Kinoshita, S.; Furusyo, M.; Takemoto, S.; Matsuzaka, H.; Uemura, M. Stereoselective Synthesis of Both Enantiomers of N-Aryl Indoles with Axially Chiral N–C Bonds. *J. Org. Chem.* **2007**, *72*, 3394–3402.
- (68) Ototake, N.; Morimoto, Y.; Mokuya, A.; Fukaya, H.; Shida, Y.; Kitagawa, O. Catalytic Enantioselective Synthesis of Atropisomeric Indoles with an N–C Chiral Axis. *Chem. - Eur. J.* **2010**, *16*, 6752–6755.
- (69) Bock, L. H.; Adams, R. The Stereochemistry of N-Phenylpyrroles. The Preparation and Resolution of N-2-Carboxyphenyl-2,5-Dimethyl-3-Carboxypyrrole XIII. *J. Am. Chem. Soc.* **1931**, *53*, 374–376.
- (70) Kanakis, A. A.; Sarli, V. Total Synthesis of (±)-Marinopyrrole A via Copper-Mediated N-Arylation. *Org. Lett.* **2010**, *12*, 4872–4875.
- (71) Cheng, C.; Pan, L.; Chen, Y.; Song, H.; Qin, Y.; Li, R. Total Synthesis of (±)-Marinopyrrole A and Its Library as Potential Antibiotic and Anticancer Agents. *J. Comb. Chem.* **2010**, *12*, 541–547.
- (72) Hughes, C. C.; Kauffman, C. A.; Jensen, P. R.; Fenical, W. Structures, Reactivities, and Antibiotic Properties of the Marinopyrroles A–F. *J. Org. Chem.* **2010**, *75*, 3240–3250.
- (73) Sugane, T.; Hamada, N.; Tobe, T.; Hamaguchi, W.; Shimada, I.; Maeno, K.; Miyata, J.; Suzuki, T.; Kimizuka, T.; Sakamoto, S.; Tsukamoto, S. -i. Practical and Efficient Synthesis of the (R)-Atropisomer of A 4-Phenyl 1,2,4-Triazole Derivative as a Selective Glyt1 Inhibitor. *Tetrahedron: Asymmetry* **2012**, *23*, 1528–1533.
- (74) Fujita, M.; Kitagawa, O.; Izawa, H.; Dobashi, A.; Fukaya, H.; Taguchi, T. Stereoselective Synthesis of an Optically Active Axially Chiral Lactam and its Reaction with Some Electrophiles. *Tetrahedron Lett.* **1999**, *40*, 1949–1952.
- (75) Kitagawa, O.; Fujita, M.; Kohriyama, M.; Hasegawa, H.; Taguchi, T. Stereoselective Synthesis of Diastereomeric Atropisomeric Lactam with Various Ring Sizes and Their Structural Characterization. *Tetrahedron Lett.* **2000**, *41*, 8539–8544.
- (76) Takahashi, M.; Tanabe, H.; Nakamura, T.; Kuribara, D.; Yamazaki, T.; Kitagawa, O. Atropisomeric Lactam Chemistry: Catalytic Enantioselective Synthesis, Application to Asymmetric Enolate Chemistry and Synthesis of Key Intermediates for NET Inhibitors. *Tetrahedron* **2010**, *66*, 288–296.
- (77) Liu, H.; Feng, W.; Kee, C. W.; Leow, D.; Loh, W.-T.; Tan, C.-H. Brønsted Base-Catalyzed Tandem Isomerization–Michael Reactions of Alkynes: Synthesis of Oxacycles and Azacycles. *Adv. Synth. Catal.* **2010**, *352*, 3373–3379.
- (78) Sakamoto, M.; Utsumi, N.; Ando, M.; Saeki, M.; Mino, T.; Fujita, T.; Katoh, A.; Nishio, T.; Kashima, C. Breaking the Symmetry of Axially Chiral N-Aryl-2(1H)-pyrimidinones by Spontaneous Crystallization. *Angew. Chem., Int. Ed.* **2003**, *42*, 4360–4363.
- (79) Kondepudi, D. K.; Laudadio, J.; Asakura, K. Chiral Symmetry Breaking in Stirred Crystallization of 1,1'-Binaphthyl Melt. *J. Am. Chem. Soc.* **1999**, *121*, 1448–1451.
- (80) Junghänel, J.; Buss, V.; Beyrich, T.; Jira, T. Circular Dichroism of Axially Chiral Methaqualone, 3-Aryl-2-Mercapto- and 3-Aryl-2-Alkylthio-4(3H)-Quinazolinones: Conformational Dependence of CD and Assignment of Absolute Configuration. *Chirality* **1998**, *10*, 253–261.
- (81) Welch, W. M.; Ewing, F. E.; Huang, J.; Menniti, F. S.; Pagnozzi, M. J.; Kelly, K.; Seymour, P. A.; Guanowsky, V.; Guhan, S.; Guinn, M. R.; Critchett, D.; Lazzaro, J.; Ganong, A. H.; DeVries, K. M.; Staigers, T. L.; Chenard, B. L. Atropisomeric Quinazolin-4-One Derivatives are Potent Noncompetitive A-Amino-3-Hydroxy-5-Methyl-4-Isoxazolepropionic Acid (AMPA) Receptor Antagonists. *Bioorg. Med. Chem. Lett.* **2001**, *11*, 177–181.
- (82) Sun, H. H.; Barrow, C. J.; Cooper, R. Benzomalvin D, a New 1,4-Benzodiazepine Atropisomer. *J. Nat. Prod.* **1995**, *58*, 1575–1580.
- (83) Dai, X.; Wong, A.; Virgil, S. C. Synthesis and Resolution of Quinazolinone Atropisomeric Phosphine Ligands. *J. Org. Chem.* **1998**, *63*, 2597–2600.
- (84) Tokitoh, T.; Kobayashi, T.; Nakada, E.; Inoue, T.; Yokoshima, S.; Takahashi, H.; Natsugari, H. Diastereoselective Synthesis of Atropisomeric 3-(2-Substituted Aryl)quinazolin-4-ones and Their Stereochemical Properties. *Heterocycles* **2006**, *70*, 93–99.
- (85) Takahashi, I.; Morita, F.; Kusagaya, S.; Fukaya, H.; Kitagawa, O. Catalytic Enantioselective Synthesis of Atropisomeric 2-Aryl-4-Quinolinone Derivatives with an N–C Chiral Axis. *Tetrahedron: Asymmetry* **2012**, *23*, 1657–1662.
- (86) Haushalter, K. A.; Lau, J.; Roberts, J. D. An NMR Investigation of the Effect of Hydrogen Bonding on the Rates of Rotation about the C–N Bonds in Urea and Thiourea. *J. Am. Chem. Soc.* **1996**, *118*, 8891–8896.

- (87) Adler, T.; Bonjoch, J.; Clayden, J.; Font-Bardia, M.; Pickworth, M.; Solans, X.; Sole, D.; Vallverdu, L. Slow Interconversion Of Enantiomeric Conformers or Atropisomers of Anilide and Urea Derivatives of 2-Substituted Anilines. *Org. Biomol. Chem.* **2005**, *3*, 3173–3183.
- (88) Clayden, J.; Lemiegre, L.; Pickworth, M.; Jones, L. Conformation and Stereodynamics of 2,2'-Disubstituted N,N'-Diaryl Ureas. *Org. Biomol. Chem.* **2008**, *6*, 2908–2913.
- (89) Clayden, J.; Turner, H. Enantiomerically enriched atropisomeric N,N'-diaryl ureas by oxidative kinetic resolution of their 2-sulfanyl derivatives. *Tetrahedron Lett.* **2009**, *50*, 3216–3219.
- (90) Nicolaou, K. C.; Boddy, C. N. C.; Bräse, S.; Winssinger, N. Chemistry, Biology, and Medicine of the Glycopeptide Antibiotics. *Angew. Chem., Int. Ed.* **1999**, *38*, 2096–2152.
- (91) Crowley, B. M.; Boger, D. L. Total Synthesis and Evaluation of [Ψ [CH₂NH]Tpg₄]Vancomycin Aglycon: Reengineering Vancomycin for Dual d-Ala-d-Ala and d-Ala-d-Lac Binding. *J. Am. Chem. Soc.* **2006**, *128*, 2885–2892.
- (92) Dahlgard, M.; Brewster, R. Q. Absorption Spectra of Some Highly Substituted Diaryl Ethers. *J. Am. Chem. Soc.* **1958**, *80*, 5861–5863.
- (93) Lehmann F., P. A. Conformations of Highly Hindered Aryl Ethers—IV PMR Studies of 2,4- And 2,6- Dinitroaryl Ethers. *Org. Magn. Reson.* **1970**, *2*, 467–490.
- (94) Bergman, J. J.; Chandler, W. D. A Study of the Barriers to Rotation in Some Highly Substituted Diphenyl Ethers. *Can. J. Chem.* **1972**, *50*, 353–363.
- (95) Duggan, B. M.; Craik, D. J. Conformational Dynamics of Thyroid Hormones by Variable Temperature Nuclear Magnetic Resonance: The Role of Side Chain Rotations and Cisoid/Transoid Interconversions. *J. Med. Chem.* **1997**, *40*, 2259–2265.
- (96) Fuji, K.; Oka, T.; Kawabata, T.; Kinoshita, T. The First Synthesis of an Optically Active Molecular Bevel Gear with Only Two Cogs on Each Wheel. *Tetrahedron Lett.* **1998**, *39*, 1373–1376.
- (97) Betson, M. S.; Clayden, J.; Worrall, C. P.; Peace, S. Three Groups Good, Four Groups Bad? Atropisomerism in ortho-Substituted Diaryl Ethers. *Angew. Chem., Int. Ed.* **2006**, *45*, 5803–5807.
- (98) Betson, M. S.; Clayden, J. Synthesis of Multiply ortho-Substituted Diaryl Ethers via Lithiation and Oxidation of a Dibenzosiloxane (Phenoxasilin). *Synlett* **2006**, 0745–0746.
- (99) Kunz, K.; Scholz, U.; Ganzer, D. Renaissance of Ullmann and Goldberg Reactions - Progress in Copper Catalyzed C-N-, C-O- and C-S-Coupling. *Synlett* **2003**, 2428–2439.
- (100) Ley, S. V.; Thomas, A. W. Modern Synthetic Methods for Copper-Mediated C(aryl)-O, C(aryl)-N, and C(aryl)-S Bond Formation. *Angew. Chem., Int. Ed.* **2003**, *42*, 5400–5449.
- (101) Krizan, T. D.; Martin, J. C. Directed Ortho Lithiation of Isophthalonitrile. New Methodology for the Synthesis of 1,2,3-Trisubstituted Benzenes. *J. Org. Chem.* **1982**, *47*, 2681–2682.
- (102) Koizumi, Y.; Suzuki, S.; Takeda, K.; Murahashi, K.; Horikawa, M.; Katagiri, K.; Masu, H.; Kato, T.; Azumaya, I.; Fujii, S.; Furuta, T.; Tanaka, K.; Kan, T. Synthesis and Characteristic Stereostructure of a Biphenanthryl Ether. *Tetrahedron: Asymmetry* **2008**, *19*, 1407–1410.
- (103) Clayden, J.; Worrall, C. P.; Moran, W. J.; Helliwell, M. Enantioselective Synthesis of an Atropisomeric Diaryl Ether. *Angew. Chem., Int. Ed.* **2008**, *47*, 3234–3237.
- (104) Betson, M. S.; Bracegirdle, A.; Clayden, J.; Helliwell, M.; Lund, A.; Pickworth, M.; Snape, T. J.; Worrall, C. P. Achieving Conformational Control Over C-C, C-N And C-O Bonds in Biaryls, N,N'-Diarylureas and Diaryl Ethers: Advantages of a Relay Axis. *Chem. Commun.* **2007**, 754–756.
- (105) Yuan, B.; Page, A.; Worrall, C. P.; Escalettes, F.; Willies, S. C.; McDouall, J. J. W.; Turner, N. J.; Clayden, J. Biocatalytic Desymmetrization of an Atropisomer with both an Enantioselective Oxidase and Ketoreductases. *Angew. Chem., Int. Ed.* **2010**, *49*, 7010–7013.
- (106) Clayden, J.; Fletcher, S. P.; Senior, J.; Worrall, C. P. Hindered Diarylether and Diarylsulfone Bisphosphine Ligands: Atropisomerism and Palladium Complexes. *Tetrahedron: Asymmetry* **2010**, *21*, 1355–1360.
- (107) Page, A.; Clayden, J. Carbamate-Directed Benzylic Lithiation for the Diastereo- and Enantioselective Synthesis of Diaryl Ether Atropisomers. *Beilstein J. Org. Chem.* **2011**, *7*, 1327–1333.
- (108) Kessler, H.; Rieker, A.; Rundel, W. Slow Rotation Around Benzene-Oxygen and Benzene-Sulphur Bonds in Aromatic Ethers, Sulphides, and Disulphides. *Chem. Commun.* **1968**, 475–476.
- (109) Casarini, D.; Foresti, E.; Gasparrini, F.; Lunazzi, L.; Misiti, D.; Macciantelli, D.; Villani, C. Conformational Studies by Dynamic NMR. 50. Atropisomerism in Hindered Naphthyl Sulfoxides: Structure, Stereodynamics, and Chiral Resolution. *J. Org. Chem.* **1993**, *58*, 5674–5682.
- (110) Casarini, D.; Lunazzi, L.; Gasparrini, F.; Villani, C.; Cirilli, M.; Gavuzzo, E. Conformational Assignment, Absolute Configuration, and Chiral Separation of All the Stereoisomers Created by the Combined Presence of Stereogenic Centers and Stereogenic Conformational Axes in a Highly Hindered 1,5-Naphthyl Sulfoxide. *J. Org. Chem.* **1995**, *60*, 97–102.
- (111) Casarini, D.; Lunazzi, L.; Alcaro, S.; Gasparrini, F.; Villani, C. Atropisomerism in Hindered Naphthyl Sulfoxides Investigated by Dynamic NMR and Dynamic HPLC Techniques. *J. Org. Chem.* **1995**, *60*, 5515–5519.
- (112) Jennings, W. B.; Kochanewycz, M. J.; Lunazzi, L. Conformation and Stereodynamics of Alkyl 9-Anthryl Sulfoxides. *J. Chem. Soc., Perkin Trans. 2* **1997**, 2271–2274.
- (113) Baker, R. W.; Kyasnoor, R. V.; Sargent, M. V. Two Pathways for the Stereomutation of 2-Substituted 1-(Tert-Butylsulfinyl)-Naphthalenes. *J. Chem. Soc., Perkin Trans. 2* **1998**, 1333–1338.
- (114) Lunazzi, L.; Mazzanti, A.; Minzoni, M. Structure and Conformational Processes of Bis(O-Cumyl)Sulfide, Sulfoxide and Sulfone. *Tetrahedron* **2005**, *61*, 6782–6790.
- (115) Villani, C.; Pirkle, W. H. Chromatographic Resolution of the Interconverting Stereoisomers of Hindered Sulfinyl and Sulfonyl Naphthalene Derivatives. *Tetrahedron: Asymmetry* **1995**, *6*, 27–30.
- (116) Clayden, J.; Senior, J.; Helliwell, M. Atropisomerism at C-S Bonds: Asymmetric Synthesis of Diaryl Sulfones by Dynamic Resolution Under Thermodynamic Control. *Angew. Chem., Int. Ed.* **2009**, *48*, 6270–6273.
- (117) Beak, P.; Anderson, D. R.; Curtis, M. D.; Laumer, J. M.; Pippel, D. J.; Weisenburger, G. A. Dynamic Thermodynamic Resolution: Control of Enantioselectivity through Diastereomeric Equilibration. *Acc. Chem. Res.* **2000**, *33*, 715–727.
- (118) Clayden, J.; Fletcher, S. P.; McDouall, J. J. W.; Rowbottom, S. J. M. Controlling Axial Conformation in 2-Arylpyridines and 1-Arylisoquinolines: Application to the Asymmetric Synthesis of QUINAP by Dynamic Thermodynamic Resolution. *J. Am. Chem. Soc.* **2009**, *131*, 5331–5343.
- (119) Lee, W. K.; Park, Y. S.; Beak, P. Dynamic Thermodynamic Resolution: Advantage by Separation of Equilibration and Resolution. *Acc. Chem. Res.* **2009**, *42*, 224–234.
- (120) Bringmann, G.; Gulder, T.; Reichert, M.; Meyer, F. Ancisheymine, the First N,C-Coupled Naphthylisoquinoline Alkaloid: Total Synthesis and Stereochemical Analysis. *Org. Lett.* **2006**, *8*, 1037–1040.
- (121) Kawabata, T.; Jiang, C.; Hayashi, K.; Tsubaki, K.; Yoshimura, T.; Majumdar, S.; Sasamori, T.; Tokitoh, N. Axially Chiral Binaphthyl Surrogates with an Inner N-H-N Hydrogen Bond. *J. Am. Chem. Soc.* **2009**, *131*, 54–55.
- (122) Ávalos, M.; Babiano, R.; Cintas, P.; Higes, F. J.; Jiménez, J. L.; Palacios, J. C.; Silvero, G.; Valencia, C. Non-Biaryl Atropisomers Derived from Carbohydrates. Part 2. Atropisomeric Behavior of Monocyclic and Bicyclic Imidazolidine-2-Ones and 2-Thiones. *Tetrahedron* **1999**, *55*, 4401–4426.
- (123) Ávalos, M.; Babiano, R.; Cintas, P.; Hursthouse, M. B.; Jiménez, J. L.; Light, M. E.; Palacios, J. C.; Silvero, G. Non-Biaryl Atropisomers Derived from Carbohydrates. Part 3: Rotational Isomerism of Sterically Hindered Heteroaryl Imidazolidine-2-Ones and 2-Thiones. *Tetrahedron* **2005**, *61*, 7931–7944.
- (124) Ávalos, M.; Babiano, R.; Cintas, P.; Hursthouse, M. B.; Jiménez, J. L.; Light, M. E.; Palacios, J. C.; Silvero, G. Non-Biaryl Atropisomers

Derived from Carbohydrates. Part 4: Absolute Stereochemistry of Carbohydrate-Based Imidazolidine-2-Ones and 2-Thiones with Axial and Central Chirality. *Tetrahedron* **2005**, *61*, 7945–7959.

(125) Wolf, C.; Bentley, K. W. Chirality Sensing Using Stereodynamic Probes with Distinct Electronic Circular Dichroism Output. *Chem. Soc. Rev.* **2013**, *42*, 5408–5424.

(126) Wolf, C. Stereolabile Chiral Compounds: Analysis by Dynamic Chromatography and Stopped-Flow Methods. *Chem. Soc. Rev.* **2005**, *34*, 595–608.

(127) Reist, M.; Testa, B.; Carrupt, P.-A.; Jung, M.; Schurig, V. Racemization, Enantiomerization, Diastereomerization, and Epimerization: Their Meaning and Pharmacological Significance. *Chirality* **1995**, *7*, 396–400.

(128) Trapp, O. Interconversion of Stereochemically Labile Enantiomers (Enantiomerization). *Topics in Current Chemistry*; Springer: Berlin, 2013; pp 1–39.

(129) Wolf, C. *Dynamic Stereochemistry of Chiral Compounds. Principles and Applications*; RSC Publishing: Cambridge, U.K., 2008.

(130) Jung, M.; Schurig, V. Determination of Enantiomerization Barriers by Computer Simulation of Interconversion Profiles: Enantiomerization of Diaziridines During Chiral Inclusion Gas Chromatography. *J. Am. Chem. Soc.* **1992**, *114*, 529–534.

(131) Stewart, W. E.; Siddall, T. H. Nuclear Magnetic Resonance Studies of Amides. *Chem. Rev.* **1970**, *70*, 517–551.

(132) Friary, R. J.; Spangler, M.; Osterman, R.; Schulman, L.; Schwerdt, J. H. Enantiomerization of an Atropisomeric Drug. *Chirality* **1996**, *8*, 364–371.

(133) Kumarasamy, E.; Jesuraj, J. L.; Omlid, J. N.; Ugrinov, A.; Sivaguru, J. Light-Induced Enantiospecific 4π Ring Closure of Axially Chiral 2-Pyridones: Enthalpic and Entropic Effects Promoted by H-Bonding. *J. Am. Chem. Soc.* **2011**, *133*, 17106–17109.

(134) Mintas, M.; Orhanović, Z.; Jakopčić, K.; Koller, H.; Stühler, G.; Mannschreck, A. Enantiomers of Sterically Hindered N-Aryl-4-Pyridones: Chromatographic Enrichment and Thermal Interconversion. *Tetrahedron* **1985**, *41*, 229–233.

(135) Kumarasamy, E.; Sivaguru, J. Light-Induced Stereospecific Intramolecular [2 + 2]-Cycloaddition of Atropisomeric 3,4-Dihydro-2-Pyridones. *Chem. Commun.* **2013**, *49*, 4346–4348.

(136) Bennett, D. J.; Blake, A. J.; Cooke, P. A.; Godfrey, C. R. A.; Pickering, P. L.; Simpkins, N. S.; Walker, M. D.; Wilson, C. Stereoselectivity in Reactions of Atropisomeric Lactams and Imides. *Tetrahedron* **2004**, *60*, 4491–4511.

(137) Suzumura, N.; Kageyama, M.; Kamimura, D.; Inagaki, T.; Dobashi, Y.; Hasegawa, H.; Fukaya, H.; Kitagawa, O. Studies on Rotational Barriers of N-C Axially Chiral Compounds: Increase in the Rotational Barrier by Aromatization. *Tetrahedron Lett.* **2012**, *53*, 4332–4336.

(138) Raghunathan, R.; Kumarasamy, E.; Iyer, A.; Ugrinov, A.; Sivaguru, J. Intramolecular Paterno-Buchi Reaction of Atropisomeric α -Oxoamides in Solution and in the Solid-State. *Chem. Commun.* **2013**, *49*, 8713–8715.

(139) Jesuraj, J. L.; Sivaguru, J. Photochemical Type II Reaction of Atropchiral Benzoylformamides to Point Chiral Oxazolidin-4-Ones. Axial Chiral Memory Leading to Enantiomeric Resolution of Photo-products. *Chem. Commun.* **2010**, *46*, 4791–4793.

(140) Curran, D. P.; Hale, G. R.; Geib, S. J.; Balog, A.; Cass, Q. B.; Degani, A. L. G.; Hernandez, M. Z.; Freitas, L. C. G. Rotational Features of Carbon-Nitrogen Bonds in Axially Chiral O-tert-Butyl Anilides and Related Molecules. Potential Substrates for the 'Prochiral Auxiliary' Approach to Asymmetric Synthesis. *Tetrahedron: Asymmetry* **1997**, *8*, 3955–3975.

(141) Curran, D. P.; Liu, W.; Chen, C. H.-T. Transfer of Chirality in Radical Cyclizations. Cyclization of o-Haloacrylanilides to Oxindoles with Transfer of Axial Chirality to a Newly Formed Stereocenter. *J. Am. Chem. Soc.* **1999**, *121*, 11012–11013.

(142) Curran, D. P.; Chen, C. H. T.; Geib, S. J.; Lapierre, A. B. Asymmetric Radical Cyclization Reactions of Axially Chiral N-Allyl-O-Iodoanilides to form Enantioenriched N-Acyl Dihydroindoles. *Tetrahedron* **2004**, *60*, 4413–4424.

(143) Petit, M.; Lapierre, A. J. B.; Curran, D. P. Relaying Asymmetry of Transient Atropisomers of o-Iodoanilides by Radical Cyclizations. *J. Am. Chem. Soc.* **2005**, *127*, 14994–14995.

(144) Lapierre, A. J. B.; Geib, S. J.; Curran, D. P. Low-Temperature Heck Reactions of Axially Chiral o-Iodoacrylanilides Occur with Chirality Transfer: Implications for Catalytic Asymmetric Heck Reactions. *J. Am. Chem. Soc.* **2007**, *129*, 494–495.

(145) Petit, M.; Geib, S. J.; Curran, D. P. Asymmetric Reactions of Axially Chiral Amides: Use of Removable Ortho-Substituents in Radical Cyclizations of o-Iodoacrylanilides and N-Allyl-N-o-Iodoacrylamides. *Tetrahedron* **2004**, *60*, 7543–7552.

(146) Guthrie, D. B.; Curran, D. P. Asymmetric Radical and Anionic Cyclizations of Axially Chiral Carbamates. *Org. Lett.* **2009**, *11*, 249–251.

(147) Guthrie, D. B.; Geib, S. J.; Curran, D. P. Synthesis of Highly Enantioenriched 3,4-Dihydroquinolin-2-ones by 6-Exo-trig Radical Cyclizations of Axially Chiral α -Halo-ortho-alkenyl Anilides. *J. Am. Chem. Soc.* **2009**, *131*, 15492–15500.

(148) Guthrie, D. B.; Geib, S. J.; Curran, D. P. Radical and Heck Cyclizations of Diastereomeric o-Haloanilide Atropisomers. *J. Am. Chem. Soc.* **2011**, *133*, 115–122.

(149) Cuyekeng, M. A.; Mannschreck, A. Liquid Chromatography on Triacetylcellulose, 14 Chromatographic Separation of Enantiomers and Barriers to Enantiomerization of Axially Chiral Aromatic Carboxamides. *Chem. Ber.* **1987**, *120*, 803–809.

(150) Ahmed, A.; Bragg, R. A.; Clayden, J.; Lai, L. W.; McCarthy, C.; Pink, J. H.; Westlund, N.; Yasin, S. A. Barriers to Rotation about the Chiral Axis of Tertiary Aromatic Amides. *Tetrahedron* **1998**, *54*, 13277–13294.

(151) Clayden, J.; Johnson, P.; Pink, J. H.; Helliwell, M. Atropisomeric Amides as Chiral Ligands: Using (–)-Sparteine-Directed Enantioselective Silylation to Control the Conformation of a Stereogenic Axis. *J. Org. Chem.* **2000**, *65*, 7033–7040.

(152) Sakamoto, M.; Unosawa, A.; Kobaru, S.; Saito, A.; Mino, T.; Fujita, T. Asymmetric Photocycloaddition in Solution of a Chiral Crystallized Naphthamide. *Angew. Chem., Int. Ed.* **2005**, *44*, 5523–5526.

(153) Sakamoto, M.; Unosawa, A.; Kobaru, S.; Fujita, K.; Mino, T.; Fujita, T. An Asymmetric S_NAr Reaction Using the Molecular Chirality in a Crystal. *Chem. Commun.* **2007**, 3586–3588.

(154) Degenhardt, C., III; Shortell, D. B.; Adams, R. D.; Shimizu, K. D. Synthesis and Structural Characterization of Adaptable Shape-Persistent Building Blocks. *Chem. Commun.* **2000**, 929–930.

(155) Dial, B. E.; Rasberry, R. D.; Bullock, B. N.; Smith, M. D.; Pellechia, P. J.; Profeta, S.; Shimizu, K. D. Guest-Accelerated Molecular Rotor. *Org. Lett.* **2011**, *13*, 244–247.

(156) Rushton, G. T.; Burns, W. G.; Lavin, J. M.; Chong, Y. S.; Pellechia, P.; Shimizu, K. D. Determination of the Rotational Barrier for Kinetically Stable Conformational Isomers via NMR and 2D TLC. *J. Chem. Educ.* **2007**, *84*, 1499.

(157) Rasberry, R. D.; Wu, X.; Bullock, B. N.; Smith, M. D.; Shimizu, K. D. A Small Molecule Diacid with Long-Term Chiral Memory. *Org. Lett.* **2009**, *11*, 2599–2602.

(158) Mino, T.; Tanaka, Y.; Yabusaki, T.; Okumura, D.; Sakamoto, M.; Fujita, T. A C(Aryl)-N(Amine) Bond Atropisomeric Aminophosphine: Preparation and Use as a Ligand in a Catalytic Asymmetric Allylic Alkylation. *Tetrahedron: Asymmetry* **2003**, *14*, 2503–2506.

(159) Kashima, C.; Katoh, A. Restricted Rotation about the Carbon-Nitrogen Single Bond of 1-Aryl-4,6-Dimethylpyrimidin-2(1H)-Ones and the Corresponding Thiones. *J. Chem. Soc., Perkin Trans. 1* **1980**, 1599–1602.

(160) Sakamoto, M.; Yagishita, F.; Ando, M.; Sasahara, Y.; Kamataki, N.; Ohta, M.; Mino, T.; Kasashima, Y.; Fujita, T. Generation and Amplification of Optical Activity of Axially Chiral N-(1-Naphthyl)-2(1H)-Pyrimidinethione by Crystallization. *Org. Biomol. Chem.* **2010**, *8*, 5418–5422.

(161) Roussel, C.; Adjimi, M.; Chemlal, A.; Djafri, A. Comparison of Racemization Processes in 1-Arylpyrimidine-2-Thione and 3-Arylthiazoline-2-Thione Atropisomers and their Oxygen Analogs. *J. Org. Chem.* **1988**, *53*, 5076–5080.

(162) Demir-Ordu, Ö.; Yılmaz, E. M.; Doğan, İ. Determination of the Absolute Stereochemistry and the Activation Barriers of Thermally Interconvertible Heterocyclic Compounds Bearing a Naphthyl Substituent. *Tetrahedron: Asymmetry* **2005**, *16*, 3752–3761.

(163) Erol, S.; Dogan, I. Axially Chiral 2-Arylimino-3-aryl-thiazolidine-4-one Derivatives: Enantiomeric Separation and Determination of Racemization Barriers by Chiral HPLC. *J. Org. Chem.* **2007**, *72*, 2494–2500.

(164) Yılmaz, E. M. j.; Doğan, I. Axially Chiral N-(O-Aryl)-2-Thioxo-Oxazolidine-4-One and Rhodanine Derivatives: Enantiomeric Separation and Determination of Racemization Barriers. *Tetrahedron: Asymmetry* **2008**, *19*, 2184–2191.

(165) Tabata, H.; Akiba, K.; Lee, S.; Takahashi, H.; Natsugari, H. Atropisomeric Properties of the Dibenzo[b,d]azepin-6-one Nucleus. *Org. Lett.* **2008**, *10*, 4871–4874.

(166) Verma, S. M.; Singh, N. B. A Study of Conformation about the Aryl C-N Bonds in N-Aryl Imides by Dynamic N.M.R. Spectroscopy. *Aust. J. Chem.* **1976**, *29*, 295–300.

(167) Kondo, K.; Fujita, H.; Suzuki, T.; Murakami, Y. A New Chiral Axis Due to N(Open-Chain Imide)-Ar Bond: Unexpected Racemization Effect of an Acyl Group. *Tetrahedron Lett.* **1999**, *40*, 5577–5580.

(168) Kondo, K.; Iida, T.; Fujita, H.; Suzuki, T.; Yamaguchi, K.; Murakami, Y. A Chiral Axis due to an Acyclic Imide-Ar Bond: a Study of Steric Effects of Acyl Groups on Racemization. *Tetrahedron* **2000**, *56*, 8883–8891.

(169) Kondo, K.; Iida, T.; Fujita, H.; Suzuki, T.; Wakabayashi, R.; Yamaguchi, K.; Murakami, Y. Further Study of Axial Chirality Due to an Acyclic Imide N-Ar Bond: Control of Rotational Barrier by Electronic Effects of Acyl Groups. *Tetrahedron* **2001**, *57*, 4115–4122.

(170) Schirok, H.; Alonso-Alija, C.; Benet-Buchholz, J.; Göller, A. H.; Grosser, R.; Michels, M.; Paulsen, H. Efficient Regioselective Synthesis of 6-Amino-5-benzoyl-1-Substituted 2(1H)-Pyridinones. *J. Org. Chem.* **2005**, *70*, 9463–9469.

(171) Kutenberger, M.; Frieser, M.; Hofweber, M.; Mannschreck, A. Axially Chiral Thioamides of Acrylic Acid: Correlated and Uncorrelated Internal Rotations. *Tetrahedron: Asymmetry* **1998**, *9*, 3629–3645.

(172) Ackerman, J. H.; Laidlaw, G. M.; Snyder, G. A. Restricted Rotational Isomers I. Hindered Triiodoisophthalic Acid Derivatives. *Tetrahedron Lett.* **1969**, *10*, 3879–3882.

(173) Ackerman, J. H.; Laidlaw, G. M. Restricted Rotational Isomers III. Cis- and Trans-3',5'-(Dimethylcarbamoyl)-2',4',6'-Triiodoaxalanilic Acid and Their N-Methyl Derivatives. *Tetrahedron Lett.* **1970**, *11*, 2381–2384.

(174) Jennings, W. B.; Tolley, M. S. Concerning Geminal Non-equivalence in Benzamides and Thiobenzamides. *Tetrahedron Lett.* **1976**, *17*, 695–698.

(175) Clayden, J.; Pink, J. H. Concerted Rotation in a Tertiary Aromatic Amide: Towards a Simple Molecular Gear. *Angew. Chem., Int. Ed.* **1998**, *37*, 1937–1939.

(176) LaPlante, S. R.; D. Fader, L.; Fandrick, K. R.; Fandrick, D. R.; Hucke, O.; Kemper, R.; Miller, S. P. F.; Edwards, P. J. Assessing Atropisomer Axial Chirality in Drug Discovery and Development. *J. Med. Chem.* **2011**, *54*, 7005–7022.

(177) Clayden, J.; Moran, W. J.; Edwards, P. J.; LaPlante, S. R. The Challenge of Atropisomerism in Drug Discovery. *Angew. Chem., Int. Ed.* **2009**, *48*, 6398–6401.

(178) Albert, J. S.; Aharony, D.; Andisik, D.; Barthlow, H.; Bernstein, P. R.; Bialecki, R. A.; Dedinas, R.; Dembofsky, B. T.; Hill, D.; Kirkland, K.; Koether, G. M.; Kosmider, B. J.; Ohnmacht, C.; Palmer, W.; Potts, W.; Rumsey, W.; Shen, L.; Shenvi, A.; Sherwood, S.; Warwick, P. J.; Russell, K. Design, Synthesis, and SAR of Tachykinin Antagonists: Modulation of Balance in NK1/NK2 Receptor Antagonist Activity. *J. Med. Chem.* **2002**, *45*, 3972–3983.

(179) Albert, J. S.; Ohnmacht, C.; Bernstein, P. R.; Rumsey, W. L.; Aharony, D.; Alelyunas, Y.; Russell, D. J.; Potts, W.; Sherwood, S. A.; Shen, L.; Dedinas, R. F.; Palmer, W. E.; Russell, K. Structural Analysis and Optimization of NK1 Receptor Antagonists through Modulation of Atropisomer Interconversion Properties. *J. Med. Chem.* **2004**, *47*, 519–529.

(180) Albert, J. S.; Ohnmacht, C.; Bernstein, P. R.; Rumsey, W. L.; Aharony, D.; Masek, B. B.; Dembofsky, B. T.; Koether, G. M.; Potts, W.; Evenden, J. L. Design and Optimization of Cyclized NK1 Antagonists with Controlled Atropisomeric Properties. *Tetrahedron* **2004**, *60*, 4337–4347.

(181) Palani, A.; Shapiro, S.; Clader, J. W.; Greenlee, W. J.; Blythin, D.; Cox, K.; Wagner, N. E.; Strizki, J.; Baroudy, B. M.; Dan, N. Biological Evaluation and Interconversion Studies of Rotamers of SCH 351125, an Orally Bioavailable CCR5 Antagonist. *Bioorg. Med. Chem. Lett.* **2003**, *13*, 705–708.

(182) Palani, A.; Shapiro, S.; Clader, J. W.; Greenlee, W. J.; Vice, S.; McCombie, S.; Cox, K.; Strizki, J.; Baroudy, B. M. Oximino-Piperidino-Piperidine-Based CCR5 Antagonists. Part 2: Synthesis, SAR and Biological Evaluation of Symmetrical Heteroaryl Carboxamides. *Bioorg. Med. Chem. Lett.* **2003**, *13*, 709–712.

(183) McCarthy, M.; Guiry, P. J. Axially Chiral Bidentate Ligands in Asymmetric Catalysis. *Tetrahedron* **2001**, *57*, 3809–3844.

(184) Jones, K.; Storey, J. M. D. Aryl Radical Cyclisations Involving an Amide Group in the Linking Chain. *J. Chem. Soc., Chem. Commun.* **1992**, 1766–1767.

(185) Curran, D. P.; DeMello, N. C. Origins of Regioselectivity in Radical Reactions of Axially Twisted Anilides. *J. Chem. Soc., Chem. Commun.* **1993**, 1314–1317.

(186) Nakazaki, A.; Mori, A.; Kobayashi, S.; Nishikawa, T. Diastereoselective Synthesis of 3,3-Disubstituted Oxindoles from Atropisomeric N-Aryl Oxindole Derivatives. *Tetrahedron Lett.* **2012**, *53*, 7131–7134.

(187) Bruch, A.; Ambrosius, A.; Fröhlich, R.; Studer, A.; Guthrie, D. B.; Zhang, H.; Curran, D. P. Memory of Axial Chirality in Aryl Radical Phosphorylations. *J. Am. Chem. Soc.* **2010**, *132*, 11452–11454.

(188) Bruch, A.; Fröhlich, R.; Grimme, S.; Studer, A.; Curran, D. P. One Product, Two Pathways: Initially Divergent Radical Reactions Reconverge To Form a Single Product in High Yield. *J. Am. Chem. Soc.* **2011**, *133*, 16270–16276.

(189) Zhang, Y.; Wang, Y.; Dai, W.-M. Efficient Remote Axial-to-Central Chirality Transfer in Enantioselective SmI₂-Mediated Reductive Coupling of Aldehydes with Crotonates of Atropisomeric 1-Naphthamides. *J. Org. Chem.* **2006**, *71*, 2445–2455.

(190) Ahmed, A.; Clayden, J.; Rowley, M. Anionic Cyclisations of an N-Benzyl Naphthamide: A Route to Benzo[E]Isoindolones. *Chem. Commun.* **1998**, 297–298.

(191) Ohno, A.; Kashiwagi, M.; Ishihara, Y.; Ushida, S.; Oka, S. NAD(P)⁺-NAD(P)H Models. 57: Stereochemistry in (Net) Hydride Transfer from and to NAD(P)⁺-NAD(P)H Models: Chirality Sink. *Tetrahedron* **1986**, *42*, 961–973.

(192) Kawamoto, T.; Tomishima, M.; Kunitomo, J.; Yoneda, F.; Hayami, J.-i. First Example of "Diastereotopic Face Activation" and Chiral Recognition Without Metal Assistance. A Novel 5-Deazaflavin Enzyme Model. *Tetrahedron Lett.* **1992**, *33*, 7173–7176.

(193) Kawamoto, T.; Tomishima, M.; Yoneda, F.; Hayami, J.-i. Diastereoface Differentiating "(Net) Hydride Transfer" in Novel 5-Deazaflavins Modified at Pyrimidine Ring. *Tetrahedron Lett.* **1992**, *33*, 3173–3176.

(194) Kawamoto, T.; Taga, T.; Bessho, K.; Yoneda, F.; Hayami, J.-i. Stereochemistry of Asymmetric "(Net) Hydride Transfer" in an Intercoenzyme Model Reaction System. *Tetrahedron Lett.* **1994**, *35*, 8631–8634.

(195) Mikata, Y.; Aida, S.; Yano, S. Carbonyl Orientation Determines Regio- and Enantioselectivity in 1,2-/1,4-Reduction of an NAD Model Compound. *Org. Lett.* **2004**, *6*, 2921–2924.

(196) De Kok, P. M. T.; Bastiaansen, L. A. M.; Van Lier, P. M.; Vekemans, J. A. J. M.; Buck, H. M. Highly Reactive and Stereoselective (R)- and (S)-3-(N,N-Dimethylcarbamoyl)-1,2,4-Trimethyl-1,4-Dihydropyridines for NADH-NAD⁺ Mimicry. *J. Org. Chem.* **1989**, *54*, 1313–1320.

(197) Mikata, Y.; Hayashi, K.; Mizukami, K.; Matsumoto, S.; Yano, S.; Yamazaki, N.; Ohno, A. Highly Reactive and Stereospecific Reaction of Quinoline-Type NADH Model Compounds With Methyl Benzoylformate. *Tetrahedron Lett.* **2000**, *41*, 1035–1038.

- (198) Kishikawa, K.; Tsuru, I.; Kohmoto, S.; Yamamoto, M.; Yamada, K. Stereoselective Synthesis of 2-Alkylamino-N-(2'-alkylphenyl)-succinimide Conformers. *Chem. Lett.* **1994**, *23*, 1605–1606.
- (199) Clayden, J.; Westlund, N.; Wilson, F. X. Asymmetric Induction Using Atropisomers: Diastereoselective Additions to 2-Acyl-1-Naphthamides. *Tetrahedron Lett.* **1996**, *37*, 5577–5580.
- (200) Clayden, J.; McCarthy, C.; Westlund, N.; Frampton, C. S. Atroposelective Attack of Nucleophiles on 2-Formyl-1-Naphthamides and Their Derivatives: Chelation and Non-Chelation Control. *J. Chem. Soc., Perkin Trans. 1* **2000**, 1363–1378.
- (201) Clayden, J.; Westlund, N.; Wilson, F. X. Synthesis of Atropisomeric 2-(1-Aminoalkyl)-1-Naphthamides by Stereoselective Addition of Organolithiums to A 2-Imino-1-Naphthamide. *Tetrahedron Lett.* **1999**, *40*, 3329–3330.
- (202) Nakamura, S.; Yasuda, H.; Watanabe, Y.; Toru, T. Diastereoselective Reaction of 1-(Arylsulfinyl)-2-Naphthaldehydes. *Tetrahedron Lett.* **2000**, *41*, 4157–4160.
- (203) Koide, H.; Uemura, M. Axially Chiral Benzamides: Diastereoselective Nucleophilic Additions to Planar Chiral (N, N-Diethyl-2-Acyl-6-Methylbenzamide)Chromium Complexes. *Tetrahedron Lett.* **1999**, *40*, 3443–3446.
- (204) Solladie-Cavallo, A. Chiral Arene-Chromium-Carbonyl Complexes in Asymmetric Synthesis. In *Advances in Metal-Organic Chemistry*; Liebeskind, L. S., Ed.; JAI Press Inc.: Greenwich, CT, USA, 1989; Vol. 1; pp 99.
- (205) Godfrey, C. R. A.; Simpkins, N. S.; Walker, M. D. High Stereochemical Fidelity in Reactions of an Atropisomeric N-Acyliminium Intermediate. *Synlett* **2000**, *2000*, 388–390.
- (206) Sakamoto, M.; Kobaru, S.; Mino, T.; Fujita, T. Absolute Asymmetric Synthesis by Nucleophilic Carbonyl Addition Using Chiral Crystals of Achiral Amides. *Chem. Commun.* **2004**, 1002–1003.
- (207) Lin, S.; Leow, D.; Huang, K.-W.; Tan, C.-H. Enantioselective Protonation of Itaconimides with Thiols and the Rotational Kinetics of the Axially Chiral C-N Bond. *Chem. - Asian J.* **2009**, *4*, 1741–1744.
- (208) Beagley, B.; Betts, M. J.; Pritchard, R. G.; Schofield, A.; Stoodley, R. J.; Vohra, S. 'Hidden' Axial Chirality as a Stereodirecting Element in Reactions Involving Enol(Ate) Intermediates. Part 1. Cyclisation Reactions of Methyl (4R)-3-(2-Diazo-3-Oxobutanoyl)Thiazolidine-4-Carboxylate and Related Compounds. *J. Chem. Soc., Perkin Trans. 1* **1993**, 1761–1770.
- (209) Fuji, K.; Kawabata, T. Memory of Chirality—A New Principle in Enolate Chemistry. *Chem. - Eur. J.* **1998**, *4*, 373–376.
- (210) Zhao, H.; Hsu, D. C.; Carlier, P. R. Memory of Chirality: An Emerging Strategy for Asymmetric Synthesis. *Synthesis* **2005**, 1–16.
- (211) Patil, N. T. Chirality Transfer and Memory of Chirality in Gold-Catalyzed Reactions. *Chem. - Asian J.* **2012**, *7*, 2186–2194.
- (212) Clayden, J.; Darbyshire, M.; Pink, J. H.; Westlund, N.; Wilson, F. X. Remote Stereocontrol Using Rotationally Restricted Amides: (1,5)-Asymmetric Induction. *Tetrahedron Lett.* **1997**, *38*, 8587–8590.
- (213) Fujita, M.; Kitagawa, O.; Yamada, Y.; Izawa, H.; Hasegawa, H.; Taguchi, T. Synthesis of Optically Active 5-Substituted-2-pyrrolidinone Derivatives Having Atropisomeric Structure and 3,5-Cis-Selective Reaction of Their Enolates with Electrophiles. *J. Org. Chem.* **2000**, *65*, 1108–1114.
- (214) Bennett, D. J.; Pickering, P. L.; Simpkins, N. S. A Novel Asymmetric Route to Succinimides and Derived Compounds: Synthesis of the Lignan Lactone (+)-hinokinin. *Chem. Commun.* **2004**, 1392–1393.
- (215) Yoshimura, T.; Tomohara, K.; Kawabata, T. Asymmetric Induction via Short-Lived Chiral Enolates with a Chiral C–O Axis. *J. Am. Chem. Soc.* **2013**, *135*, 7102–7105.
- (216) Snieckus, V. Directed Ortho Metalation. Tertiary Amide and O-Carbamate Directors in Synthetic Strategies for Polysubstituted Aromatics. *Chem. Rev.* **1990**, *90*, 879–933.
- (217) Beak, P.; Brown, R. A. The Tertiary Amide as an Effective Director of Ortho Lithiation. *J. Org. Chem.* **1982**, *47*, 34–46.
- (218) Beak, P.; Zajdel, W. J.; Reitz, D. B. Metalation and Electrophilic Substitution of Amine Derivatives Adjacent to Nitrogen: α -Metallo Amine Synthetic Equivalents. *Chem. Rev.* **1984**, *84*, 471–523.
- (219) Clayden, J.; Pink, J. H. Atroposelectivity in the Reactions of Laterally Lithiated Tertiary Amides. *Tetrahedron Lett.* **1997**, *38*, 2561–2564.
- (220) Clayden, J.; Pink, J. H. Configurational Stability and Stereospecificity in the Reactions of Amide-Stabilised Organolithiums: A Non-Stereospecific Tin-Lithium Exchange. *Tetrahedron Lett.* **1997**, *38*, 2565–2568.
- (221) Clayden, J.; Helliwell, M.; Pink, J. H.; Westlund, N. Stereospecificity and Stereoselectivity in Electrophilic Substitution Reactions of Non- α -Heterosubstituted Organolithiums and Stannanes: A Rotationally Restricted Amide as an Internal Stereochemical Marker. *J. Am. Chem. Soc.* **2001**, *123*, 12449–12457.
- (222) Clayden, J.; Pink, J. H.; Westlund, N.; Frampton, C. S. Atroposelectivity in the Electrophilic Substitution Reactions of Laterally Lithiated and Silylated Tertiary Amides. *J. Chem. Soc., Perkin Trans. 1* **2002**, 901–917.
- (223) Clayden, J.; Lai, L. W.; Helliwell, M. Using Amide Conformation to 'Project' the Stereochemistry of an (–)-ephedrine-Derived Oxazolidine: A Pair of Pseudoenantiomeric Chiral Amido-Phosphine Ligands. *Tetrahedron: Asymmetry* **2001**, *12*, 695–698.
- (224) Ach, D.; Reboul, V.; Metzner, P. Atroposelectivity of Reactions of Benzylic Metalated Thiobenzamides and Thionaphthamides. *Eur. J. Org. Chem.* **2003**, *2003*, 3398–3406.
- (225) Thayumanavan, S.; Park, Y. S.; Farid, P.; Beak, P. Fluoride Activated Stereoinformation Transfer from a C-Si Bond of a Chiral Benzyl Silane to C-C Bonds. *Tetrahedron Lett.* **1997**, *38*, 5429–5432.
- (226) Clayden, J.; Pink, J. H.; Yasin, S. A. Conformationally Interlocked Amides: Remote Asymmetric Induction by Mechanical Transfer of Stereochemical Information. *Tetrahedron Lett.* **1998**, *39*, 105–108.
- (227) Clayden, J.; Westlund, N.; Wilson, F. X. Synthesis of Atropisomeric Diamides with Remotely Related Stereogenic Axes by Stereoselective Additions to Imines. *Tetrahedron Lett.* **1999**, *40*, 3331–3334.
- (228) Clayden, J.; Westlund, N.; Frampton, C. S.; Helliwell, M. Diastereoselective Synthesis of Atropisomers Containing Two Non-Biaryl Stereogenic Axes: Stereochemical Relay Through Stereogenic Centres in Dihydrostilbene-2,2'-dicarboxamides. *Org. Biomol. Chem.* **2006**, *4*, 455–461.
- (229) Clayden, J.; Kenworthy, M. N.; Youssef, L. H.; Helliwell, M. Axial Chirality in Xanthene-4,5-Dicarboxamides: 1,9-Stereocontrol Mediated by Remote Interactions Between Conformationally Constrained Amide Groups. *Tetrahedron Lett.* **2000**, *41*, 5171–5175.
- (230) Clayden, J.; Lund, A.; Youssef, L. H. Conformational Preference and Remote (1,10) Stereocontrol in Biphenyl-2,2'-dicarboxamides. *Org. Lett.* **2001**, *3*, 4133–4136.
- (231) Clayden, J.; Vallverdu, L.; Helliwell, M. Transmitting Information along Oligo-Para-Phenylenes: 1,12-Stereochemical Control in a Terphenyl Tetracarboxamide. *Chem. Commun.* **2007**, 2357–2359.
- (232) Clayden, J.; Turner, H.; Pickworth, M.; Adler, T. Ring-Selective Functionalization of N,N'-Diaryleureas by Regioselective N-Alkylation and Directed Ortho Metalation. *Org. Lett.* **2005**, *7*, 3147–3150.
- (233) Clayden, J.; Turner, H.; Helliwell, M.; Moir, E. N,N'-Diaryleureas: A New Family of Atropisomers Exhibiting Highly Diastereoselective Reactivity. *J. Org. Chem.* **2008**, *73*, 4415–4423.
- (234) Clayden, J.; Helliwell, M.; McCarthy, C.; Westlund, N. Atropisomeric Benzamides and Naphthamides as Chiral Auxiliaries. *J. Chem. Soc., Perkin Trans. 1* **2000**, 3232–3249.
- (235) Clayden, J.; McCarthy, C.; Cumming, J. G. Dynamically Resolved Peri-Substituted 2-Formyl Naphthamides: A New Class of Atropisomeric Chiral Auxiliary. *Tetrahedron Lett.* **2000**, *41*, 3279–3283.
- (236) Dantale, S.; Reboul, V.; Metzner, P.; Philouze, C. First Use of Axially Chiral Thioamides for the Stereocontrol of C–C Bond Formation. *Chem. - Eur. J.* **2002**, *8*, 632–640.
- (237) Trost, B. M.; Van Vranken, D. L. Asymmetric Transition Metal-Catalyzed Allylic Alkylations. *Chem. Rev.* **1996**, *96*, 395–422.

- (238) Dai, X.; Virgil, S. Asymmetric allylic alkylation catalyzed by palladium complexes with atropisomeric quinazolinone phosphine ligands. *Tetrahedron Lett.* **1999**, *40*, 1245–1248.
- (239) Mino, T.; Kashihara, K.; Yamashita, M. New Chiral Phosphine–Amide Ligands in Palladium-Catalyzed Asymmetric Allylic Alkylations. *Tetrahedron: Asymmetry* **2001**, *12*, 287–291.
- (240) Dai, W.-M.; Yeung, K. K. Y.; Liu, J.-T.; Zhang, Y.; Williams, I. D. A Novel Class of Nonbiaryl Atropisomeric P,O-Ligands for Palladium-Catalyzed Asymmetric Allylic Alkylation†. *Org. Lett.* **2002**, *4*, 1615–1618.
- (241) Tanaka, Y.; Mino, T.; Akita, K.; Sakamoto, M.; Fujita, T. Development of Chiral (S)-Prolinol-Derived Ligands for Palladium-Catalyzed Asymmetric Allylic Alkylation: Effect of a Siloxymethyl Group on the Pyrrolidine Backbone. *J. Org. Chem.* **2004**, *69*, 6679–6687.
- (242) Mino, T.; Tanaka, Y.; Hattori, Y.; Yabusaki, T.; Saotome, H.; Sakamoto, M.; Fujita, T. Synthesis and Optical Resolution of Aminophosphines with Axially Chiral C(aryl)–N(amine) Bonds for Use as Ligands in Asymmetric Catalysis. *J. Org. Chem.* **2006**, *71*, 7346–7353.
- (243) Mino, T.; Wakui, K.; Oishi, S.; Hattori, Y.; Sakamoto, M.; Fujita, T. Kinetic Resolution of Allylic Esters in Palladium-Catalyzed Asymmetric Allylic Alkylations Using C–N Bond Axially Chiral Aminophosphine Ligands. *Tetrahedron: Asymmetry* **2008**, *19*, 2711–2716.
- (244) Mino, T.; Komatsu, S.; Wakui, K.; Yamada, H.; Saotome, H.; Sakamoto, M.; Fujita, T. N-Aryl Indole-Derived C–N Bond Axially Chiral Phosphine Ligands: Synthesis and Application in Palladium-Catalyzed Asymmetric Allylic Alkylation. *Tetrahedron: Asymmetry* **2010**, *21*, 711–718.
- (245) Mino, T.; Yamada, H.; Komatsu, S.; Kasai, M.; Sakamoto, M.; Fujita, T. Atropisomerism at C–N Bonds of Acyclic Amines: Synthesis and Application to Palladium-Catalyzed Asymmetric Allylic Alkylations. *Eur. J. Org. Chem.* **2011**, *2011*, 4540–4542.
- (246) Wang, F.; Li, S.; Qu, M.; Zhao, M.-X.; Liu, L.-J.; Shi, M. A Highly Efficient Kinetic Resolution of Morita-Baylis-Hillman Adducts Achieved by N-Ar Axially Chiral Pd-Complexes Catalyzed Asymmetric Allylation. *Chem. Commun.* **2011**, *47*, 12813–12815.
- (247) Mino, T.; Ishikawa, M.; Nishikawa, K.; Wakui, K.; Sakamoto, M. Palladium-Catalyzed Asymmetric Allylic Alkylation of Indoles by C–N Bond Axially Chiral Phosphine Ligands. *Tetrahedron: Asymmetry* **2013**, *24*, 499–504.
- (248) Dai, W.-M.; Yeung, K. K. Y.; Chow, C. W.; Williams, I. D. Study on Enantiomerically Pure 2-Substituted N,N-Dialkyl-1-Naphthamides: Resolution, Absolute Stereochemistry, and Application to Desymmetrization of Cyclic Meso Anhydrides. *Tetrahedron: Asymmetry* **2001**, *12*, 1603–1613.
- (249) Horibe, H.; Kazuta, K.; Kotoku, M.; Kondo, K.; Okuno, H.; Murakami, Y.; Aoyama, T. Further Application of an N-Ar Axially Chiral Mimetic-Type Ligand: Asymmetric Grignard Cross-Coupling Reaction. *Synlett* **2003**, 2047–2051.
- (250) Dai, W.-M.; Yeung, K. K. Y.; Wang, Y. The First Example of Atropisomeric Amide-Derived P,O-Ligands Used for an Asymmetric Heck Reaction. *Tetrahedron* **2004**, *60*, 4425–4430.
- (251) Dai, W.-M.; Li, Y.; Zhang, Y.; Yue, C.; Wu, J. Generation of an Aromatic Amide-Derived Phosphane (Aphos) Library by Self-Assisted Molecular Editing and Applications of Aphos in Room-Temperature Suzuki–Miyaura Reactions. *Chem. - Eur. J.* **2008**, *14*, 5538–5554.
- (252) Pesch, J.; Harms, K.; Bach, T. Preparation of Axially Chiral N,N'-Diarylimidazolium and N-Arylthiazolium Salts and Evaluation of Their Catalytic Potential in the Benzoin and in the Intramolecular Stetter Reactions. *Eur. J. Org. Chem.* **2004**, *2004*, 2025–2035.
- (253) Brandes, S.; Niess, B.; Bella, M.; Prieto, A.; Overgaard, J.; Jørgensen, K. A. Non-Biaryl Atropisomers in Organocatalysis. *Chem. - Eur. J.* **2006**, *12*, 6039–6052.
- (254) Bai, X.-F.; Song, T.; Xu, Z.; Xia, C.-G.; Huang, W.-S.; Xu, L.-W. Aromatic Amide-Derived Non-Biaryl Atropisomers as Highly Efficient Ligands in Silver-Catalyzed Asymmetric Cycloaddition Reactions. *Angew. Chem., Int. Ed.* **2015**, *54*, 5255–5259.
- (255) Faigl, F.; Erdélyi, Z.; Deák, S.; Nyerges, M.; Mátravölgyi, B. A New Pyrrolidine-Derived Atropisomeric Amino Alcohol as a Highly Efficient Chiral Ligand for the Asymmetric Addition of Diethylzinc to Aldehydes. *Tetrahedron Lett.* **2014**, *55*, 6891–6894.
- (256) Faigl, F.; Mátravölgyi, B.; Szöllösy, Á.; Czugler, M.; Tárkányi, G.; Vékey, K.; Kubinyi, M. Synthesis of Atropisomeric 1-Phenylpyrrole-Derived Amino Alcohols: New Chiral Ligands. *Chirality* **2012**, *24*, 532–542.
- (257) Faigl, F.; Mátravölgyi, B.; Holczbauer, T.; Czugler, M.; Madarász, J. Resolution of 1-[2-Carboxy-6-(Trifluoromethyl)Phenyl]-1H-Pyrrole-2-Carboxylic Acid with Methyl (R)-2-Phenylglycinate, Reciprocal Resolution and Second Order Asymmetric Transformation. *Tetrahedron: Asymmetry* **2011**, *22*, 1879–1884.
- (258) Faigl, F.; Vas-Feldhoffer, B.; Kudar, V.; Czugler, M.; Pál, K.; Kubinyi, M. Synthesis and Optical Resolution of 1-[(3-Carboxy-1,1'-Biphenyl)-2-Yl]-1H-Pyrrole-2-Carboxylic Acid. *Chirality* **2009**, *21*, 905–910.
- (259) Fogassy, K.; Harmat, V.; Böcskei, Z.; Tárkányi, G.; Tőke, L.; Faigl, F. Efficient Synthesis and Resolution of (±)-1-[2-Carboxy-6-(Trifluoromethyl)Phenyl]Pyrrole-2-Carboxylic Acid. *Tetrahedron: Asymmetry* **2000**, *11*, 4771–4780.
- (260) Bach, T.; Schröder, J.; Harms, K. Diastereoselective Photocycloaddition of an Axial Chiral Enamide. *Tetrahedron Lett.* **1999**, *40*, 9003–9004.
- (261) Müller, C.; Bach, T. Chirality Control in Photochemical Reactions: Enantioselective Formation of Complex Photoproducts in Solution. *Aust. J. Chem.* **2008**, *61*, 557–564.
- (262) Ayitou, A. J.-L.; Ugrinov, A.; Sivaguru, J. 6π-Photocyclization of O-tert-butylacrylanilides. N-substitution Dictates the Regiochemistry of Cyclization. *Photochem. Photobiol. Sci.* **2009**, *8*, 751–754.
- (263) Ayitou, A.; Pemberton, B. C.; Kumarasamy, E.; Vallavoju, N.; Sivaguru, J. Fun with Photons: Selective Light Induced Reactions in Solution and in Water Soluble Nano-containers. *Chimia* **2011**, *65*, 202–209.
- (264) Pemberton, B. C.; Raghunathan, R.; Volla, S.; Sivaguru, J. From Containers to Catalysts: Supramolecular Catalysis within Cucurbiturils. *Chem. - Eur. J.* **2012**, *18*, 12178–12190.
- (265) Havinga, E.; Schlatmann, J. L. M. A. Remarks on the Specificities of the Photochemical and Thermal Transformations in the Vitamin D Field. *Tetrahedron* **1961**, *16*, 146–152.
- (266) Maessen, P. A.; Jacobs, H. J. C.; Cornelisse, J.; Havinga, E. Photochemistry of Previtamin D3 at 92 K; Formation of an Unstable Tachysterol3 Rotamer. *Angew. Chem., Int. Ed. Engl.* **1983**, *22*, 718–719.
- (267) Jacobs, H. J. C. Photochemistry of Conjugated Trienes: Vitamin D Revisited. *Pure Appl. Chem.* **1995**, *67*, 63–70.
- (268) Ayitou, A. J.-L.; Sivaguru, J. Reactive Spin State Dependent Enantiospecific Photocyclization of Axially Chiral α-Substituted Acrylanilides. *Chem. Commun.* **2011**, *47*, 2568–2570.
- (269) Ayitou, A. J.-L.; Vallavoju, N.; Ugrinov, A.; Sivaguru, J. Enantiospecific 6π-Photocyclization of Atropisomeric α-Substituted Acrylanilides in the Solid-State: Role of Crystalline Confinement on Enantiospecificity. *Photochem. Photobiol. Sci.* **2011**, *10*, 1380–1383.
- (270) Ayitou, A. J.-L.; Clay, A.; Kumarasamy, E.; Jockusch, S.; Sivaguru, J. Enantiospecific Photochemical 6π-ring Closure of α-substituted Atropisomeric Acrylanilides - Role of Alkali Metal Ions. *Photochem. Photobiol. Sci.* **2014**, *13*, 141–144.
- (271) Sieburth, S. McN. Photochemical Reactivity of Pyridones. In *CRC Handbook of Organic Photochemistry and Photobiology*, 2nd ed.; Horspool, W., Lenci, F., Eds.; CRC Press: Boca Raton, FL, USA, 2003; Vols. 1 and 2.
- (272) Bach, T.; Bergmann, H.; Brummerhop, H.; Lewis, W.; Harms, K. The [2 + 2]-Photocycloaddition of Aromatic Aldehydes and Ketones to 3,4-Dihydro-2-pyridones: Regioselectivity, Diastereoselectivity, and Reductive Ring Opening of the Product Oxetanes. *Chem. - Eur. J.* **2001**, *7*, 4512–4521.
- (273) Corey, E. J.; Streith, J. Internal Photoaddition Reactions of 2-Pyrone and N-Methyl-2-pyridone: A New Synthetic Approach to Cyclobutadiene. *J. Am. Chem. Soc.* **1964**, *86*, 950–951.

- (274) Tanaka, K.; Fujiwara, T.; Urbanczyk-Lipkowska, Z. Highly Enantioselective Photocyclization of 1-Alkyl-2-pyridones to β -Lactams in Inclusion Crystals with Optically Active Host Compounds. *Org. Lett.* **2002**, *4*, 3255–3257.
- (275) Taylor, E. C.; Kan, R. O.; Paudler, W. W. The Photolysis of 2-Aminopyridines and 2-Pyridones. *J. Am. Chem. Soc.* **1961**, *83*, 4484–4485.
- (276) Bach, T. Stereoselective Intermolecular [2 + 2]-Photocycloaddition Reactions and Their Application in Synthesis. *Synthesis* **1998**, 1998, 683.
- (277) Schreiber, S. L. [2 + 2] Photocycloadditions in the Synthesis of Chiral Molecules. *Science* **1985**, *227*, 857–863.
- (278) Clay, A.; Kumarasamy, E.; Ayitou, A. J. L.; Sivaguru, J. Photochemistry of Atropisomers: Non-biaryl Atropisomers for Stereospecific Phototransformations. *Chem. Lett.* **2014**, *43*, 1816–1825.
- (279) Kumarasamy, E.; Raghunathan, R.; Jockusch, S.; Ugrinov, A.; Sivaguru, J. Tailoring Atropisomeric Maleimides for Stereospecific [2 + 2] Photocycloaddition—Photochemical and Photophysical Investigations Leading to Visible-Light Photocatalysis. *J. Am. Chem. Soc.* **2014**, *136*, 8729–8737.
- (280) Roscini, C.; Cubbage, K. L.; Berry, M.; Orr-Ewing, A. J.; Booker-Milburn, K. I. Reaction Control in Synthetic Organic Photochemistry: Switching between [5 + 2] and [2 + 2] Modes of Cycloaddition. *Angew. Chem., Int. Ed.* **2009**, *48*, 8716–8720.
- (281) Gülten, Ş.; Sharpe, A.; Baker, J. R.; Booker-Milburn, K. I. Use of Temporary Tethers in the Intramolecular [2 + 2] Photocycloaddition Reactions of Tetrahydrophthalimide Derivatives: A New Approach to Complex Tricyclic Lactones. *Tetrahedron* **2007**, *63*, 3659–3671.
- (282) Bach, T. The Paternò-Büchi Reaction of 3-Heteroatom-Substituted Alkenes as a Stereoselective Entry to Polyfunctional Cyclic and Acyclic Molecules. *Liebigs Ann.* **1997**, 1997, 1627–1634.
- (283) Abe, M. Recent Progress Regarding Regio-, Site-, and Stereoselective Formation of Oxetanes in Paternò-Büchi Reactions. *J. Chin. Chem. Soc.* **2008**, *55*, 479–486.
- (284) Iyer, A.; Jockusch, S.; Sivaguru, J. Dictating Photoreactivity through Restricted Bond Rotations: Cross-Photoaddition of Atropisomeric Acrylimide Derivatives under UV/Visible-Light Irradiation. *J. Phys. Chem. A* **2014**, *118*, 10596–10602.
- (285) Ayitou, A. J.-L.; Jesuraj, J. L.; Barooah, N.; Ugrinov, A.; Sivaguru, J. Enantiospecific Photochemical Norrish/Yang Type II Reaction of Nonbiaryl Atropchiral α -Oxoamides in Solution-Axial to Point Chirality Transfer. *J. Am. Chem. Soc.* **2009**, *131*, 11314–11315.
- (286) Ramamurthy, V.; Venkatesan, K. Photochemical Reactions of Organic Crystals. *Chem. Rev.* **1987**, *87*, 433–481.
- (287) Sakamoto, M. Spontaneous Chiral Crystallization of Achiral Materials and Absolute Asymmetric Photochemical Transformation Using the Chiral Crystalline Environment. *J. Photochem. Photobiol., C* **2006**, *7*, 183–196.
- (288) Inoue, Y. Asymmetric Photochemical Reactions in Solution. *Chem. Rev.* **1992**, *92*, 741–770.
- (289) Griesbeck, A. G.; Meierhenrich, U. J. Asymmetric Photochemistry and Photochirogenesis. *Angew. Chem., Int. Ed.* **2002**, *41*, 3147–3154.
- (290) Sakamoto, M. Absolute Asymmetric Synthesis from Achiral Molecules in the Chiral Crystalline Environment. *Chem. - Eur. J.* **1997**, *3*, 684–689.
- (291) Sakamoto, M.; Unosawa, A.; Kobaru, S.; Hasegawa, Y.; Mino, T.; Kasashima, Y.; Fujita, T. Diastereoselective Photocycloaddition Using Memory Effect of Molecular Chirality Controlled by Crystallization. *Chem. Commun.* **2007**, 1632–1634.
- (292) Sakamoto, M.; Iwamoto, T.; Nono, N.; Ando, M.; Arai, W.; Mino, T.; Fujita, T. Memory of Chirality Generated by Spontaneous Crystallization and Asymmetric Synthesis Using the Frozen Chirality. *J. Org. Chem.* **2003**, *68*, 942–946.
- (293) Yagishita, F.; Sakamoto, M.; Mino, T.; Fujita, T. Asymmetric Intramolecular Cyclobutane Formation via Photochemical Reaction of N,N-Diallyl-2-quinolone-3-carboxamide Using a Chiral Crystalline Environment. *Org. Lett.* **2011**, *13*, 6168–6171.
- (294) Sakamoto, M.; Yagishita, F.; Saito, A.; Kobaru, S.; Unosawa, A.; Mino, T.; Fujita, T. Asymmetric Photocycloaddition of Naphthamide With a Diene Using the Provisional Molecular Chirality in a Chiral Crystal. *Photochem. Photobiol. Sci.* **2011**, *10*, 1387–1389.
- (295) Sakamoto, M.; Kato, M.; Aida, Y.; Fujita, K.; Mino, T.; Fujita, T. Photosensitized 2 + 2 Cycloaddition Reaction Using Homochirality Generated by Spontaneous Crystallization. *J. Am. Chem. Soc.* **2008**, *130*, 1132–1133.
- (296) Ayitou, A. J. L.; Fukuhara, G.; Kumarasamy, E.; Inoue, Y.; Sivaguru, J. Enantiospecific Photochemical Transformations under Elevated Pressure. *Chem. - Eur. J.* **2013**, *19*, 4327–4334.
- (297) Rebek, J., Jr. Molecular Recognition with Model Systems. *Angew. Chem., Int. Ed. Engl.* **1990**, *29*, 245–255.
- (298) Iwamura, H.; Mislou, K. Stereochemical Consequences of Dynamic Gearing. *Acc. Chem. Res.* **1988**, *21*, 175–182.
- (299) Rebek, J.; Marshall, L.; Wolak, R.; McManis, J. Epoxidations With Selective Peracids. *J. Am. Chem. Soc.* **1984**, *106*, 1170–1171.
- (300) Rebek, J.; Marshall, L.; Wolak, R.; Parris, K.; Killoran, M.; Askew, B.; Nemeth, D.; Islam, N. Convergent Functional Groups: Synthetic and Structural Studies. *J. Am. Chem. Soc.* **1985**, *107*, 7476–7481.
- (301) Shimizu, K. D.; Dewey, T. M.; Rebek, J., Jr. Convergent Functional Groups. 15. Synthetic and Structural Studies of Large and Rigid Molecular Clefs. *J. Am. Chem. Soc.* **1994**, *116*, 5145–5149.
- (302) Shimizu, K. D.; Rebek, J. A Rigid Trans-Spanning Dinitrile Ligand. *Proc. Natl. Acad. Sci. U. S. A.* **1996**, *93*, 4257–4260.
- (303) Choi, D.-S.; Chong, Y. S.; Whitehead, D.; Shimizu, K. D. Molecules with Shape Memory Based on Restricted Rotation. *Org. Lett.* **2001**, *3*, 3757–3760.
- (304) Rasberry, R. D.; Shimizu, K. D. Molecular Playdough: Conformationally Programmable Molecular Receptors Based on Restricted Rotation. *Org. Biomol. Chem.* **2009**, *7*, 3899–3905.
- (305) Degenhardt, C. F.; Lavin, J. M.; Smith, M. D.; Shimizu, K. D. Conformationally Imprinted Receptors: Atropisomers with “Write”, “Save”, and “Erase” Recognition Properties. *Org. Lett.* **2005**, *7*, 4079–4081.
- (306) Chong, Y. S.; Smith, M. D.; Shimizu, K. D. A Conformationally Programmable Ligand. *J. Am. Chem. Soc.* **2001**, *123*, 7463–7464.
- (307) Shinkai, S.; Ikeda, M.; Sugasaki, A.; Takeuchi, M. Positive Allosteric Systems Designed on Dynamic Supramolecular Scaffolds: Toward Switching and Amplification of Guest Affinity and Selectivity†. *Acc. Chem. Res.* **2001**, *34*, 494–503.
- (308) Chong, Y. S.; Dial, B. E.; Burns, W. G.; Shimizu, K. D. Covalent Locking and Unlocking of an Atropisomeric Molecular Switch. *Chem. Commun.* **2012**, *48*, 1296–1298.
- (309) Lavin, J. M.; Shimizu, K. D. Rapid Screening of a Receptor with Molecular Memory. *Org. Lett.* **2006**, *8*, 2389–2392.
- (310) Degenhardt, C. F.; Smith, M. D.; Shimizu, K. D. A Chiral 28-Membered Macrocyclic with Symmetry and Structure Similar to That of trans-Cyclooctene. *Org. Lett.* **2002**, *4*, 723–726.
- (311) Chong, Y. S.; Shimizu, K. D. Shape-Persistent and Shape-Adaptable Macrocycles Based on Restricted Rotation: Studies Building Toward ‘Macromolecular Playdough’. *Synthesis* **2002**, 2002, 1239–1244.
- (312) Clayden, J.; Vallverdu, L.; Clayton, J.; Helliwell, M. Conformational Switching Between Diastereoisomeric Atropisomers of Arenedicarboxamides Induced by Complexation With Lewis Acids. *Chem. Commun.* **2008**, 561–563.
- (313) Alfonso, I.; Burguete, M. I.; Luis, S. V. A Hydrogen-Bonding-Modulated Molecular Rotor: Environmental Effect in the Conformational Stability of Peptidomimetic Macrocyclic Cyclophanes. *J. Org. Chem.* **2006**, *71*, 2242–2250.
- (314) Dial, B. E.; Pellechia, P. J.; Smith, M. D.; Shimizu, K. D. Proton Grease: An Acid Accelerated Molecular Rotor. *J. Am. Chem. Soc.* **2012**, *134*, 3675–3678.
- (315) Carroll, W. R.; Pellechia, P.; Shimizu, K. D. A Rigid Molecular Balance for Measuring Face-to-Face Arene–Arene Interactions. *Org. Lett.* **2008**, *10*, 3547–3550.
- (316) Chong, Y. S.; Carroll, W. R.; Burns, W. G.; Smith, M. D.; Shimizu, K. D. A High-Barrier Molecular Balance for Studying Face-to-

Face Arene–Arene Interactions in the Solid State and in Solution. *Chem. - Eur. J.* **2009**, *15*, 9117–9126.

(317) Zhao, C.; Parrish, R. M.; Smith, M. D.; Pellechia, P. J.; Sherrill, C. D.; Shimizu, K. D. Do Deuteriums Form Stronger CH– π Interactions? *J. Am. Chem. Soc.* **2012**, *134*, 14306–14309.

(318) Clayden, J.; Lund, A.; Vallverdu, L.; Helliwell, M. Ultra-Remote Stereocontrol by Conformational Communication of Information Along a Carbon Chain. *Nature* **2004**, *431*, 966–971.